

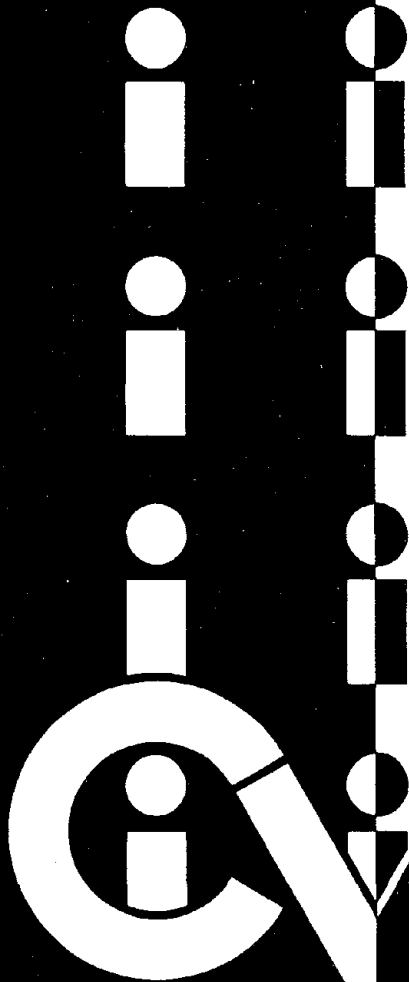
## Structural Engineering

CE-STR-80-18

DATA ANALYSIS FOR  
SAFETY EVALUATION OF  
EXISTING STRUCTURES

Shwu-Jen Hong Chen

James T. P. Yao



REPRODUCED BY  
NATIONAL TECHNICAL  
INFORMATION SERVICE  
U.S. DEPARTMENT OF COMMERCE  
SPRINGFIELD, VA 22161

INFORMATION RESOURCES  
NATIONAL SCIENCE FOUNDATION





<b>REPORT DOCUMENTATION PAGE</b>	<b>1. REPORT NO.</b> NSF/RA-800423	<b>2.</b>	<b>3. Recipient's Accession No.</b> <b>PB01 186074</b>
<b>4. Title and Subtitle</b> Data Analysis for Safety Evaluation of Existing Structures			<b>5. Report Date</b> December 1980
<b>7. Author(s)</b> S.-J. Hong Chen, J. T. P. Yao			<b>6.</b>
<b>9. Performing Organization Name and Address</b> Purdue University School of Civil Engineering West Lafayette, IN 47907			<b>8. Performing Organization Rept. No.</b> CE-STR-80-18
<b>12. Sponsoring Organization Name and Address</b> Office of Planning and Resources Management (OPRM) National Science Foundation 1800 G Street, N.W. Washington, D.C. 20550			<b>10. Project/Task/Work Unit No.</b>
<b>15. Supplementary Notes</b>			<b>11. Contract(C) or Grant(G) No.</b> (C) (G) PFR7906296
<b>16. Abstract (Limit: 200 words)</b> The state of structural safety is evaluated by using rational indicators which are related to the physical deterioration of existing structures. Two such indicators-- natural fundamental frequency, and damping ratio are studied. An approach for safety evaluation of existing structures utilizing system identification techniques is emphasized. Specifically, changes of estimated parameters such as natural frequencies and damping ratios during an earthquake are correlated with the observed structural damage. The application of simple methods of system identification to existing structures from observations of responses to earthquake inputs is elucidated. Numerical examples of two existing buildings and two test structural models with various damage levels are given to demonstrate the effectiveness of these new methods. The significance of changes in structural characteristics with respect to time is discussed. Results which are improved by imposing various conditions to remove undesirable data points and the treatment of measurement noise and error are presented. Available data are summarized and plotted to show the relationship between damage ratio and change in natural frequency of structures. Recommendations are made for the further improvement of this approach.			<b>13. Type of Report &amp; Period Covered</b>
<b>17. Document Analysis a. Descriptors</b> Damage assessment                      Safety factor                      Buildings Damping                                      Systems engineering              Earthquakes Resonant frequency                      Structural analysis			
<b>b. Identifiers/Open-Ended Terms</b> Seismic response  Earthquake Hazards Mitigation			
<b>c. COSATI Field/Group</b>			
<b>18. Availability Statement</b>  NTIS	<b>19. Security Class (This Report)</b>	<b>21. No. of Pages</b>	
	<b>20. Security Class (This Page)</b>	<b>22. Price</b>	



## NOTICE

THIS DOCUMENT HAS BEEN REPRODUCED FROM THE BEST COPY FURNISHED US BY THE SPONSORING AGENCY. ALTHOUGH IT IS RECOGNIZED THAT CERTAIN PORTIONS ARE ILLEGIBLE, IT IS BEING RELEASED IN THE INTEREST OF MAKING AVAILABLE AS MUCH INFORMATION AS POSSIBLE.



DATA ANALYSES FOR SAFETY EVALUATION OF  
EXISTING STRUCTURES

by

Shwu-Jen Hong Chen

and

James T. P. Yao

Technical Report No. CE-STR-80-18

Supported by

The National Science Foundation

through

Grant No. PFR 7906296

December 1980

School of Civil Engineering  
Purdue University  
West Lafayette, IN 47907

Any opinions, findings, conclusions  
or recommendations expressed in this  
publication are those of the author(s)  
and do not necessarily reflect the views  
of the National Science Foundation.

*i-a*



TABLE OF CONTENTS

	<u>Page</u>
1. INTRODUCTION . . . . .	1
1.1 General Remarks . . . . .	1
1.2 Objective and Scope . . . . .	2
2. LITERATURE REVIEW. . . . .	2
2.1 System Identification . . . . .	2
2.2 Damage Assessment and Damageability Evaluation. . . . .	5
2.3 Degradation of Structural Characteristics . . . . .	12
3. EFFECT OF DAMAGE ON NATURAL FREQUENCY. . . . .	15
3.1 General Remarks . . . . .	15
3.2 Methodology . . . . .	16
3.3 Idealized Model . . . . .	19
3.4 Union Bank Building . . . . .	20
3.5 Jet Propulsion Laboratory, Building 180 . . . . .	21
3.6 Test Structure I. . . . .	21
3.7 Test Structure II . . . . .	22
4. SUMMARY AND DISCUSSION . . . . .	23
4.1 Summary of Results. . . . .	23
4.2 Conclusion and Recommendation . . . . .	24
ACKNOWLEDGMENT . . . . .	26
APPENDIX A Method I Criterion . . . . .	27
APPENDIX B Method II Criterion. . . . .	29
APPENDIX C Heuristic Derivation For A Suitable Value of $\Delta t$ . . . . .	31
APPENDIX D Computer Program Listing For Methods I And II. . . . .	32
APPENDIX E References . . . . .	36
TABLES . . . . .	40
FIGURES. . . . .	53



## 1. INTRODUCTION

### 1.1 General Remarks

It is important to evaluate the safety condition (or damage state) of existing structures after the occurrence of each strong-motion earthquake. Although there are competent and experienced structural engineers who can perform such tasks successfully, the detailed methodology and decision-making process remain to be privileged information for the select few.

To assess the damage state, it must be defined first. One example of such damage state definitions is given by Housner and Jennings [19]. Another possible definition can be obtained through the use of reliability functions [45,49]. Although the theory of structural reliability has been successfully applied in the development of a rational design code [15], it is still difficult to use in the case of existing structures [16,17,25].

One approach to the problem of safety evaluation of existing structures is the application of pattern recognition [13], which refers to those mathematical techniques representing human experience. The existing structure consists of infinite dimensions, and its responses are measured with the use of transducers to produce a measurement space with a finite number of dimensions. These measurements are then analyzed to obtain a feature space with a smaller number of dimensions. Finally a classifier is required to yield the desired classification.

System identification techniques can be used for the analysis of measurements in obtaining a feature space. The traditional approach to the system identification problem in structural engineering is to obtain "more realistic" equations of motion for the structure by analyzing dynamic test data with known forcing functions. The problem of interest herein is safety evaluation or damage assessment of existing structures through the application of system identification techniques using earthquake input and measured response data.

## 1.2 Objective and Scope

The ultimate objectives of this research project are to formulate reliability criteria and to analyze available data concerning damage assessment for the safety evaluation of existing structures. The objective of this phase of investigation is to develop two simple methods for the estimation of fundamental natural frequencies, the changes of which during a strong earthquake can be considered as a feature in the context of pattern recognition.

Recently developed methods of structural identification, techniques of damage assessment and damageability evaluation are reviewed and summarized. Two simple methods for identification of degrading structural characteristics and their changes due to destructive excitation are then presented. Numerical examples illustrating the application of these methods using recorded data are also included. Available data of natural frequency and damage ratio of structures are summarized and plotted to establish a relationship for damage assessment in terms of changes in natural frequency. Advantages, disadvantages and possible extensions of this approach are also discussed.

## 2. LITERATURE REVIEW

### 2.1 System Identification

The available literature on system identification in structural engineering was reviewed and summarized by Chen in 1976 [7,40]. In Reference 7, various methods were classified as to the type of excitation, model, and response. Excitations were classified as being random or deterministic, and ambient or moderate-to-strong. Models were classified as linear or nonlinear, lumped parameter or distributed parameter, time domain or frequency domain, and whether or not noise was considered. Responses were also classified as being acceleration, velocity, displacement, or some combination of these, or frequency responses when frequency domain was used. In the following, an attempt is made to present a review of additional literature on system identification techniques as applied

to structural dynamics to-date.

A method was presented by Rodeman [34] for the estimation of structural parameters using noise-polluted transient response data. A set of nonlinear algebraic equations involving the parameters and obtained with the use of Maximum Likelihood method were then solved to obtain estimates of mass, damping, and stiffness of structures. In addition, the Cramer-Rao bounds on the covariance matrix of the estimates for different runs were obtained. Later, Krieger [24] developed a methodology for the estimation of structural parameters recursively in the frequency domain. The Maximum likelihood simulation runs were designed to indicate how well the estimated values of Young's modules and the damping proportionality constant compared with the actual values. The Bayesian estimation runs were designed to reflect their particular generalization over the maximum likelihood approach. The methodology was then applied to a 138-KV Air Core Line Trap structure which was not a linear and viscously damped model.

A second-order nonlinear differential equation containing the linear viscous damping coefficient and a three-parameter Ramberg-Osgood type hysteretic force-deformation relation was formulated to represent a single-story steel structure [27]. An integral squared error function was applied to evaluate the "goodness-of-fit" between the acceleration and displacement of this structure and those of its nonlinear mathematical model. The set of parameters corresponding to the minimum squared error is considered as the best set possible for the given model and test data. Three different models in increasing order of complexity have been used to identify the seismic behavior of a three-story steel frame subjected to arbitrary forcing functions, all of which cause responses within the elastic range [23]. In this report, more than five parameters related to stiffness characteristics and Rayleigh type damping were established using a modified Gauss-Newton algorithm and obtained by minimizing an error function.

Methods of parameter estimation based on the observed data of applied

forces and responses for linear multi-degree-of-freedom structural systems were studied by Shinozuka et al., [37]. The auto-regressive and moving-average model was found to be a convenient model representing linear multi-degree-of-freedom structural dynamic systems. It was also compatible with the instrumental variable method and the maximum likelihood method but not with the ordinary least square method and the limited information maximum likelihood method. All of these methods were applied to identify the aerodynamic coefficient matrices of a suspension bridge using field measurement data. This study was extended by Yun and Shinozuka [51], who found that the extended Kalman filter and the iterated linear filter-smoother to be highly useful for the identification of the parameters in non-linear multi-degree-of-freedom structural dynamic systems. The identification of hydrodynamic coefficient matrices of a fixed offshore tower was considered as a numerical example.

A general formulation called the output-error approach was presented by Beck et al. [4,5] to minimize a selected measure-of-fit between the calculated response using the mathematical model and the recorded structural response. A new technique, called the modal minimization method, was developed to overcome difficulties which were encountered when an optimal filter method was applied to analyze records of two multi-story buildings from the 1971 San Fernando Earthquake. It is interesting to note that the optimal estimates of the period for different segments of the records are showing a tendency to increase with respect to time during San Fernando earthquake. In addition, estimates of the parameters before and after the 1971 San Fernando earthquake were also compared. A method was developed by McVerry [28] to identify the parameters of the lower modes of a linear time-invariant model of a structure from a portion of recorded earthquake response. In this method, the parameters are selected from results of a least-squares-fit over a specified frequency band between the finite Fourier transform of the recorded acceleration response and the corresponding transform calculated from the response of the

model. In addition, short segments of the records were used to study the time-variation of the equivalent linear parameters of nonlinear systems.

## 2.2 Damage Assessment and Damageability Evaluation

It is desirable to evaluate the damage state of existing structures because of the requirement of disaster mitigation. For the purpose of comparison, a numerical quantity is often assigned to express the structural damage level. Such a damage index can be based on such quantities as cost of repairs, stress ratio, and probability of failure. Estimation of structural damage can be classified as damage assessment and damageability evaluation. In this report, "damage assessment" refers to the assessment of the current damage state of structures by making a judgement through a detailed field survey or from an empirical damage function. Meanwhile, "damage ability evaluation" refers to the prediction of the future damage of existing structures based on current structural conditions as well as available knowledge of past loading history in the general area. Several examples of damage assessment and damageability evaluation are reviewed and summarized in the following. Some damage functions, either time-dependent or time-independent are also included.

In 1971, Wiggins and Moran [42] proposed an empirical procedure for grading existing buildings in Long Beach, California. A total of up to 180 points is assigned to each structure according to the evaluation of the following five items:

- (a) Framing system and/or walls (0, 20, 40 points). A well-designed reinforced concrete or steel building less than 3 stories in height is assigned a zero-value. On the other hand, an unreinforced masonry filler and bearing walls with poor quality mortar is assigned a value of 40 points.
- (b) Diaphragm and/or Bracing System (0, 10, 20 points). As

an example, zero values corresponds to well-anchored reinforced slabs and fills. On the other hand, incomplete or inadequate bracing systems correspond to the high 20 points on the scale.

- (c) Partitions (0, 10, 20 points). Those partitions with many wood or metal stud bearings rate zero points. On the other hand, unreinforced masonry partitions with poor mortar will draw 20 points.
- (d) Special Hazards (0, 5, 10, 15, 20, 35, 50 points). The high hazards include the presence of non-bearing, unreinforced masonry walls, parapet walls, or appendages.
- (e) Physical Condition (0, 10, 15, 20, 35, 50 points). The high hazards include serious bowing or leaning, signs of incipient structural failure, serious deterioration of structural materials, and other serious unrepaired earthquake damage.

All of these assigned points are summed for each building thus inspected. Rehabilitation is not required if the sum is less than 50 points (low hazard). Some strengthening is required if the sum is between 51 and 100 points (intermediate hazard). Demolition or major strengthening is necessary when the sum exceeds 100 points (high hazard).

A safety evaluation program in disaster investigations was developed recently [43]. The exposure to structures, the critical vulnerability of structure, and combined safety index are primarily considered by investigators. A digital scale of 0 through 9 is used in a subjective manner with 0 denoting no damage and 9 denoting severe damage. Weighting factors are also applied to obtain a combined index for safety evaluation.

Culver et al. [11] proposed the field evaluation method (FEM) which is particularly applicable when building plans are not available. A rating of 1 through 4 is assigned for each general rating, GR, grading the material of frame, structural system rating, s, combining connection, roof, and floor ratings, etc., and Modified Mercalli Intensity I. Then a composite rating, CR, is computed as follows:

$$CR = \frac{GR + 2s}{3I} \quad (1)$$

If  $CR < 1.0$ ; the building is said to be in good condition, if  $1.0 < CR < 1.4$ ; it is in fair condition, if  $1.4 < CR < 2.0$ ; it is in poor condition, if  $CR > 2.0$ ; it is in very poor condition. A detailed methodology was also presented for survey and evaluation of existing buildings to determine the risk to life safety under natural hazard conditions and estimate the amount of expected damage. There are four major parts in this report as follows:

- (a) generation of site loads,
- (b) generation of a structural model,
- (c) computation of response, drift and ductility, and
- (d) assessment of damage.

The damage on  $i^{\text{th}}$  story,  $D_i$ , resulting from extreme natural environments is expressed in percent of total damage as follows:

$$D_i \% = 100 \times F(\mu_i), \text{ and} \quad (2)$$

$$\mu_i = \frac{\Delta_i}{(\Delta_y)_i} \quad (3)$$

where  $F(\mu_i)$  = distribution function of ductility to yield of  $i^{\text{th}}$  story,

$\mu_i, \Delta_i$  = calculated interstory ductility and drift of  $i^{\text{th}}$  story, respectively, and

$(\Delta_y)_i$  = user specified interstory drift to yield of  $i^{\text{th}}$  story.

The damage is classified into 3 categories: structural, nonstructural and glass. It is further subdivided into frame, walls and diaphragms in the case of structural damage.

Rich et al. [33] presented a method for assessing the residual strength of structural components which have sustained impact penetration damage. This method is based upon the application of the Weibull probability density function to account for the significant scatter in residual strengths which result from the random nature of impact damage detail (cracks, holes, and spall surfaces). The impact damage  $d_{im}$  is defined as follows:

$$d_{im} = \text{Max} (\rho \sin^2 \beta) \quad (4)$$

The damage parameters  $\rho$  and  $\beta$  are the total crack length and the crack inclined angle, respectively. In this paper, three primary forms of damage have been investigated:

- (a) No damage-where no machined damage is present and failure is controlled by the inherent material weaknesses which determine the ultimate tensile strength (0.00");
- (b) Smooth damage-where failure is initiated at a smooth machined hole (0.593");
- (c) Sharp damage-where failure is initiated at sharp crack tips (0.160", 0.320", 0.450", and 0.630").

The numbers in parentheses refer to the size of machined hole or crack tips corresponding to six nominal values of  $d_{im}$  in an example.

In studying the building damage resulting from the Caracas Earthquake of 29 July 1967, Seed et al. [36] used several quantities representing building damage for the purpose of comparison. For a given region, the structural damage intensity denotes the ratio of the number of damaged buildings to the

total number of buildings in this region. For individual buildings, the ratio of maximum induced dynamic lateral force to static design lateral force is used for brittle structures, and the ratio of spectral velocity to lateral force coefficient is used for ductile structures.

More generally, Bresler, Okada, Zisling, and Bertero [6] suggested a procedure similar to Wiggins and Morans' [42]. A total of up to 180 points is also adopted to grade a structure. In the second part of the report, a capacity ratio  $C$  and the leniency ratio  $L$  which are proposed for hazard abatement of structures are defined as follows:

$$C = \frac{r_c}{r_d}, \text{ and } L = 1 - C \quad (5)$$

where  $r_c$  and  $r_d$  denote calculated and design earthquake resistance of the structure, respectively. The last part presented a damageability criteria between local and global structure. The local damage  $d_i$  is the ratio of demand response to resistance in the  $i^{\text{th}}$  element. The global damage  $d_g$  is a summation of products of each local damage and its importance factor  $w_i$  which depends upon life hazard and cost. Similarly, a cumulative damageability index of structure subjected to cyclic loading conditions is defined as follows:

$$d_c = \sum_{i=1}^n \frac{w_i \eta_i d_i}{x_i} \quad (6)$$

where  $\eta_i$  and  $x_i$  denote the service history influence coefficients for demand and capacity, respectively.

Yao and Munse [50] suggested the following damage function for axially-loaded steel members, which are subjected to low-cycle and high-amplitude reversed plastic deformations:

$$D = \sum_{i=1}^n \left( \frac{Z_i - Y_{di}}{C_i - Y_{di}} \right)^{\alpha_i} \quad (7)$$

where  $\alpha_i$  is a function of a ratio of the cyclic compressive change in plastic strain to the subsequent tensile change in plastic strain,

$Z_i - Y_{di}$  denotes cyclic tensile change in plastic true strain,

$C_i - Y_{di}$  denotes cyclic tensile change in plastic true strain in  $n=1$ , and

$n$  is the number of applications of tensile load prior to fracture.

Equation 7 was applied to evaluate the damageability of seismic structures by Kasiraj and Yao [22] and Tang and Yao [39].

Oliveira [30] defined a damage ratio function (DRF) for structures as follows:

$$DRF = \left( \frac{z - Y_d}{C - Y_d} \right)^\alpha, \text{ if } Y_d \leq z \leq C \quad (8)$$

In this expression, DRF is in terms of the yield displacement  $Y_d$  and collapse displacement  $C$  which are considered as random variables. This is a measure of structural response or an index of the level of damage suffered by a building during an earthquake. The individual loss function (ILF) and global loss function (GLF) are also defined and studied. The individual risk function (IRF) used for a building and global risk function (GRF) used for metropolitan area are derived from ILF and GLF respectively. The risk analysis with the use of an probabilistic methodology is also presented.

Whitman, Reed, and Hong [41] presented a methodology for compiling and presenting statistics concerning damage to different types of buildings as result of earthquakes with various intensities. Each number in the damage probability matrix (DPM) is the probability that a building will experience a particular level of damage as the result of a particular intensity. The scale of damage runs from 0 to 8. Each damage state is identified by: (a) a

subjective description of physical damage including structural and nonstructural damage, and (b) an objective ratio, damage ratio (DR), of repair cost to replacement cost. A mean damage ratio (MDR) is also obtained as an indication of the relative damage to different types of buildings during different earthquakes.

A manual as prepared by Pinkham and Hart [32] describes a method of structural analysis, design and analysis of costs for the determination of strengthening of multi-story buildings. The method of evaluation is given in terms of the behavior of the critical structural elements in the building. An analysis of the structural response of the building to prescribed forces is first required. Therefore, the elements which should be considered as critical ones are the vertical shear resisting elements such as shear walls, braced frames, moment-resisting frames, and the horizontal diaphragm systems. Stress ratio of the calculated stress to the allowable stress of critical element is also calculated according to the type of structure such as masonry, concrete, or steel. This information is then used to make appropriate decisions as to which elements are satisfactory and which elements need to be strengthened.

Arias-Soto [2] suggested a damage function for structural integrity.

$$D = \frac{\sum_{i=1}^N (D_i M_i)}{\sum_{i=1}^N M_i} \quad (9)$$

where  $D_i$  = grade of damage of element  $i$ , and

$M_i$  = magnitude of damage of fault of element  $i$ .

Four categories are also assigned to an element or a structure with 0 denoting intact, 1 denoting cracked, 2 denoting broken and 3 indicating completely collapsed element or structure.

A possible application of pattern recognition in damage assessment of

existing structures is recently discussed by Fu and Yao [13]. This approach can be used to make a practical definition of "structural damage" and to develop a more rational method for the comparison and calibration of procedures for grading existing building structures. The application of pattern recognition to structural damage is to reduce physical damage data from a pattern space and finally apply a decision function to assess the damage state of structures.

Although there exist highly qualified engineers who are capable of conducting such estimations on the basis of their intuition and experience, the reliability of the results of these methods are still not widely known. In any event, a more rational solution for the damage assessment of existing structures is highly desirable. Based on a reliable method of assessment, the damageability can then be evaluated.

### 2.3 Degradation of Structural Characteristics

Crack size, plastic deformation, and ductilities have been used as damage factors in some methods of damage estimation which are discussed in Section 2.2. Recently, many meaningfully destructive tests have been performed to study the problem of structural deterioration. The degradation of natural frequency and stiffness of a structure after it is significantly damaged can be found in the following experimental investigations.

Otani and Sozen [31] investigated the inelastic dynamic response of reinforced concrete frames by subjecting a series of one-by three-story small-scale structures to strong base motions simulating one horizontal component of representative earthquake acceleration records. As a result of cracking and bond slip, the measured frequencies changed drastically during the first test run. As the intensity of the base motion was increased in successive tests, the observed frequencies decreased because of further cracking of the concrete and local yielding of the reinforcement. The first-mode frequency at the end of the last test run was reduced to a quarter of the calculated frequency. In

this paper, the total displacement range rather than the absolute maximum displacement was used as a damage index.

Aristizabal-Ochoa and Sozen [3] presented tests of four ten-story small-scale perforated walls which were subjected to an initial earthquake selected to cause serious damage. Before and after each seismic run, maximum base acceleration, spectrum intensity, response spectra, response displacements and accelerations, crack pattern, etc. were measured. The frequencies associated with the first mode and second mode were also measured to decrease with time and with run.

An analytical study of the static hysteretic response of six-story reinforced concrete walls to seismic loading was undertaken by Lybas and Sozen [26]. The main experimental variables were the strength and stiffness of the connecting beams. A damage ratio,  $\mu_{dr}$ , for an element of a linearly elastic substitute structure is expressed by

$$\mu_{dr} = \frac{K_{el}}{K_r} \quad (10)$$

where  $K_{el}$  = spring stiffness for a linearly elastic single-degree-of-freedom system, which has not yet yielded, and

$K_r$  = spring stiffness, reduced for equivalent linear response, of a single-degree-of-freedom system.

The apparent natural frequency of the test structures decreased continuously as the structures deteriorated under successive and increasingly severe application of the base motion. Equivalent viscous damping factors, the variation of damping factor with response mode and response amplitude was also studied.

Healey and Sozen [18] reported the response data obtained in three earthquake simulation tests of a ten-story reinforced concrete frame. Changes in the dynamic properties of the test structure, such as apparent frequencies and equivalent damping, are discussed. Because the apparent natural frequency

decreased with the maximum amplitude of motion in this study, the measured frequencies from the free-vibration tests were found to be consistently high while those from the earthquake simulation tests were consistently low. The measured frequencies of the test structure are listed in Table 13. Damping factors, estimated from the free-vibration test data using the logarithmic decrement method, were found to have increased after each earthquake simulation run.

Moehle and Sozen [29] subjected successively a small-scale ten-story reinforced concrete frame structure with relatively flexible lower stories to simulated earthquakes of increasing intensity. In this report, extensive experimental data were presented. Recorded dynamic responses were discussed in relation to stiffness, strength, and energy-dissipative capacity of the test structure. In addition, apparent natural frequencies of the test structures were estimated from data of free-vibration tests, simulated earthquake tests, and steady-state tests. Changes of apparent natural frequencies can be obtained from Fourier Amplitude Spectra of displacements at each run.

Hudson [20] presented a paper for dynamic tests of full scale structures including free-vibration and forced-vibration tests. A comparison of the natural frequencies is summarized to show that the natural frequencies obtained from forced vibration tests are always less than those from ambient vibration tests because of a considerable increase over the low-level value indicating a definite nonlinear behavior. In an example of a nine-story reinforced concrete building, the roof response was excited well into the nonlinear range. The period of this building during the San Fernando earthquake of February 9, 1971, was 1.01 seconds. In this case no significant structural damage occurred and the permanent period change can be attributed to minor alterations in non-structural ornamental facades. A period of about 0.79 seconds from man-excited vibration after earthquake is also found to be greater

than the one, 0.65 seconds, obtained before the earthquake.

Small-amplitude as well as large-amplitude dynamic tests of a full-scale building were performed by Galambos and Mayes [14]. Their data can be used to study the change of dynamic characteristics. The damping and the period were determined and changed at various input force levels. Finally, permanent changes of characteristics consisted on beam hinging, joint shear cracking and hinging of the stairwall occurred in all lower input force level tests performed after a series of large amplitude tests.

The application of a degrading-stiffness model to determine the seismic response [1, 21] shows another agreement with the importance of the degradation of structural characteristics. Most recently, a structural identification concept was advanced by Liu and Yao [25]. Structural damage as a function of fundamental frequency and damping coefficient which can be estimated with the use of methods of structural identification was also discussed [9,10,44-49].

### 3. EFFECT OF DAMAGE ON NATURAL FREQUENCY

#### 3.1 General Remarks

The properties of various structural elements in an existing structure do not necessarily remain the same as those when the structure was newly constructed. Therefore, it is desirable to detect any deterioration or other changes in a given structure. To date, most structural identification studies deal with the estimation of a set of constant parameters either through the analysis of nondestructive or destructive test data. It is believed that some of these parameters change during a strong earthquake, and these changes may provide an indication of structural damage. In this chapter, two simple methods are applied to recorded earthquake response data for the identification of linear parameters as functions of time during a given earthquake. The extent of the natural frequency as experienced by a damaged structure during an earthquake is also expressed on a segment-by-segment basis and their

changes are investigated. Results of this study compare favorably with those using other methods, and may be used to establish the relationship between dynamic characteristics and structural damage.

### 3.2 Methodology

Destructive tests of large-scale or full-scale structures are usually too expensive to be performed in the laboratory or in the field. However, an increasing number of records from natural earthquakes are becoming available in recent years. Recently, Sozen [18], Hudson [20] and others have already found that the natural frequencies obtained from both ambient tests and earthquake excitations decreased after each earthquake. Because ambient tests are always conducted at extremely low-level vibrations, they can be performed as many times as it is needed without causing any apparent damage to the structure. Nevertheless, the forced vibration test which may cause structural damage are of interest herein. Only earthquake records are available for the purpose of damage analysis in most cases. Based on the assumption of an existing structure, aged or new, with only a recent earthquake record available, the record of this earthquake can be divided into two or more segments for the purpose of this investigation. In general, the complete record of an earthquake can be separated into the following three main portions with different characteristics:

- (a) strongly-excited portion with higher modes contribution at the beginning of an earthquake,
- (b) much larger amplitude portion with nonlinear behavior,  
and
- (c) very low level vibration portion at the end of an earthquake.

In system identification problems, parameters identified from portion (a) can not be very accurate although a contribution of higher modes has been considered

in the analysis because of higher irregularity of earthquake input and response data. Because portion (c) is equivalent to very low level ambient vibration, natural frequency identified from portion (c) is always higher than and can not be compared with that from portion (b). However, the period of portion (a) and the relatively low amplitude of portion (c) can not be determined because they depend on the duration and intensity of earthquake and structural characters. Therefore, one approach used in this investigation is to deal with the identification of structural characteristics only in portion (b) by dividing this portion into several segments in order to study and compare the changes among those characteristics.

Method I is applied to find parameters  $\omega_n$  and  $\xi$  as functions of time from two linear equations of motion at time  $t$  and time  $t + \Delta t$  by using measured earthquake and response data. Parameters at any time  $t$  can be found as follows:

$$\omega_n^2(t) = \frac{(\ddot{x}_o(t) + \ddot{y}(t))\dot{y}(t + \Delta t) - (\ddot{x}_o(t + \Delta t) + \ddot{y}(t + \Delta t))\dot{y}(t)}{\dot{y}(t)y(t + \Delta t) - \dot{y}(t + \Delta t)y(t)} \quad (11)$$

and

$$\xi(t) = - \frac{\ddot{x}_o(t) + \ddot{y}(t) + \omega_n^2(t)y(t)}{2\omega_n(t)\dot{y}(t)} \quad (12)$$

When the denominators of Equation 11 and Equation 12 approach zero due to inadequate  $\Delta t$  nonlinear behavior, higher mode contribution, and measurement noise, it is difficult to estimate the values of  $\omega_n(t)$  and  $\xi(t)$  using this method. The selection of a suitable value of  $\Delta t$  by maximizing the denominator of Equation 11 is discussed in Appendix C, and the resulting mean values of  $\bar{\omega}_n$  and  $\bar{\xi}$ , have less variances. To improve these calculations, a set of conditions are applied to modify Method I as presented above.

It is well known that the Least-square-error-fit is simple and useful to identify a single degree-of-freedom model. By using this fit, natural frequency,  $\omega_n$ , and damping ratio,  $\xi$ , can be estimated by minimizing the integral-squared difference,  $E$ , between the excitation,  $\ddot{x}_{oi}$ , input to a structure and

the excitation,  $\ddot{x}_{oi}^{(1)}$ , calculated from its linear model. Here,

$$E = \sum_{i=n_j}^{n_k} (\ddot{x}_{oi} - \ddot{x}_{oi}^{(1)})^2 \quad (13)$$

$$= \sum_{i=n_j}^{n_k} (\ddot{x}_{oi} + y_i + 2\xi\omega_n \dot{y}_i + \omega_n^2 y_i)^2$$

$$\omega_n^2 = \frac{(\sum \dot{y}_i \dot{y}_i + \sum \ddot{x}_{oi} \dot{y}_i) \sum \dot{y}_i y_i - (\sum \dot{y}_i y_i + \sum \ddot{x}_{oi} y_i) \sum \dot{y}_i^2}{\sum \dot{y}_i^2 \sum y_i^2 - (\sum \dot{y}_i y_i)^2} \quad (14)$$

and

$$\xi = - \frac{\sum \dot{y}_i y_i + \sum \ddot{x}_{oi} y_i + \omega_n^2 \sum y_i^2}{2\omega_n \sum \dot{y}_i y_i} \quad (15)$$

where  $x_{oi}$ ,  $y_i$ ,  $\dot{y}_i$ , and  $\ddot{x}_{oi}$  are measured data during an earthquake and intervals  $n_j$ ,  $n_k$  are segments of the records to be used for identification of  $\omega_n$  and  $\xi$ . In addition, values  $\omega_{n1}$  and  $\xi_1$ ,  $\omega_{n2}$ , and  $\xi_2$ , ...,  $\omega_{nn}$  and  $\xi_n$  are identified from segments  $(n_1, n_2)$ ,  $(n_2, n_3)$ , ...,  $(n_n, n_{n+1})$ , respectively. Note that Equation 14 and Equation 15 are reduced to Equation 11 and Equation 12 when only two points of record are taken in Least-square-error-fit.

Method II is developed to apply conditions obtained from Method I to Least-square-error-fit such that each point of interest is over the linear range as applied to Method I. Available points to be used in segment  $n_j$ ,  $n_k$  is then less than or equal to  $n_k - n_j + 1$  whenever conditions are applicable.

Both Method I and Method II are specially developed and modified for the easy identification of structural characteristics and their changes during an earthquake. The main advantage of using such simple methods and linear models is the ease in checking the results and in preventing unnecessary errors associated with complicated calculation. In a possible future application to structural control [47], such simple methods can be advantageous. Moreover, the exact nonlinear characteristics for any given full-scale structure are not readily known in most cases.

These methods are demonstrated by an application to generated test data, as well as to measured earthquake response. Several numerical examples with different structural characteristics identified by the proposed methods using damage data are presented and discussed in the following.

### 3.3 Idealized Model

Response data generated from a linear first-mode model with a natural frequency of 2.0 rps and a damping ratio of 0.05 to a particular 1971 San Fernando earthquake excitation are utilized in this example. The relative displacement of this idealized system is shown in Figure 1. Table 1 lists a number of available points used for identification of  $\omega_n(t)$  and  $\xi(t)$ , mean and variance of  $\omega_n(t)$  and  $\xi(t)$  at different  $\Delta t$  by using Method I. The optimum value of 0.7 second is then selected from this table where the variances of  $\omega_n(t)$  and/or  $\xi(t)$  are the smallest. By using Method I and a fixed value of  $\Delta t$ , the natural frequency and the damping ratio as functions of time are solved and are plotted on Figures 2 through 5, and Figures 6 through 9, respectively, under different conditions. These time-variant parameters vary strongly in the beginning and fairly at the end of records because of irregular amplitude and small amplitude of displacement and velocity which cause small denominators. Table 2 presents results obtained from different conditions. No data point is to be used when a more restricted limitation of denominator is applicable, because all denominators at the end of records are smaller than  $10.0 \text{ cm}^2/\text{sec}$  as shown on Figure 10. However, the natural frequency and the damping ratio obtained from using Method I and Method II are found to be practically constant and accurate in the middle portion of an earthquake. By including the effects of the initial and final conditions in the analysis, the identification algorithm produce accurate estimates of the parameters for nearly ideal structural models or structures without being damaged.

### 3.4 Union Bank Building

The Union Bank Building is a 42-story steel-frame structure in downtown Los Angeles as shown in Figure 11. Prior to the 1971 San Fernando Earthquake strong-motion accelerographs with synchronized timing were installed in the sub-basement, on the 19th floor and on the 39th floor. However, the instruments on the 39th floor failed to record. The ground acceleration is illustrated in Figure 12. The S38°W components of the digitized relative acceleration, velocity and displacement at the 19th floor as shown in Figure 12 through 15 were used as the response data in the analysis.

The dominance of the lower modes in the earthquake response of this structure is essentially in first mode. Because the Union Bank building was strongly excited by a large pulse in the ground motion at approximately 10 seconds during the 1971 San Fernando Earthquake, the denominator in Equation 11 is near zero as shown in Figure 16. Therefore, the calculated natural frequency with high variance in first segment is not accurate and should be ignored. Consequently, the damping ratio,  $\xi$ , is also inaccurate due to such irregular values of  $\omega_n$ . When Method I and a  $\Delta t$ , 1.2 seconds, are applicable, the time-variant natural frequency and damping ratio can be estimated and are plotted in Figure 17 and 18. The distribution of the natural frequency as obtained from using Method I is listed in Table 3. The mode value is found to be between 1.25 rps and 1.35 rps. However, the properties at large amplitudes of displacement are more relevant for the application of these methods by comparing the displacement record and the results of parameters. Due to the presence of noise and errors in measured data, several conditions are imposed to improve the results such as those shown in Tables 4 and 5.

The proposed methods are found to be useful and efficient to determine the parameters for linear structures. As given in Table 6 and in Figure 19, the results of these methods show agreement with those of modal minimization method by Beck [4]. The natural frequency is shown to decrease segment by

segment except for the last value obtained from Method II. The loss of stiffness as indicated by this change in natural frequency seems to be the results of cracking and other types of damage of nonstructural elements during the occurrence of large-amplitude earthquake response. Its rough estimate of earthquake repairs was \$50,000 out of an initial construction cost of \$30,000,000 [12].

### 3.5 Jet Propulsion Laboratory, Building 180

Building 180 is a 9-story steel-frame structure as shown in Figure 20 on the grounds of the Jet Propulsion Laboratory, Pasadena, California. The S82°E components of the ground acceleration, relative acceleration, velocity and displacement at the roof were used as the excitation and response data as shown in Figure 21 through 24, respectively. The dominance of the first mode in the earthquake response and the fitness of a linear model of this building were found by Beck [4]. Results of the present study consisting of the changes in the natural frequency and the damping ratio are given in Tables 7 through 9 and Figures 25 through 27. Table 9 and Figure 28 show results from Method I, Method II, and Modal Minimization method by Beck [4]. The amplitude of the acceleration response of this building during the earthquake was twice that of the Union Bank but damage was limited to minor nonstructural cracking. However, very little changes in the natural frequency result in this analysis due to relatively minor damage involved.

### 3.6 Test Structure I

Test data as shown in Figures 30 through 33 for a single story steel structure subjected to a simulated earthquake [27] are analyzed through the use of proposed methods. The time-variant natural frequency and damping ratio obtained from Method I with a  $\Delta t$ -value of 0.1 second are plotted in Figures 34 through 37 for several different conditions. The averages of these parameters are listed on Table 10 segment by segment. Since a nonlinear hysteretic behavior was recorded during the excitation test, the slope of the hysteretic

model decreased as the force reached a certain high level and recovered at unloading point during a cycle. As long as the time of unloading situation is known, the natural frequency at this moment can be obtained from Method I to be compared with the one obtained from the slope of the hysteretic model listed in Table 11. Since these methods always yield good results in the range of linear behavior, an attempt to detect the presence of nonlinear behavior can be made by comparing the natural frequency identified from linear method and small ranges. A linear least-square-fit of a few records less than  $1/4$  of the number of records in a cycle can be suggested.

### 3.7 Test Structure II

The base acceleration and the tenth-level response data observed in three earthquake simulation tests of a ten-story reinforced concrete frame as shown in Figure 38 [18] are described in Figures 39 through 41. The maximum observed base accelerations for Runs Number One, Two, and Three were found to be 0.4g, 0.98g and 1.42g, respectively. The structure experienced little additional cracking during Run No. One, extensive cracking after Run No. Two and additional cracking and spalling at the base of columns after Run No. Three. The reduction in the frequencies of the test structure is given in Table 13 and in figure 42 by comparing the dominant mode frequencies of three runs. Test data during the first 16 seconds such as these mentioned above are used to identify the changes of natural frequencies during and between runs. Since the test structure was subjected to strong excitations during the first several seconds, higher modes and nonlinear behavior are present and pre-dominate in this period. Therefore, results obtained from Method I in the last segment can only be considered. A further restrictive condition is imposed by using a reasonable range of damping ratio. The introduction of this condition improved the results with the use of Method I.

## 4. SUMMARY AND DISCUSSION

### 4.1 Summary of Results

It is reasonably well understood that the natural frequency is non-increasing while the excited structure exhibits a considerable amount of damage at the end of the earthquake. The question to be answered is what levels, if any, of structural damage can be inferred from data of this parameter during earthquakes. Table 13 summarizes the type of structure, structural periods before, during and after earthquake, and damage ratios which are defined as ratios in percent of repair cost to replacement cost in non-structural, structural and total damage. Except the two test structures, all the buildings were subjected to the 1971 San Fernando earthquake with certain observations reported in [35]. In Table 14, the change of natural frequency of each structure is calculated and corresponds to the cost ratios of structural damage and total damage. These data points are also plotted in Figure 43 for the case during earthquake excitation and in Figure 44 on the basis of ambient excitations before and after earthquake. A curve can then be drawn through the approximate mean damage ratio on a given percent decrease in natural frequency for each data set. As an indicator of the occurrence of structural damage, the decrease in natural frequency provides more consistent correlation with the structural damage rather than with the total damage of structures. For example, it is obvious that such buildings as Bank of California and Holiday Inns showing high percent decrease in natural frequency have observable structural damage but have inconsistent total damage. However, non-decreasing natural frequency shows no damage or only very small nonstructural damage following an earthquake. Therefore, the identification of structural parameters takes into consideration not only a realistic mathematical model but also the identification of structural damage.

#### 4.2 Conclusion and Recommendation

Some existing methodologies for the estimation of structural damage require many input parameters such as historical seismic and meteorological records and detailed structural data. However, the more parameters are manipulated, the more uncertainties exist in the result. The principal advantage of this approach is its simplicity in assessing the damage of existing structures directly from the change of identified structural characteristics in handling available earthquake time-history records from a small number of locations in a structure. From a review of the results of this proposed approach, general discussion and recommendations given to further study are outlined in the following paragraphs.

The importance of this research can best be appreciated by recognizing that it brings together the relationship between the damage and the natural frequency of existing structures. However, this has to be accomplished using the statistical data as a basis of this relation. Sufficient data points in Figure 43 and Figure 44 are still necessary to define the threshold of the percent decrease in natural frequency at a hundred percent damage level, and to obtain a validated mathematical expression for damage assessment through regression analyses.

Current techniques in system identification which are acceptable in giving more accurate mathematical models of structures can be modified on a segment-by-segment basis to evaluate the relative decrease in natural frequency due to earthquakes. However, a consistent method may be more useful to prevent uncertainties resulting from various techniques. Proposed Methods I and II as described in the previous chapter have the advantage that it is easy to calculate.

To test the applicability of Methods I and/or II on Union Bank building, JPL building 180, and nonlinear test structure I, results gained within middle

portion of earthquake records can be useful in the identification of structural natural frequency. On the other hand, the damping ratio is not an apparent damage indicator by itself, but is considered as an important condition to improve the results of natural frequency as applied in test structure II. The overestimate of the damping ratio can also be improved by adding this condition in the method.

Because both methods are based on a linear, first-mode mathematical model in this thesis, suitable conditions can be applied to prevent undesired results due to nonlinear behavior, higher mode, and measurement noise which cause small denominators in Equation 11, and to give a reduced mean square error associated with the estimate. Because the result in the nonlinear range may be ignored by conditions or inconsistent with the linear one, these methods can be extended as a technique to investigate the presence of nonlinear behaviors in structural vibration. In addition, the first mode responses make relatively smaller contributions to the overall response as the base-motion intensity is increased. Research extension is needed into the consideration of higher modes so as to identify the initial natural frequency in first seconds of earthquake.

To obtain insight into the selection of numerical values for  $\Delta t$ , results of a study as given in Appendix C provide a value of a quarter structural period. However, examples described in Chapter Four result in consistent ratios of  $\Delta t$  to structural period, such as 0.7 seconds to 3.14 seconds for idealized model, 1.2 seconds to 4.72 seconds for Union Bank building, 0.4 seconds to 1.27 seconds for JPL building, 0.1 seconds to 0.54 seconds for test structure I, and 0.14 seconds to 0.5 seconds for test structure II. Because natural frequencies can change during the earthquake,  $\Delta t$  can be adjusted accordingly to obtain more accurate results during the analysis.

In conclusion, the changes in fundamental natural frequency are found to be important indicators for seismic damage of existing structures. Both Methods

I and II are simple and effective in estimating the natural frequency of existing buildings which vibrate primarily in the first mode during the earthquake.

For further improvement of these proposed methods, the concept of pattern recognition can be applied to make decisions for selecting adequate conditions. Then, the reliability of proposed approach for damage assessment can be greatly enhanced.

#### ACKNOWLEDGMENT

This report is based in part on results of S. J. Hong Chen's thesis research [8] under the direction of J. T. P. Yao. Both investigators appreciate the support of the National Science Foundation during these past several years. In addition, they wish to thank M. P. Gaus, J. L. Bogdanoff, K. S. Fu, E. C. Ting, and C. C. Chen for their advice and encouragement during the course of this investigation. Mrs. Vicki Gascho capably typed this report.

## APPENDIX A

## Method I Criterion

For a one-degree-of-freedom system, the linear equation of motion is as follows:

$$\ddot{y}(t) + 2\xi\omega_{\eta}\dot{y}(t) + \omega_{\eta}^2 y(t) = -\ddot{x}_o(t) \quad (\text{A-1})$$

where  $\ddot{y}$ ,  $\dot{y}$ ,  $y$  and  $\ddot{x}_o$  are relative acceleration, velocity, displacement and base acceleration, respectively.

Quantities  $\ddot{y}$ ,  $\dot{y}$ ,  $y$  and  $\ddot{x}_o$  are given, we wish to estimate  $\omega_{\eta}$  and  $\xi$ . Assume that  $\omega_{\eta}$  and  $\xi$  remain constants at time  $t_1$  and time  $t_2$ , solve  $\omega_{\eta}$  and  $\xi$  from two equations of motion at  $t_1$  and  $t_2$ .

$$\ddot{y}(t_1) + 2\xi\omega_{\eta}\dot{y}(t_1) + \omega_{\eta}^2 y(t_1) = -\ddot{x}_o(t_1) \quad (\text{A-2})$$

and 
$$\ddot{y}(t_2) + 2\xi\omega_{\eta}\dot{y}(t_2) + \omega_{\eta}^2 y(t_2) = -\ddot{x}_o(t_2) \quad (\text{A-3})$$

Multiplying both sides of (A-2) with  $\dot{y}(t_2)$

$$\begin{aligned} \ddot{y}(t_1)\dot{y}(t_2) + 2\xi\omega_{\eta}\dot{y}(t_1)\dot{y}(t_2) + \omega_{\eta}^2 y(t_1)\dot{y}(t_2) \\ = -\ddot{x}_o(t_1)\dot{y}(t_2) \end{aligned} \quad (\text{A-4})$$

Multiplying both sides of (A-3) with  $\dot{y}(t_1)$

$$\begin{aligned} y(t_2)\dot{y}(t_1) + 2\xi\omega_{\eta}\dot{y}(t_2)\dot{y}(t_1) + \omega_{\eta}^2 y(t_2)\dot{y}(t_1) \\ = -\ddot{x}_o(t_2)\dot{y}(t_1) \end{aligned} \quad (\text{A-5})$$

and subtracting (A-5) from (A-4), we obtain

$$\omega_{\eta}^2 = \frac{(\ddot{x}_o(t_1) + \ddot{y}(t_1))\dot{y}(t_2) - (\ddot{x}_o(t_2) + \ddot{y}(t_2))\dot{y}(t_1)}{\dot{y}(t_1)y(t_2) - \dot{y}(t_2)y(t_1)} \quad (\text{A-6})$$

If we consider many sets of  $t_1$  and  $t_2$  during the earthquake, the  $\omega_{\eta}$  and  $\xi$  become functions of time as follows:

$$\omega_{\eta}^2(t) = \frac{(\ddot{x}_o(t) - \ddot{y}(t))\dot{y}(t+\Delta t) - (\ddot{x}_o(t+\Delta t) + \ddot{y}(t+\Delta t))\dot{y}(t)}{\dot{y}(t)y(t+\Delta t) - \dot{y}(t+\Delta t)y(t)} \quad (\text{A-7})$$

$$\xi(t) = -\frac{\ddot{x}_o(t) + \ddot{y}(t) + \omega_{\eta}^2(t)}{2\omega_{\eta}(t)\dot{y}(t)} \quad (\text{A-8})$$

where  $\Delta t = t_2 - t_1$ .

## APPENDIX B

## Method II Criterion

Consider a one-degree-of-freedom system, the square error  $E$ , between measured excitation,  $\ddot{x}_{oi}$ , and excitation  $\ddot{x}_{oi}^{(1)}$ , solved from a linear model is as follows:

$$\begin{aligned} E &= \sum_{i=1}^n (\ddot{x}_{oi} - \ddot{x}_{oi}^{(1)})^2 \\ &= \sum_{i=1}^n (\ddot{x}_{oi} + \ddot{y}_i + 2\xi\omega\dot{y}_i + \omega^2 y_i)^2 \end{aligned} \quad (B-1)$$

Minimizing the square error,  $E$ , by taking  $\frac{\partial E}{\partial \xi} = 0$  and  $\frac{\partial E}{\partial \omega} = 0$ , we get

$$\sum_{i=1}^n (\dot{y}_i \ddot{y}_i + 2\xi\omega \dot{y}_i^2 + \omega^2 y_i \dot{y}_i + \ddot{x}_{oi} \dot{y}_i) = 0 \quad (B-2)$$

and

$$\begin{aligned} \sum_{i=1}^n (\xi \ddot{y}_i \dot{y}_i + \omega \ddot{y}_i y_i + 2\xi^2 \omega \dot{y}_i^2 + 3\xi\omega \dot{y}_i y_i + \omega^3 y_i^2 \\ + \xi \ddot{x}_{oi} \dot{y}_i + \omega \ddot{x}_{oi} y_i) = 0 \end{aligned} \quad (B-3)$$

Let

$$a = \sum_{i=1}^n \ddot{y}_i \dot{y}_i, \quad b = \sum_{i=1}^n \dot{y}_i^2, \quad c = \sum_{i=1}^n \dot{y}_i y_i, \quad d = \sum_{i=1}^n \ddot{x}_{oi} \dot{y}_i,$$

$$e = \sum_{i=1}^n \ddot{y}_i y_i, \quad f = \sum_{i=1}^n y_i^2, \quad \text{and } g = \sum_{i=1}^n \ddot{x}_{oi} y_i,$$

(B-2) and (B-3) become

$$a + 2\xi\omega b + \omega^2 c + d = 0, \quad (\text{B-4})$$

and  $\xi a + \omega e + 2\xi^2\omega b + 3\xi\omega^2 c + \omega^3 f + \xi d + \omega g = 0$  (B-5)

Multiplying (B-4) with  $\xi$  and then subtracting (B-5)

$$\xi = \frac{-e-g-\omega^2 f}{2\omega c} \quad (\text{B-6})$$

Substituting  $\xi$  in (B-4), we have

$$\omega^2 = \frac{ac + dc - be - bg}{bf - c^2}$$

$$= \frac{(\sum \ddot{y}_i \dot{y}_i + \sum \ddot{x}_{oi} \dot{y}_i) \sum \dot{y}_i y_i - (\sum \ddot{y}_i y_i + \sum \ddot{x}_{oi} y_i) \sum \dot{y}_i^2}{\sum \dot{y}_i^2 y_i^2 - (\sum y_i \dot{y}_i)^2} \quad (\text{B-7})$$

When  $n = 2$ , (B-7) is equivalent to (A-6) as derived in the following,

$$\omega^2 = \frac{(\ddot{y}_1 \dot{y}_1 + \ddot{y}_2 \dot{y}_2 + \ddot{x}_{o1} \dot{y}_1 + \ddot{x}_{o2} \dot{y}_2)(\dot{y}_1 y_1 + \dot{y}_2 y_2) - (\ddot{y}_1 y_1 + \ddot{y}_2 y_2 + \ddot{x}_{o1} y_1 + \ddot{x}_{o2} y_2)(\dot{y}_1^2 + \dot{y}_2^2)}{(\dot{y}_1^2 + \dot{y}_2^2)(y_1^2 + y_2^2) - (\dot{y}_1 y_1 + \dot{y}_2 y_2)^2}$$

$$= \frac{(\dot{y}_2 y_1 - \dot{y}_1 y_2)[(\ddot{x}_{o2} + \ddot{y}_2) \dot{y}_1 - (\ddot{x}_{o1} + \ddot{y}_1) \dot{y}_2]}{(\dot{y}_2 y_1 - \dot{y}_1 y_2)^2}$$

$$= \frac{(\ddot{x}_{o2} + \ddot{y}_2) \dot{y}_1 - (\ddot{x}_{o1} + \ddot{y}_1) \dot{y}_2}{\dot{y}_2 y_1 - \dot{y}_1 y_2} \quad (\text{B-8})$$

## APPENDIX C

Heuristic Derivation For A Suitable Value of  $\Delta t$ 

The denominator in Equation (4.1) can be close to zero when two data points are selected inadequately. Before analysis we have to choose a suitable  $\Delta t$  between two data points in order to obtain a large value for the denominator. The following derivation verifies that  $\Delta t$  equal to a quarter of period,  $T$ , maximizes the absolute of denominator,  $Z$ .

$$\text{For an ideal model, let } Z = y_1 \dot{y}_2 - y_2 \dot{y}_1, \quad (\text{C-1})$$

$$\begin{aligned} \text{where } y_1 &= \sin \omega t, & \dot{y}_1 &= \omega \cos \omega t \\ y_2 &= \sin \omega(t + \Delta t), & \dot{y}_2 &= \omega \cos \omega(t + \Delta t) \end{aligned} \quad (\text{C-2})$$

Therefore, we have

$$Z = \omega \sin \omega t \cos \omega(t + \Delta t) - \omega \sin \omega(t + \Delta t) \cos \omega t \quad (\text{C-3})$$

Taking the derivative of  $Z$  with respect to  $\Delta t$ , we get

$$\begin{aligned} \frac{\partial Z}{\partial \Delta t} &= -\omega^2 \sin \omega t \sin \omega(t + \Delta t) - \omega^2 \cos \omega(t + \Delta t) \cos \omega t \\ &= -\omega^2 \cos \omega \Delta t \end{aligned} \quad (\text{C-4})$$

When  $\frac{\partial Z}{\partial \Delta t} = 0$  and  $\frac{\partial^2 Z}{\partial \Delta t^2}$  is positive, i.e.  $\Delta t = \frac{T}{4}$  where  $T = \frac{2\pi}{\omega}$ , it will give us  $Z_{\min}$  or  $|Z|_{\max}$

## APPENDIX D

## Computer Program Listing For Methods I And II

```

PROGRAM HPIOT(INPUT,OUTPUT,PLOT,TAPE5=INPUT,TAPE6=OUTPUT)
C
C   THIS PROGRAM IS TO IDENTIFY THE NATURAL FREQUENCY AND
C   DAMPING RATIO SEGMENT BY SEGMENT USING METHOD I AND
C   METHOD II.
C
C   PARAMETER AS A FUNCTION OF TIME IS PLOTTED.
C
C   DESCRIPTION OF PARAMETERS :
C       CC - DENOMINATOR
C       WN - NATURAL FREQUENCY OBTAINED FROM METHOD I
C       S  - DAMPING RATIO OBTAINED FROM METHOD I
C       AVW - THE AVERAGE OF WN
C       AVS - THE AVERAGE OF S
C       VARW - THE VARIANCE OF WN
C       VARS - THE VARIANCE OF S
C       W1 - NATURAL FREQUENCY OBTAINED FROM METHOD II
C       S1 - DAMPING RATIO OBTAINED FROM METHOD II
C
REAL XDOT2(2870),YDOT2(3060),YV(1528),YDOT(3056),YD(616),Y(3080)
REAL XV(1440),XD(576),TT(300)
REAL W2(2868),WN(2868),S(2868),CC(2868)
C
READ 1,NX,DX,(XDOT2(I),I=1,2868)
READ 3,NXV,DXV,(XV(I),I=1,1440)
READ 3,NXD,DXD,(XD(I),I=1,576)
READ 1,NY,DY,(YDOT2(I),I=1,3060)
READ 3,NV,DV,(YV(I),I=1,1528)
READ 3,ND,DYD,(YD(I),I=1,616)
1  FORMAT(///,I5,F5.2,/, (12F6.1))
3  FORMAT(/,I5,F5.2,/(8F9.4))
C
C   OBTAIN RELATIVE RESPONSES
C
DO 4 I=1,2868
4  YDOT2(I)=YDOT2(I)-XDOT2(I)
DO 5 I=1,1440
5  YV(I)=YV(I)-XV(I)
DO 6 I=1,576
6  YD(I)=YD(I)-XD(I)
C
C   LET ALL DT EQUAL TO 0.02 SECONDS
C
Y0=0.0
YDOT(1)=(YV(1)+Y0)/2.0
YDOT(2)=YV(1)
DO 13 I=1,1433
YDOT(2*I+1)=(YV(I+1)+YV(I))/2.0

```

```

YDOT(2*I+2)=YV(I+1)
13 CONTINUE
DO 14 J=1,5
Y(J)=(YD(1)-YD)*FLOAT(J)/5.0
14 CONTINUE
DO 44 I=1,573
DO 44 J=1,5
Y(5*I+J)=YD(I)+(YD(I+1)-YD(I))*FLOAT(J)/5.0
44 CONTINUE
DI=0.02
C
C IDENTIFY WN AND S USING T AND T+1.2 SEC. IN METHOD I
C
IT=60
DO 7 I=10,2800,10
AA=(XDOT2(I+IT)+YDOT2(I+IT))*YDOT(I)
BB=(XDOT2(I)+YDOT2(I))*YDOT(I+IT)
CC(I)=Y(I)+YDOT(I+IT)-Y(I+IT)+YDOT(I)
W2(I)=(AA-BB)/CC(I)
WW=ABS(W2(I))
WN(I)=SORT(WW)
S(I)=-((XDOT2(I)+YDOT2(I)+W2(I)*Y(I))/(2.0*WN(I)+YDOT(I)))
7 CONTINUE
C
C PLOT WN VS. TIME
C
DO 20 I=1,280
TT(I)=FLOAT(I)+0.2
WN(I)=WN(10*I)
20 CONTINUE
CALL PLOTS
CALL FACTOR(0.6)
WN(281)=0.0
WN(282)=3.0
TT(281)=0.0
TT(282)=4.0
CALL AXIS(0.0,0.0,12H NAT. FREQ.,12,10.0,90.0,WN(281),WN(282),-1)
CALL AXIS(0.0,0.0,12H TIME(SEC) ,-12,15.0,0.0,TT(281),TT(282),0)
CALL PLOT(0.0,0.0,3)
DO 21 I=10,2800,10
J=I/10
IF(ABS(CC(I)).LT.10.0) GO TO 22
IF(W2(I).LE.0.0) GO TO 22
IF(S(I).GT.1.0 .AND. S(I).LT.0.0) GO TO 22
CALL PLOT(I(J)/TT(282),WN(J)/WN(282),2)
GO TO 21
22 CALL PLOT(TT(J+1)/TT(282),WN(J+1)/WN(282),3)
21 CONTINUE
CALL PLOT(0,0,999)
C
C FIND AVERAGE AND STANDARD DEVIATION OF WN AND S FOR METHOD I

```

```

C
  PRINT 10
10  FORMAT(9X,*PERIOD*,4X,*NO. OF *W2*,2X,*NAT. FREQ.*,2X,*DAMP. RAT.*,
      13X,*VAR. OF U*,4X,*VAR. OF S*)
      IN=10
      DO 8 J=1,4
      IF=IN+690
      SIT=FLOAT(IN)*DT
      SIF=FLOAT(IF)*DT
      NUB=70
      SUMW=SUMS=0.0
      K=0
      DO 70 I=IN,IF,10
      AA=(XDOT2(I+IT)+YDOT2(I+IT))*YDOT(I)
      BB=(XDOT2(I)+YDOT2(I))*YDOT(I+IT)
      CC(I)=Y(I)*YDOT(I+IT)-Y(I+IT)*YDOT(I)
      IF(ABS(CC(I)).LT.10.0) GO TO 57
      W2(I)=DD(I)/CC(I)
      IF(W2(I).LE.0.0) GO TO 57
      K=K+1
      WN(K)=SORT(W2(I))
      IF(YDOT(I).EQ.0.0) GO TO 55
      S(K)=-((XDOT2(I)+YDOT2(I)+W2(I)*Y(I))/(2.0*WN(K)*YDOT(I)))
      GO TO 56
55  S(K)=S(K-1)
56  SUMW=SUMW+WN(K)
      SUMS=SUMS+S(K)
      GO TO 70
57  NUB=NUB-1
70  CONTINUE
      AVW=SUMW/FLOAT(NUB)
      AVS=SUMS/FLOAT(NUB)
      VAW=VAS=0.0
      K=0
      DO 71 I=IN,IF,10
      IF(ABS(CC(I)).LT.10.0) GO TO 71
      IF(W2(I).LE.0.0) GO TO 71
      K=K+1
      VAW=VAW+(WN(K)-AVW)**2
      VAS=VAS+(S(K)-AVS)**2
71  CONTINUE
      VARW=VAW/FLOAT(NUB)
      VARS=VAS/FLOAT(NUB)
      PRINT 17,SIT,SIF,NUB,AVW,AVS,VARW,VARS
17  FORMAT(5X,F5.2,* TO *,F5.2,1X,I5,4F13.5)
      IN=IF
8   CONTINUE
C
C   IDENTIFY WN AND S USING METHOD II AND CONDITIONS USED IN METHOD I
C
PRINT 77

```

```

77  FORMAT(6X,*PERIOD*,7X,*NAT. FREQ.*,5X,*DAMP. RAT.*)
    IN=10
    DO 28 J=1,4
    IF=IN+700
    SIT=FLOAT(IN)*DT
    SIF=FLOAT(IF)*DT
    SUMA=SUMB=SUMC=SUMD=SUMF=SUNG=0.0
    DO 27 I=IN,IF,10
    IF(ABS(CC(I)).LT.10.0) GO TO 27
    IF(S(I).GT.1.0 .OR. S(I).LT.0.0) GO TO 27
    SUHA=SUMA+YDOT(I)*YDOT2(I)
    SUMB=SUMB+YDOT(I)**2
    SUMC=SUMC+Y(I)*YDOT(I)
    SUMD=SUMD+XDOT2(I)*YDOT(I)
    SUME=SUME+YDOT2(I)*Y(I)
    SUMF=SUMF+Y(I)**2
    SUNG=SUNG+XDOT2(I)*Y(I)
27  CONTINUE
    A=SUMC-SUMB+SUMF/SUMC
    C=SUMA+SUMD-SUMB+SUME/SUMC-SUMB+SUNG/SUMC
    W1=SQRT(-C/A)
    S1=(-SUMF-SUNG-W1+W1*SUMF)/2.0/W1/SUMC
    PRINT 72,SIT,SIF,W1,S1
72  FORMAT(F7.2,* TD *,F5.2,2E15.7)
    IN=IF
28  CONTINUE
    STOP
    END

```

I

APPENDIX E  
REFERENCES

- [1] Anderson, J. C., and Townsend, W. H., "Models for RC Frames with Degrading Stiffness," Journal of the Structural Division, ASCE, v. 103, n. ST12, December 1977, pp. 2361-2376.
- [2] Arias-Soto, Santiago, "Metodologia Para La Reparacion De Una Estructura Denada Por Sismo" Segundas Jornadas Chilenas de Sismologia E Ingenieria Antisismica, Santiago de Chile, v. 2, Julio 1976, pp. 26-30.
- [3] Aristizabal-Ochoa, J. D., and Sozen, M. A., Behavior of Ten-Story R/C walls Subjected to Earthquake Motion, Report No. UILU-ENG-76-2017, Dept. of Civil Engineering, University of Illinois, Urbana, Illinois, Oct. 1976.
- [4] Beck, J. L., Determining Models of Structures from Earthquake Records, Report No. EERL-78-01, California Institute of Technology, Pasadena, CA, June 1978.
- [5] Beck, J. L. and Jennings, P. C., "Structural Identification Using Linear Models and Earthquake Records", California Institute of Technology, Pasadena, CA.
- [6] Bresler, B., Okada, T., Zisling, D., and Bertero, V. V., "Assessment of Earthquake Safety and of Hazard Abatement," Developing Methodologies for Evaluating the Earthquake Safety of Existing Buildings, Earthquake Engineering Research Center, University of California at Berkeley, Report No. UCB/EERC-77-06, February 1977, pp. 17-49.
- [7] Chen, S. J. H., Methods of System Identification in Structural Engineering, M.S. Thesis, School of Civil Engineering, Purdue University, W. Lafayette, IN, August 1976.
- [8] Chen, S. J. H., System Identification and Damage Assessment of Existing Structures, Ph.D. Thesis, School of Civil Engineering, Purdue University, W. Lafayette, IN, December 1980.
- [9] Chen, S. J. H., Ting, E. C., and Yao, J. T. P., "Evaluation of Structural Damage Using Measurable Data", Proceedings, at the ASCE EMD-STD Specialty Conference on Probabilistic Mechanics and Structural Reliability, Tucson, AZ, Jan. 10-12, 1979, pp. 141-145.
- [10] Chen, S. J. H., and Yao, J. T. P., "Identification of a Structural Damage Using Earthquake Response Data", Proceedings at the ASCE/EMD Specialty Conference, Austin, Texas, September 17-19, 1979, pp. 661-664.
- [11] Culver, C. G., Lew, H. S., Hart, G. C., and Pinkham, C. W., Natural Hazards Evaluation of Existing Buildings, National Bureau of Standards, Building Science Series No. 61, January 1975.
- [12] Foutch, D. A., Housner, G. W., and Jennings, P. C., Dynamic Responses of Six Multistory Buildings During the San Fernando Earthquake, Report No. EERL-75-02, California Institute of Technology, Pasadena, CA, 1975.
- [13] Fu, K. S., and Yao, J. T. P., "Pattern Recognition and Damage Assessment", Proceedings, ASCE Third EMD Specialty Conference, University of Texas, Austin, Texas, 17-19 September 1979, pp. 344-347.

- [14] Galambos, T. V., and Mayes, R. L., Dynamic Tests of a Reinforced Concrete Building, Department of Civil Engineering, School of Engineering and Applied Science, Washington University, St. Louis, Missouri, June 1978.
- [15] Galambos, T. V., and Ravindra, M. D., Tentative Load and Resistance Factor Design Criteria for Steel Buildings, Research Report No. 18, Structural Division, Civil Engineering Department, Washington University, St. Louis, MO, September 1973.
- [16] Galambos, T. V., and Yao, J. T. P., "Additional Comments on Code Formats," DIALOG 2-76, Edited by O. Kitlevsen and G. Mohr, Denmarks Ingeniorakademi, Denmark, 1976, pp. 24-26.
- [17] Hart, G. C., and Yao, J. T. P., "System Identification in Structural Dynamics," Journal of the Engineering Mechanics Division, ASCE, v. 103, n. EM6, December 1977, pp. 1089-1104.
- [18] Healey, T. J., and Sozen, M. A., Experimental Study of the Dynamic Response of a Ten-Story Reinforced Concrete Frame with a Tall First Story, Report No. UILU-ENG-78-2012, Department of Civil Engineering, University of Illinois, Urbana, Illinois, Aug. 1978.
- [19] Housner, G. W., and Jennings, P. C., Earthquake Design Criteria for Structures, Report No. EERC-77-06, California Institute of Technology, Pasadena, CA, November 1977.
- [20] Hudson, D. E., "Dynamic Tests of Full-Scale Structures," Journal of the Engineering Mechanics Division, ASCE, v. 103, n. EM6, December 1977, pp. 1141-1157.
- [21] Imbeault, F. A., and Nielsen, N. N., "Effects of Degrading Stiffness on the Response of Multistory Frames Subjected to Earthquake," Proceedings, Fifth World Conference on Earthquake Engineering, Rome, Italy, 1973.
- [22] Kasiraji, I., and Yao, J. T. P., "Fatigue Damage in Seismic Structures," Journal of the Structural Division, ASCE, v. 95, n. ST8, August 1969, pp. 1673-1692.
- [23] Kaya, I., and McNiven, H. D., Investigation of the Elastic Characteristics of a Three-Story Steel Frame Using System Identification, Report No. EERC-78-24, Earthquake Engineering Research Center, University of California, Berkeley, California, 1978.
- [24] Krieger, W. F., Frequency Domain Structural Parameter Estimation, Ph.D Thesis, School of Aeronautics and Astronautics, Purdue University, West Lafayette, IN, December 1977.
- [25] Liu, S. C., and Yao, J. T. P., "Structural Identification Concept," Journal of the Structural Division, ASCE, v. 104, n. ST12, December 1978, pp. 1845-1858.
- [26] Lybas, J. M., and Sozen, M. A., Effect of Beam Strength and Stiffness on Dynamic Behavior of R/C Coupled Walls, Report No. UILU-ENG-77-2016, Dept. of Civil Engineering, University of Illinois, Urbana, Illinois, July 1977.

- [27] Matzen, V. C., and McNiven, H. D., Investigation of the Inelastic Characteristics of a Single-Story Steel Structure Using System Identification and Shaking Table Experiments, Report No. EERC-76-20, Earthquake Engineering Research Center, University of California, Berkeley, California, August 1976.
- [28] McVerry, G. H., "Structural Identification in the Frequency Domain from Earthquake Records," Applied Mechanics Department, Mail Code 104-44, California Institute of Technology, Pasadena, California 91125.
- [29] Moehle, J. P., and Sozen, M. A., Earthquake-Simulation Tests of a Ten-Story Reinforced Concrete Frame with a Discontinued First-Level Beam, Report No. UILU-ENG-78-2014, Department of Civil Engineering, University of Illinois, Urbana, Illinois, August 1978.
- [30] Oliveira, C. S., Seismic Risk Analysis for a Site and a Metropolitan Area, Report No. EERC-75-3, Earthquake Engineering Research Center, University of California, Berkeley, California, August 1975.
- [31] Otani, S., and Sozen, M. A., "Simulated Earthquake Tests of R/C Frames," Journal of the Structural Division, ASCE, v. 100, n. ST3, March 1974, pp. 687-701.
- [32] Pinkham, C. W., and Hart, G. C., "A Methodology for Seismic Evaluation of Existing Multistory Residential Buildings," U.S. Department of Housing and Urban Development, Office of Policy Development and Research Division of Energy, Building Technology and Standards, v. 1-3, June 1977.
- [33] Rich, T. P., Tracy, P. G., Tramontozzi, L. R., Adachi, J., Benicek, M., Katz, A. H., and Foster, W., "Probability Based Fracture Mechanics for Impact Penetration Damage," International Journal of Fracture, v. 13, No. 4, August 1977, pp. 409-430.
- [34] Rodeman, R., Estimation of Structural Dynamic Model Parameters from Transient Response Data, Ph.D. Thesis, School of Civil Engineering, Purdue University, West Lafayette, IN, August 1974.
- [35] "San Fernando, California, Earthquake of February 9, 1971", U.S. Department of Commerce, National Oceanic and Atmospheric Administration, v. I, Part A & B, 1973.
- [36] Seed, H. B., Idriss, I. M., and Dezfulian, H., Relationships Between Soil Conditions and Building Damage in the Caracas Earthquake of July 29, 1967, Earthquake Engineering Research Center, University of California at Berkeley, Report No. EERC-70-2, February 1970.
- [37] Shinozuka, M., Yun, C. B., and Imai, H., Identification of Linear Structural Systems, Technical Report No. NSF-ENG-76-12257-2, Department of Civil Engineering and Engineering Mechanics, Columbia University in the City of New York, May 1978.
- [38] Takeda, T., Sozen, M. A., and Nielsen, N. N., "Reinforced Concrete Beam Column Connection," Journal of the Structural Division, ASCE, v. 96, n. ST12, December 1970, pp. 2557-2573.

- [39] Tang, J. P., and Yao, J. T. P., "Expected Fatigue Damage of Seismic Structures," Journal of the Engineering Mechanics Division, ASCE, v. 98, n. EM3, June 1972, pp. 695-709.
- [40] Ting, E. C., Chen, S. J. Hong, and Yao, J. T. P., System Identification, Damage Assessment and Reliability Evaluation of Structures, Report No. CE-STR-78-1, School of Civil Engineering, Purdue University, W. Lafayette, Indiana, February 1978.
- [41] Whitman, R. V., Reed, J. W., and Hong, S. T., "Earthquake Damage Probability Matrices," Proceedings, 5th World Conference on Earthquake Engineering, Rome, Italy, 1973.
- [42] Wiggins, J. H., Jr., and Moran, D. F., Earthquake Safety in the City of Long Beach Based on the Concept of Balanced Risk, J. H. Wiggins Company, Redondo Beach, California, September 1971.
- [43] Bresler, B., Hanson, J. M., Comartin, C. D., and Thomasen, S. E., "Practical Evaluation of Structural Reliability," Preprint No. 80-596, ASCE Convention, Florida, 27-31 October 1980.
- [44] Yao, J. T. P., "Assessment of Seismic Damage in Existing Structures," presented at U.S.-S.E. Asia Joint Symposium on Engineering for Natural Hazard Protection, Manila, Philippines, 26-30 September 1977.
- [45] Yao, J. T. P., "Damage Assessment and Reliability Evaluation of Existing Structures," Engineering Structures, England, v. 1, October 1979, pp. 245-251.
- [46] Yao, J. T. P., An Approach to Damage Assessment of Existing Structures, Report No. CE-STR-79-4, School of Civil Engineering, Purdue University, West Lafayette, IN, October 1979; also "Damage Assessment of Existing Structures," Journal of the Engineering Mechanics Division, ASCE, v. 106, n. EM4, August 1980, pp. 785-799.
- [47] Yao, J. T. P., Reliability of Existing Buildings in Earthquake Zones, Report No. CE-STR-79-6, School of Civil Engineering, Purdue University, W. Lafayette, IN, December 1979.
- [48] Yao, J. T. P., "Identification and Control of Structural Damage," Solid Mechanics Archives, v. 5, Issue 3, August 1980, pp. 325-345.
- [49] Yao, J. T. P., and Anderson, C. A., "Reliability Analysis and Assessment of Existing Structural Systems," presented at the Fourth International Conference on Structural Mechanics in Reactor Technology, San Francisco, CA, August 15-19, 1977.
- [50] Yao, J. T. P., and Munse, W. H., "Low-Cycle Axial Fatigue Behavior of Mild Steel," ASTM Special Technical Publication No. 338, 1962, pp. 5-24.
- [51] Yun, C. B., and Shinozuka, M., Identification of Nonlinear Structural Systems, Technical Report No. NSF-ENG-76-12257-3, Department of Civil Engineering and Engineering Mechanics, Columbia University in the City of New York, June 1978.

Table 1. Analysis of the Idealized Model-Results Obtained From Method I Under 1 Condition

t & t + $\Delta t$ AT WHICH EQUATIONS ARE SOLVED FOR $\omega_n(t)$ & $\xi(t)$ , (SEC)	TIME SEGMENTS (SEC)	NUMBER OF RECORDS USED	$\bar{\omega}_n$ (RPS)	$\bar{\xi}$	VARIANCE OF $\omega_n$	VARIANCE OF $\xi$
t & t + 0.1	0 TO 14	577	2.700	.022	8.373	1.012
	14 TO 28	701	1.998	.050	.005	.001
	28 TO 42	700	1.990	.050	.049	.016
	42 TO 56	695	1.986	.057	.155	.149
t & t + 0.2	0 TO 14	604	2.309	.101	1.330	3.264
	14 TO 28	701	1.999	.050	.001	.000
	28 TO 42	701	1.996	.050	.012	.004
	42 TO 56	700	1.992	.056	.038	.023
t & t + 0.3	0 TO 14	624	2.187	.036	.858	.689
	14 TO 28	701	1.999	.050	.001	.000
	28 TO 42	701	1.998	.050	.005	.002
	42 TO 56	701	1.997	.056	.023	.027
t & t + 0.4	0 TO 14	625	2.207	.013	.993	.546
	14 TO 28	701	1.999	.050	.000	.000
	28 TO 42	701	1.999	.050	.003	.001
	42 TO 56	699	2.001	.056	.019	.018
t & t + 0.5	0 TO 14	625	2.158	.036	.638	.343
	14 TO 28	701	1.999	.050	.000	.000
	28 TO 42	701	1.999	.050	.002	.001
	42 TO 56	701	1.996	.049	.011	.004
t & t + 0.6	0 TO 14	630	2.234	.003	5.060	.538
	14 TO 28	701	2.000	.050	.000	.000
	28 TO 42	701	1.999	.050	.002	.001
	42 TO 56	700	1.999	.050	.011	.002
t & t + 0.7	0 TO 14	640	2.090	.058	.440	.267
	14 TO 28	701	1.999	.050	.000	.000
	28 TO 42	701	1.999	.050	.001	.001
	42 TO 56	698	2.001	.050	.017	.002

Table 1. Analysis of the Idealized Model-Results Obtained From Method I Under 1 Condition (Continued)

t & t + $\Delta t$ AT WHICH EQUATIONS ARE SOLVED FOR $\omega_n(t)$ & $\xi(t)$ , (SEC)	TIME SEGMENTS (SEC)	NUMBER OF RECORDS USED	$\bar{\omega}_n$ (RPS)	$\bar{\xi}$	VARIANCE OF $\omega_n$	VARIANCE OF $\xi$
t & t + 0.8	0 TO 14	628	3.835	-.138	1716.780	13.037
	14 TO 28	701	1.999	.050	.000	.000
	28 TO 42	701	1.999	.050	.001	.001
	42 TO 56	696	2.010	.048	.068	.005
t & t + 0.9	0 TO 14	620	2.155	.069	.641	.707
	14 TO 28	701	2.000	.050	.000	.000
	28 TO 42	701	1.999	.050	.001	.001
	42 TO 56	696	2.006	.050	.049	.008
t & t + 1.0	0 TO 14	609	2.217	.013	.987	.380
	14 TO 28	701	1.999	.050	.000	.000
	28 TO 42	701	1.999	.050	.002	.001
	42 TO 56	686	2.011	.050	.061	.021

Table 2. Comparison of Results of the Idealized Model Under Different Conditions by Using Method I and  $\Delta t = 0.7$  Seconds.

CONDITIONS	TIME SEGMENTS (SEC)	NUMBER OF RECORDS USED	$\bar{\omega}_n$ (RPS)	$\bar{\xi}$	VARIANCE OF $\omega_n$	VARIANCE OF $\xi$
UNDER 1 CONDITION	0 TO 14	640	2.090	.059	.440	.267
	14 TO 28	701	1.999	.050	.000	.000
	28 TO 42	701	1.999	.050	.001	.001
	42 TO 56	698	2.001	.050	.017	.002
UNDER 2 CONDITIONS	0 TO 14	569	2.043	.055	.295	.126
	14 TO 28	701	1.999	.050	.000	.000
	28 TO 42	701	1.999	.050	.001	.001
	42 TO 56	267	1.998	.050	.003	.001
UNDER 2 CONDITIONS W/MORE RESTRICTED DENOMINATOR	0 TO 14	399	1.986	.063	.116	.050
	14 TO 28	701	1.999	.050	.000	.000
	28 TO 42	409	1.999	.050	.001	.000
	42 TO 56	0	-	-	-	-

Table 3. Analysis of Union Bank Data - Distribution of Natural Frequency Obtained from Method I Under 1 Condition.

$\omega_n$ (RPS)	<	0.95 TO	1.05 TO	1.15 TO	1.25 TO	1.35 TO	1.45 TO	1.55 TO	1.65 TO	1.75 TO	1.85 TO	1.95 TO	>
NUMBER	26	23	16	29	36	29	30	17	11	4	6	6	27

Table 4. Comparison of Results of Union Bank Data From Method I Under Different Conditions.

CONDITIONS	TIME SEGMENTS (SEC)	NO. OF RECORDS USED	$\bar{\omega}_n$ (RPS)	$\bar{\xi}$	VARIANCE OF $\omega_n$	VARIANCE OF $\xi$
UNDER 1 CONDITION	0 TO 14	53	2.605	-.189	2.746	1.469
	14 TO 28	70	1.323	.080	.033	.015
	28 TO 42	70	1.302	.083	.062	.059
	42 TO 56	67	1.246	.072	.114	.107
UNDER 2 CONDITIONS	0 TO 14	41	2.356	.017	2.017	.732
	14 TO 28	70	1.323	.080	.033	.015
	28 TO 42	70	1.302	.083	.062	.039
	42 TO 56	61	1.217	.088	.098	.102
UNDER 3 CONDITIONS	0 TO 14	41	2.356	.017	2.017	.732
	14 TO 28	70	1.323	.080	.033	.015
	28 TO 42	70	1.302	.085	.062	.058
	42 TO 56	61	1.217	.084	.098	.105

Table 5. Comparison of Results of Union Bank Data Obtained From Method II Under Different Conditions.

TIME SEGMENTS (SEC)	UNDER NO CONDITIONS		UNDER 1 CONDITION (CONDITION a)		UNDER 1 CONDITION (CONDITION b)	
	$\omega_n$ (RPS)	$\xi$	$\omega_n$ (RPS)	$\xi$	$\omega_n$ (RPS)	$\xi$
0 TO 14	1.441	0.154	1.566	0.182	1.437	0.151
14 TO 28	1.344	0.090	1.344	0.090	1.344	0.090
28 TO 42	1.250	0.085	1.250	0.085	1.250	0.085
42 TO 56	1.312	0.113	1.339	0.115	1.283	0.106

Table 6. Comparison of Analytical Results of Union Bank Data Obtained at Different Methods.

METHOD I UNDER 2 CONDITIONS			METHOD II UNDER 1 CONDITION		MODAL MINIMIZATION METHOD BY BECK {4}	
TIME SEGMENTS (SEC)	$\bar{\omega}_n$ (RPS)	$\bar{\xi}$	$\omega_n$ (RPS)	$\xi$	TIME SEGMENTS (SEC)	$\omega_n$ (RPS)
0 TO 14	2.356	0.017	1.437	0.151	5 TO 15	1.425
14 TO 28	1.323	0.080	1.344	0.090	10 TO 20	1.372
28 TO 42	1.302	0.083	1.250	0.085	15 TO 25	1.354
42 TO 56	1.217	0.088	1.283	0.106	20 TO 30	1.331

Table 7. Results of JPL Building 180 Under Different Conditions by Using Method I and  $\Delta t = 0.4$  Seconds.

CONDITIONS	TIME SEGMENTS (SEC)	NUMBER OF RECORDS USED	$\omega_n$ (RPS)	$\xi$	VARIANCE OF $\omega_n$	VARIANCE OF $\xi$
UNDER 1 CONDITION	0 TO 12	48	6.048	.520	6.275	3.112
	12 TO 24	59	5.087	.227	.434	.014
	24 TO 36	58	4.087	.245	1.105	.046
	36 TO 47	48	5.594	.636	16.311	6.422
UNDER 2 CONDITIONS	0 TO 12	43	5.843	.548	6.295	3.445
	12 TO 24	59	5.087	.227	.434	.014
	24 TO 36	58	5.087	.245	1.105	.046
	36 TO 47	13	4.598	.261	1.220	.068
UNDER 2 CONDITIONS WITH MORE RESTRICTED DENOMINATOR	0 TO 12	32	5.594	.222	4.577	.495
	12 TO 24	59	5.087	.227	.434	.014
	24 TO 36	18	5.004	.240	.154	.005
	36 TO 47	0	-	-	-	-

Table 8. Results of JPL Building 180 Under Different Conditions by Using Method II.

TIME SEGMENTS (SEC)	UNDER NO CONDITIONS		UNDER 1 CONDITION	
	$\bar{\omega}_n$ (RPS)	$\bar{\xi}$	$\omega_n$ (RPS)	$\xi$
0 TO 12	5.435	0.170	5.436	0.170
12 TO 24	4.893	0.221	4.893	0.221
24 TO 36	4.976	0.238	4.981	0.234
36 TO 48	3.877	0.179	4.942	0.048

Table 9. Comparison of Analytical Results of  
JPL Building 180 Data.

METHOD I UNDER 2 CONDITIONS			METHOD II UNDER 1 CONDITION		MODAL MINIMIZATION METHOD BY BECK {4}	
TIME SEGMENTS (SEC)	$\bar{\omega}_n$ (RPS)	$\bar{\xi}$	$\omega_n$ (RPS)	$\xi$	TIME SEGMENTS (SEC)	$\omega_n$ (RPS)
0 TO 12	5.594	0.222	5.436	0.170	0 TO 10	5.108
12 TO 24	5.087	0.227	4.893	0.221	10 TO 20	4.947
24 TO 36	5.004	0.240	4.981	0.234	-	-

Table 10. Comparison of the Natural Frequency of Nonlinear Model I [27] Obtained in the Beginning of Each Hysteretic Cycle at Different Methods.

TIME $t_i$ IN THE BEGINNING OF EACH CYCLE (SEC)	PERIOD OF EACH CYCLE (SEC)	$\omega_n(t_i)$ OBTAINED FROM METHOD I (RPS)	$\omega_n(t_i)$ OBTAINED FROM THE SLOPE OF FIGURE 3.1 (RPS)
.03	-	16.43	11.73
.64	.61	17.74	11.73
1.19	.55	12.36	11.73
1.81	.61	12.24	11.73
2.36	.55	10.77	11.71
2.95	.60	11.01	11.69
3.45	.49	11.70	11.73
4.08	.63	11.40	11.73
4.65	.58	11.91	11.73
5.22	.57	10.31	11.69
5.82	.60	10.79	11.70
6.39	.57	10.03	11.73
6.93	.54	10.10	11.73
7.45	.52	11.11	11.73
7.99	.54	10.86	11.73
8.54	.55	10.12	11.73
9.05	.52	10.80	11.73
9.54	.49	10.65	11.73
10.05	.51	11.12	11.73
10.61	.56	10.68	11.73
11.17	.56	10.49	11.73
11.67	.50	10.59	11.73
12.17	.50	11.58	11.73
12.76	.60	10.67	11.69
13.36	.59	10.91	11.72
13.94	.58	10.72	11.72
14.49	.55	11.01	11.73
15.07	.58	8.87	11.73
15.55	.49	11.75	11.73
16.08	.53	11.11	11.73
16.61	.53	10.98	11.73
17.14	.53	10.55	11.73
17.70	.56	8.03	11.73

Table 11. Results of Nonlinear Model I Under Different Conditions by Using Method I and  $\Delta t = 0.1$  Seconds

CONDITIONS	TIME SEGMENTS (SEC)	NUMBER OF RECORDS USED	$\bar{\omega}_n$ (RPS)	$\bar{\xi}$	VARIANCE OF $\omega_n$	VARIANCE OF $\xi$
UNDER 1 CONDITION	.0 TO 4.3	411	12.198	.029	15.936	.067
	4.3 TO 8.6	431	11.964	.030	4.447	.022
	8.6 TO 12.9	431	12.021	.029	3.249	.018
	12.9 TO 17.2	418	12.571	.031	13.787	.081
UNDER 2 CONDITIONS	.0 TO 4.3	282	11.500	.039	.748	.005
	4.3 TO 8.6	431	11.964	.030	4.447	.022
	8.6 TO 12.9	431	12.021	.029	3.249	.018
	12.9 TO 17.2	379	11.857	.023	3.976	.031
UNDER 2 CONDITIONS WITH MORE RESTRICTED DENOMINATOR	.0 TO 4.3	251	11.457	.043	.806	.005
	4.3 TO 8.6	297	11.287	.042	1.299	.012
	8.6 TO 12.9	351	11.463	.024	1.942	.016
	12.9 TO 17.2	259	11.470	.021	1.598	.015

Table 12. Results of Nonlinear Model II [18] Obtained by Using Method I and  $\Delta t = 0.14$  Seconds at Each Run of Strong Excitation.

CONDITIONS	TIME SEGMENTS (SEC)	NUMBER OF RECORDS USED	$\bar{\omega}_n$ (RPS)	$\bar{\xi}$	VARIANCE OF $\omega_n$	VARIANCE OF $\xi$
RUN 1						
UNDER 1 CONDITION	0 TO 4	447	26.125	.001	565.998	.066
	4 TO 8	248	21.947	.007	653.206	4.200
	8 TO 12	389	22.096	-.003	630.891	.077
	12 TO 12	517	19.637	-.001	318.100	.010
UNDER 2 CONDITIONS	0 TO 4	220	17.753	.021	136.960	.035
	4 TO 8	245	19.899	.035	312.765	4.143
	8 TO 12	388	21.273	-.007	368.923	.072
	12 TO 16	517	19.637	-.001	318.100	.010
UNDER 3 CONDITIONS	0 TO 4	118	15.836	.085	94.848	.018
	4 TO 8	145	22.300	.255	432.085	.052
	8 TO 12	238	23.719	.154	413.474	.019
	12 TO 16	305	19.908	.052	235.571	.002
RUN 2						
UNDER 1 CONDITION	0 TO 4	498	25.525	.169	674.220	1.067
	4 TO 8	350	29.054	.016	13987.376	.790
	8 TO 12	152	12.533	.308	1244.892	2.759
	12 TO 16	346	15.624	-.082	426.650	.995
UNDER 2 CONDITIONS	0 TO 4	134	14.338	.100	83.384	.042
	4 TO 8	194	13.492	.143	65.194	1.220
	8 TO 12	151	9.712	.251	42.808	2.274
	12 TO 16	344	14.828	-.060	283.146	.885
UNDER 3 CONDITIONS	0 TO 4	112	14.498	.112	83.342	.006
	4 TO 8	61	17.178	.208	103.073	.068
	8 TO 12	89	10.401	.419	25.083	.061
	12 TO 16	138	15.630	.235	212.460	.027
RUN 3						
UNDER 1 CONDITION	0 TO 4	467	22.813	.005	717.566	.010
	4 TO 8	468	22.178	.120	1109.408	.359
	8 TO 12	250	16.865	.061	855.664	3.686
	12 TO 16	403	16.256	.077	396.454	2.415
UNDER 2 CONDITIONS	0 TO 4	384	14.777	.001	81.354	.008
	4 TO 8	395	15.604	.134	88.169	.413
	8 TO 12	249	15.384	.136	310.733	2.318
	12 TO 16	402	15.553	.051	197.987	2.158

Table 12. Results of Nonlinear Model II [18] Obtained by Using Method I and  $\Delta t = 0.14$  Seconds at Each Run of Strong Excitation.

CONDITIONS	TIME SEGMENTS (SEC)	NUMBER OF RECORDS USED	$\bar{\omega}_n$ (RPS)	$\bar{\xi}$	VARIANCE OF $\omega_n$	VARIANCE OF $\xi$
UNDER 3 CONDITIONS	0 TO 4	203	14.759	.051	83.887	.005
	4 TO 8	174	14.430	.108	68.037	.046
	8 TO 12	109	15.848	.438	358.543	.076
	12 TO 16	150	13.572	.447	54.584	.089

Table 13. Summary of Structural Period and Damage Ratio of Buildings Before, During, and After Real or Simulated Earthquake

STRUCTURE OR BUILDING NAME	FRAME TYPE	DIRECTION	PERIOD OF 1ST MODE (SEC)				DAMAGE COST RATIO (%)			REFER
			DURING EARTHQUAKE		PRE- EARTHQUAKE	POST- EARTHQUAKE	NONSTRUCTURAL	STRUCTURAL	TOTAL	
			INITIAL	FINAL						
UNION BANK	STEEL	TRANSVERSE	4.41	4.72	3.1	3.8	0.16	NONE	0.16	4,35
UPL BUILDING 180	STEEL	S82°E	1.23	1.27	.93	1.01	MINOR	NONE	-	4,35
TEST FRAME	STEEL		0.54		-	-	-	-	-	27
TEST STRUC- TURE	RC		0.50 (RUN 1)	0.71 (RUN 2)	0.31	0.34	MINOR	NONE	-	18
			0.71 (RUN 2)	0.91 (RUN 3)	0.34	0.43	EXTENSIVE	NONE	-	
			0.91 (RUN 3)		0.43	0.53	EXTENSIVE	MINOR	-	
BANK OF CALIFORNIA	RC	TRANSVERSE	1.33	2.5	-	1.7	NOTICEABLE	0.3	1.7	35
ORION HOLI- DAY INN	RC	TRANSVERSE	0.7	1.6	0.48	0.68	EXTENSIVE	0.15	11.0	35
MARENGO HOLIDAY INN	RC	TRANSVERSE	0.63	1.15	0.53	0.64	EXTENSIVE	0.2	7.0	35
BUNKER HILL TOWER	STEEL	TRANSVERSE	3.98		-	2.62	MINOR	NONE	-	35
KE VALLEY CENTER	STEEL	TRANSVERSE	3.43	2.98	-	-	0.08	NONE	0.08	35
MUIR MEDICAL CENTER	RC	TRANSVERSE	1.6		1.03	1.14	0.04	NONE	0.04	35
KAJIMA BLDG.	STEEL	TRANSVERSE	3.19	2.8	1.88	2.15	0.03	NONE	0.03	35
CERTIFIED LIFE BLDG.	RC	TRANSVERSE	1.08		0.81	0.90	0.07	NONE	1.0	35
SHERATON- UNIVERSAL HOTEL	RC	TRANSVERSE	2.22		1.26	1.5	0.03	NONE	0.03	35
1901 AVE OF THE STARS	STEEL	S44°W	3.6		2.45	2.72	MINOR	NONE	-	35

Table 14. Percent Change in Natural Frequency and Damage Ratio of Structures [4,18,27,35].

STRUCTURE OR BUILDING NAME	PERCENT DECREASE IN $\omega_n$ (%)		PERCENT DAMAGE (%)	
	FROM INITIAL TO FINAL DURING EARTH- QUAKE	FROM PRE- TO POST- EARTHQUAKE	STRUCTURAL	TOTAL
UNION BANK	6.6	18.4	0.	0.16
JPL BUILDING 180	3.2	7.9	0.	-
TEST STRUCTURE	-	8.8	0.	-
	-	20.9	0.	-
	-	18.9	MINOR	-
BANK OF CALIFORNIA	46.8	-	0.3	1.1
ORION HOLIDAY INN	56.2	29.4	0.15	11.0
MARENGO HOLIDAY INN	45.2	17.2	0.2	7.0
KB VALLEY CTR.	0.	-	0.	0.08
MUIR MEDICAL CENTER	-	9.7	0.	0.04
KAJIMA BUILDING	0.	12.6	0.	0.03
CERTIFIED LIFE BUILDING	-	10.0	0.	1.0
SHERATON- UNIVERSAL HOTEL	-	16.0	0.	0.03
1901 AVENUE OF THE STARS	-	9.9	0.	-

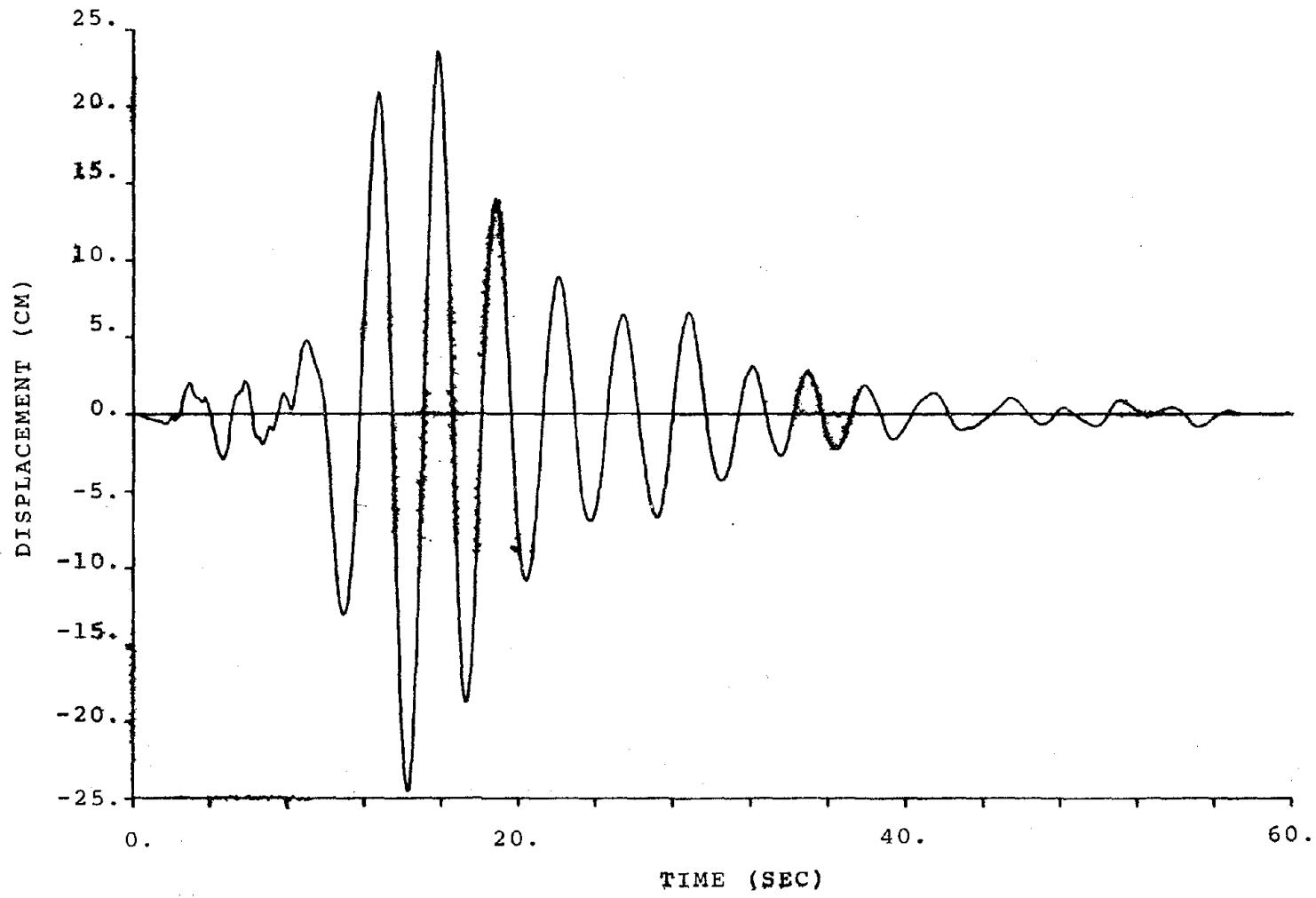


Figure 1. Relative Displacement Generated From an Idealized Model Subjected to a 1971 San Fernando Earthquake Acceleration Record.

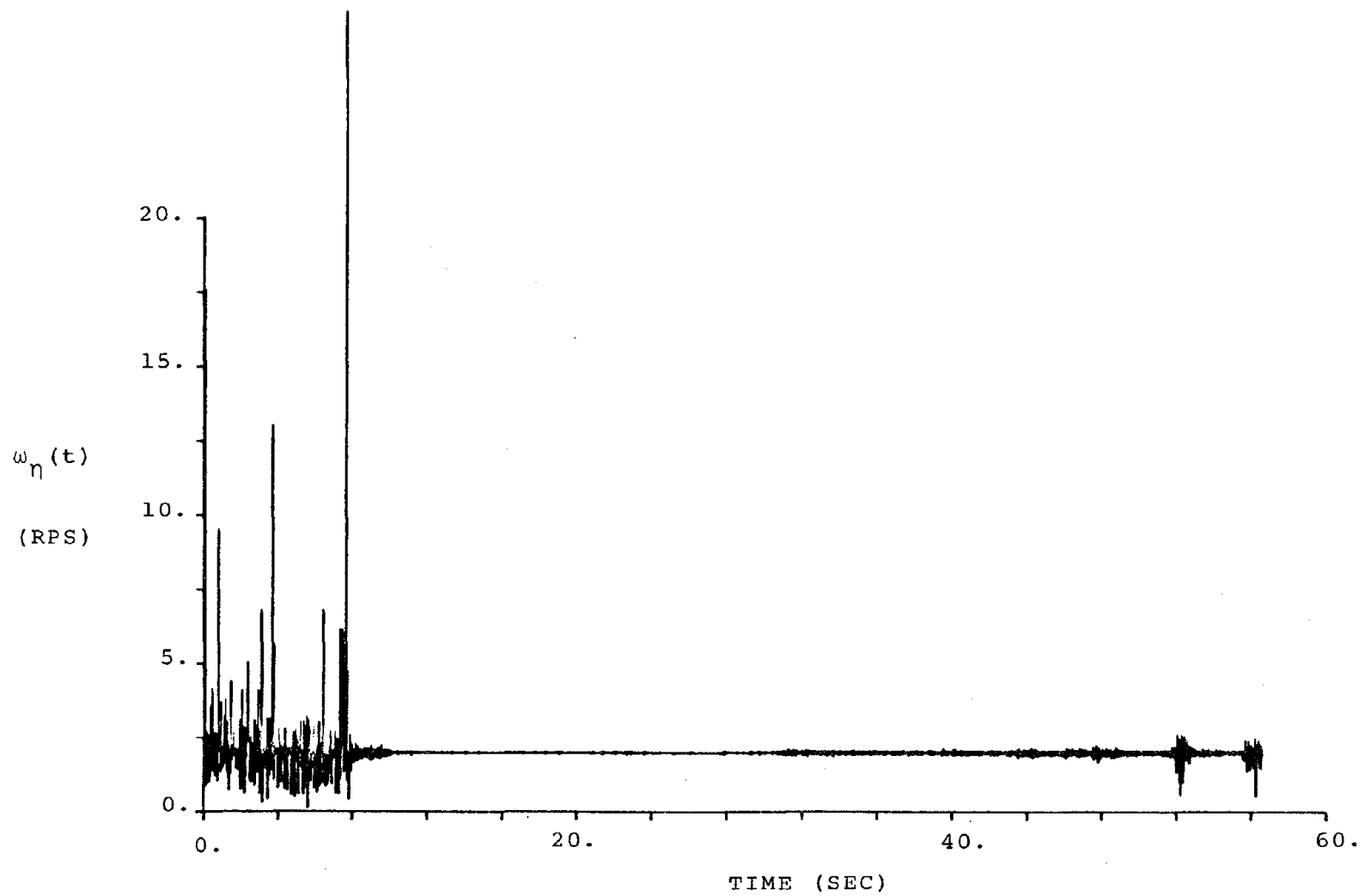


Figure 2. Natural Frequency Identified From the Data of Idealized Model Under No Conditions.

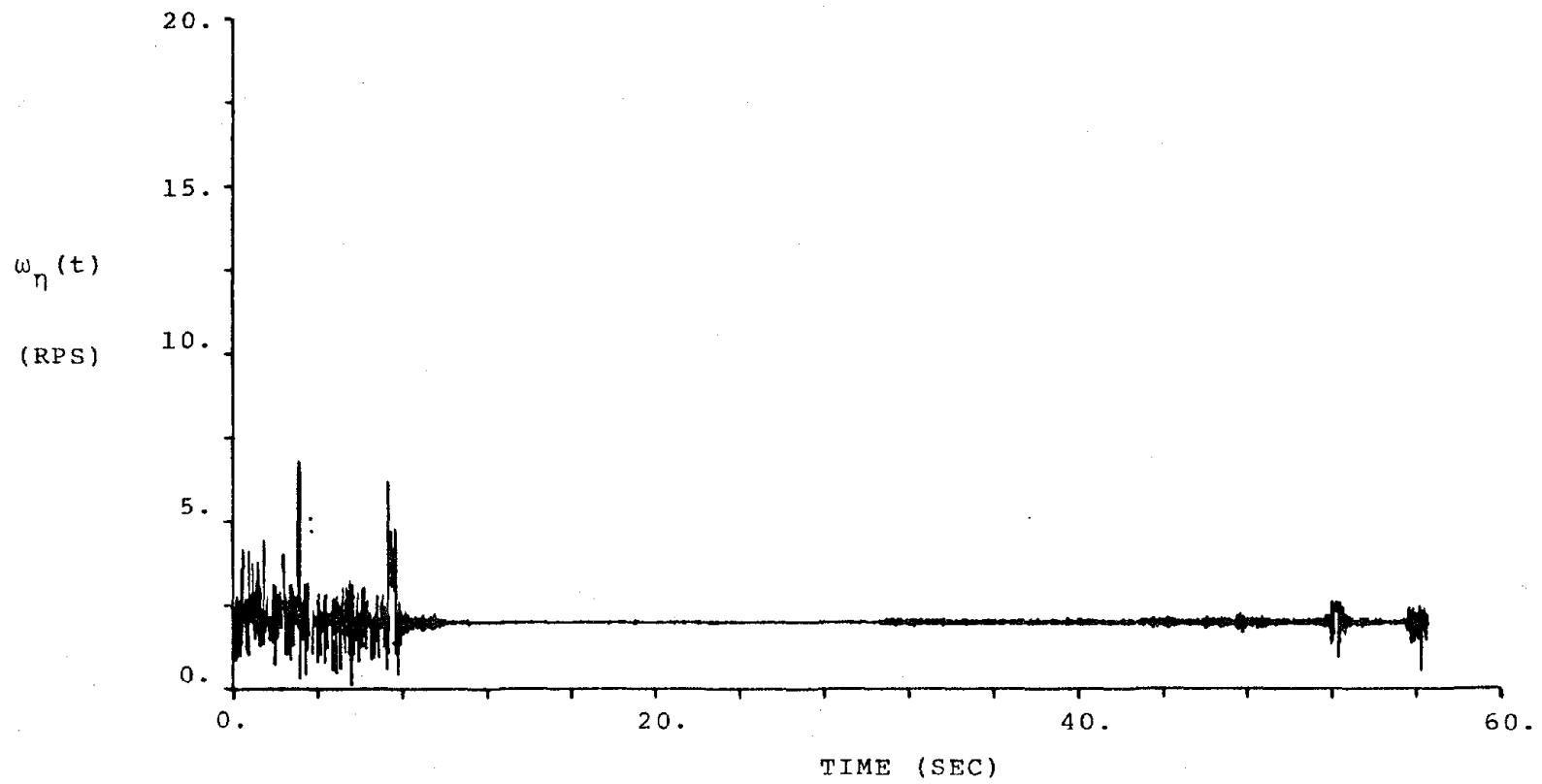


Figure 3. Natural Frequency Identified From the Data of Idealized Model Under One Condition.

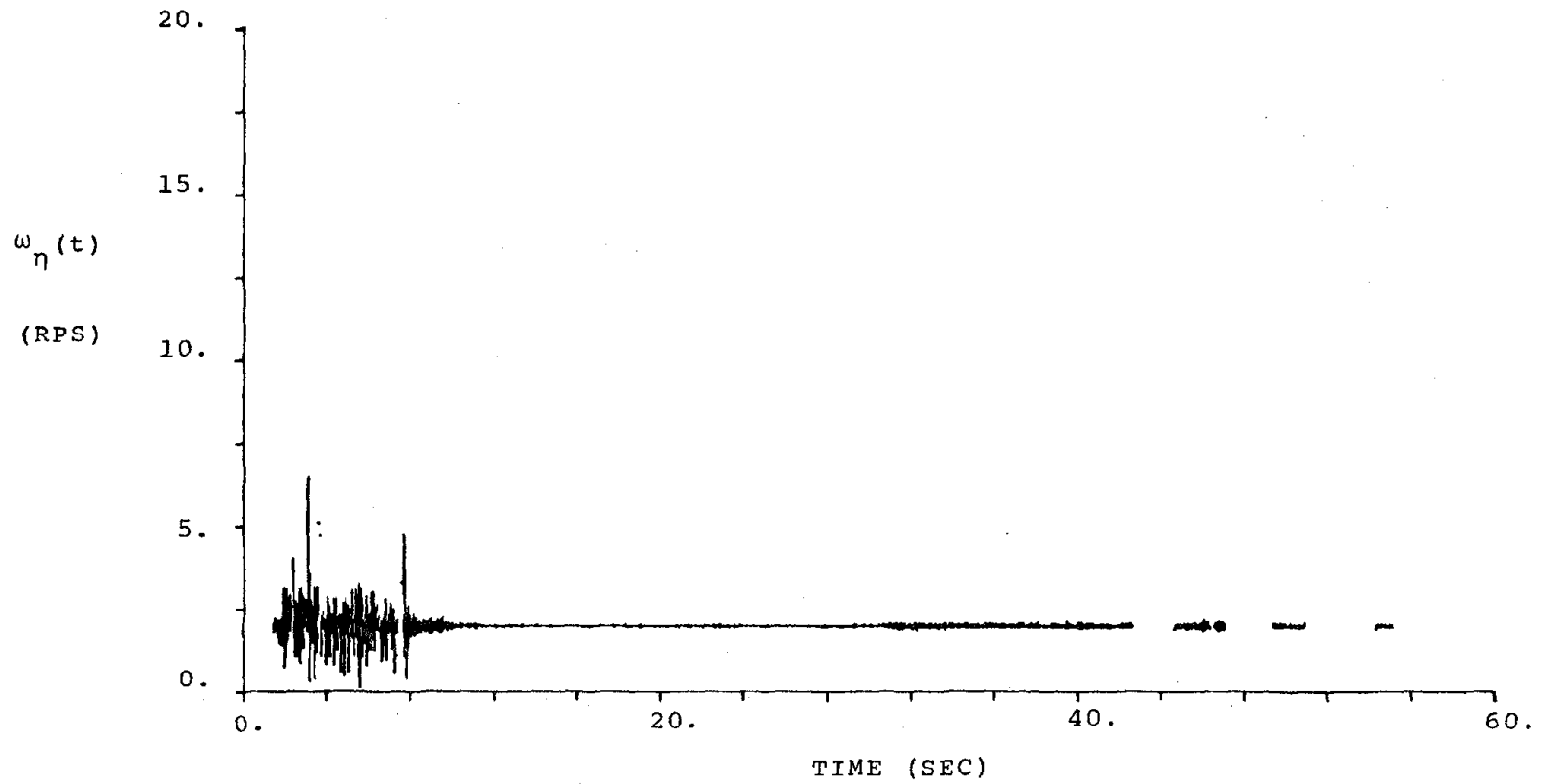


Figure 4. Natural Frequency Identified From the Data of Idealized Model Under Two Conditions.

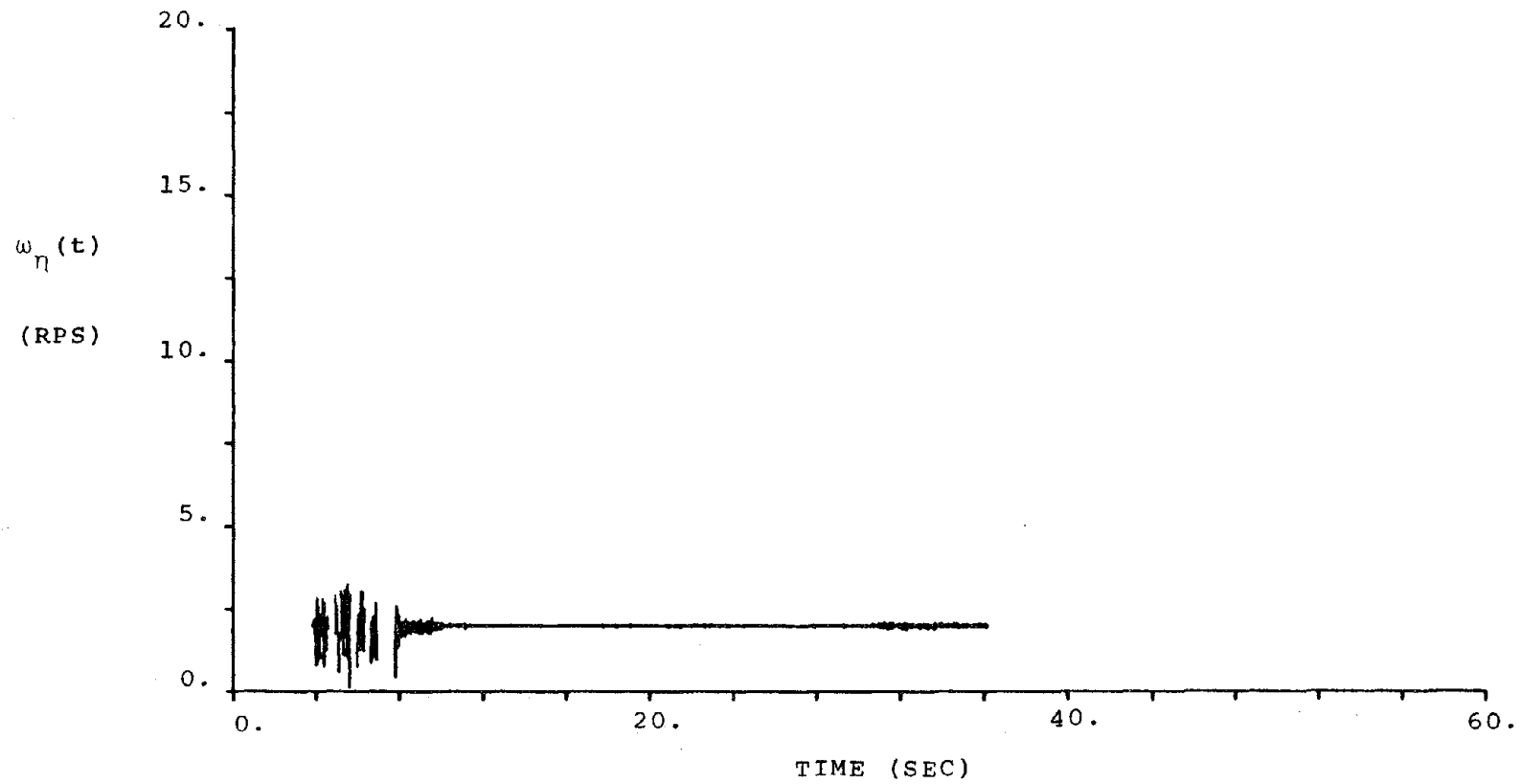


Figure 5. Natural Frequency Identified From the Data of Idealized Model Under Two Conditions with More Restricted Denominator.

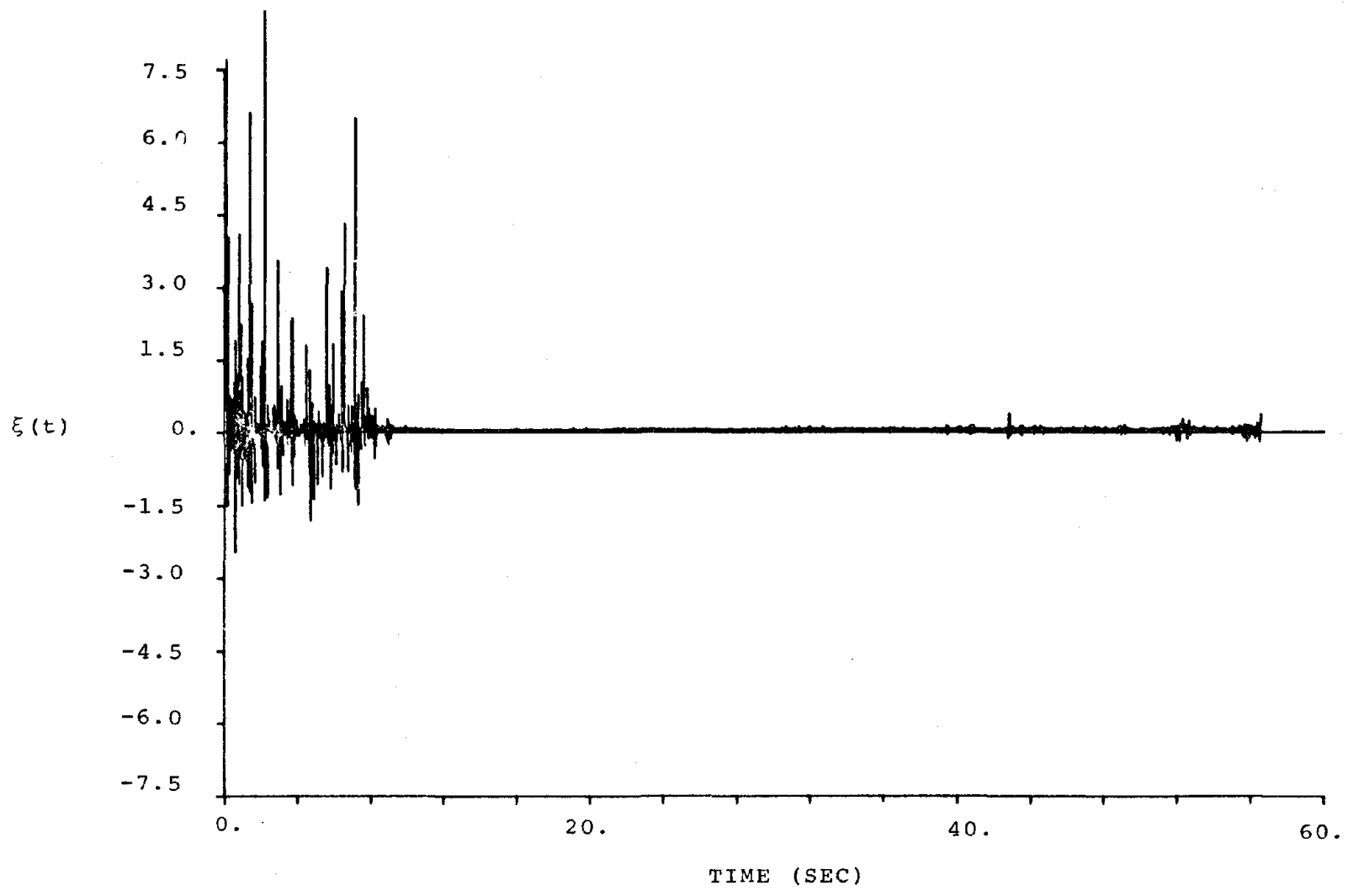


Figure 6. Damping Ratio Identified From the Data of Idealized Model and the Natural Frequency of Figure 2.

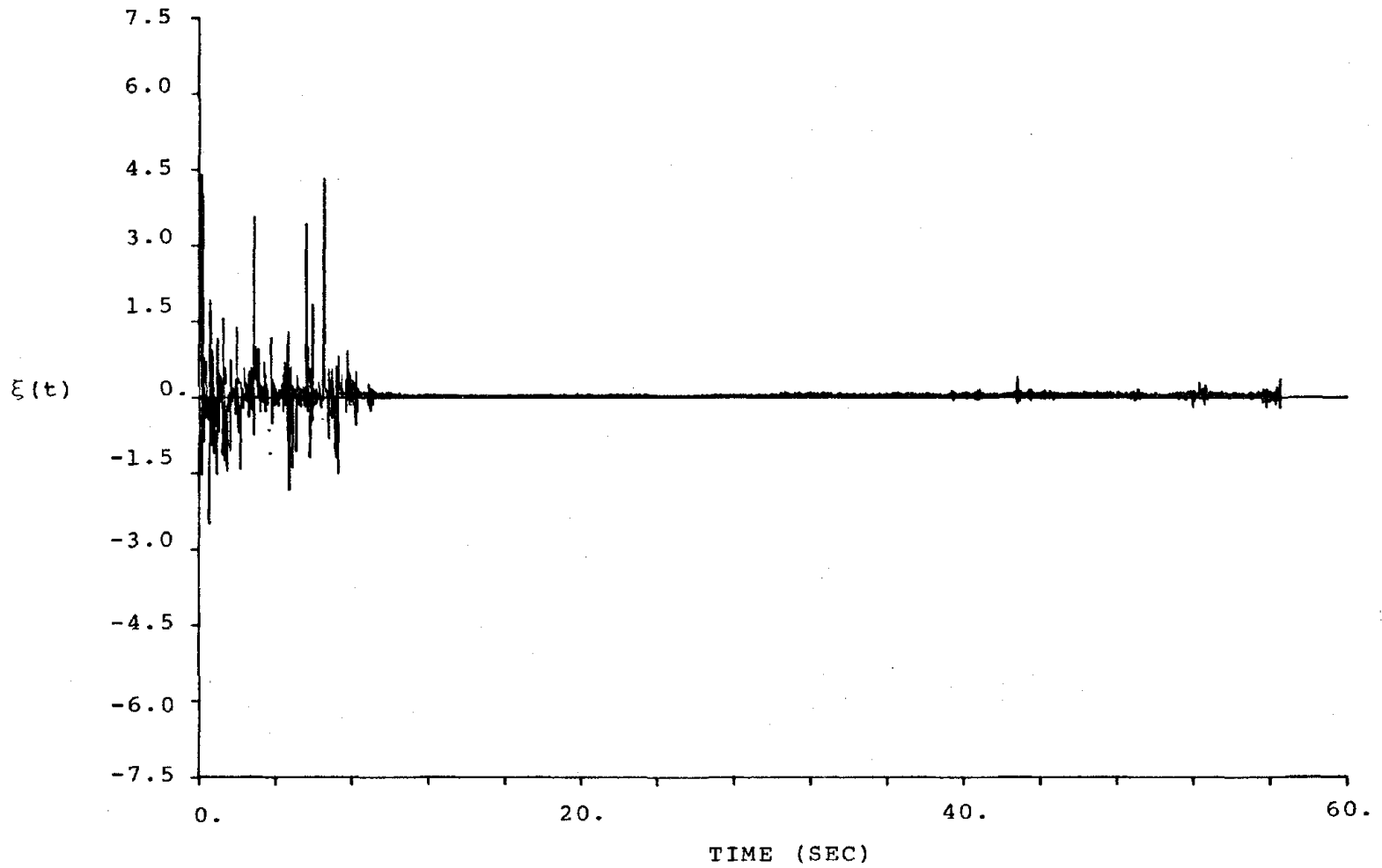


Figure 7. Damping Ratio Identified From the Data of Idealized Model and the Natural Frequency of Figure 3.

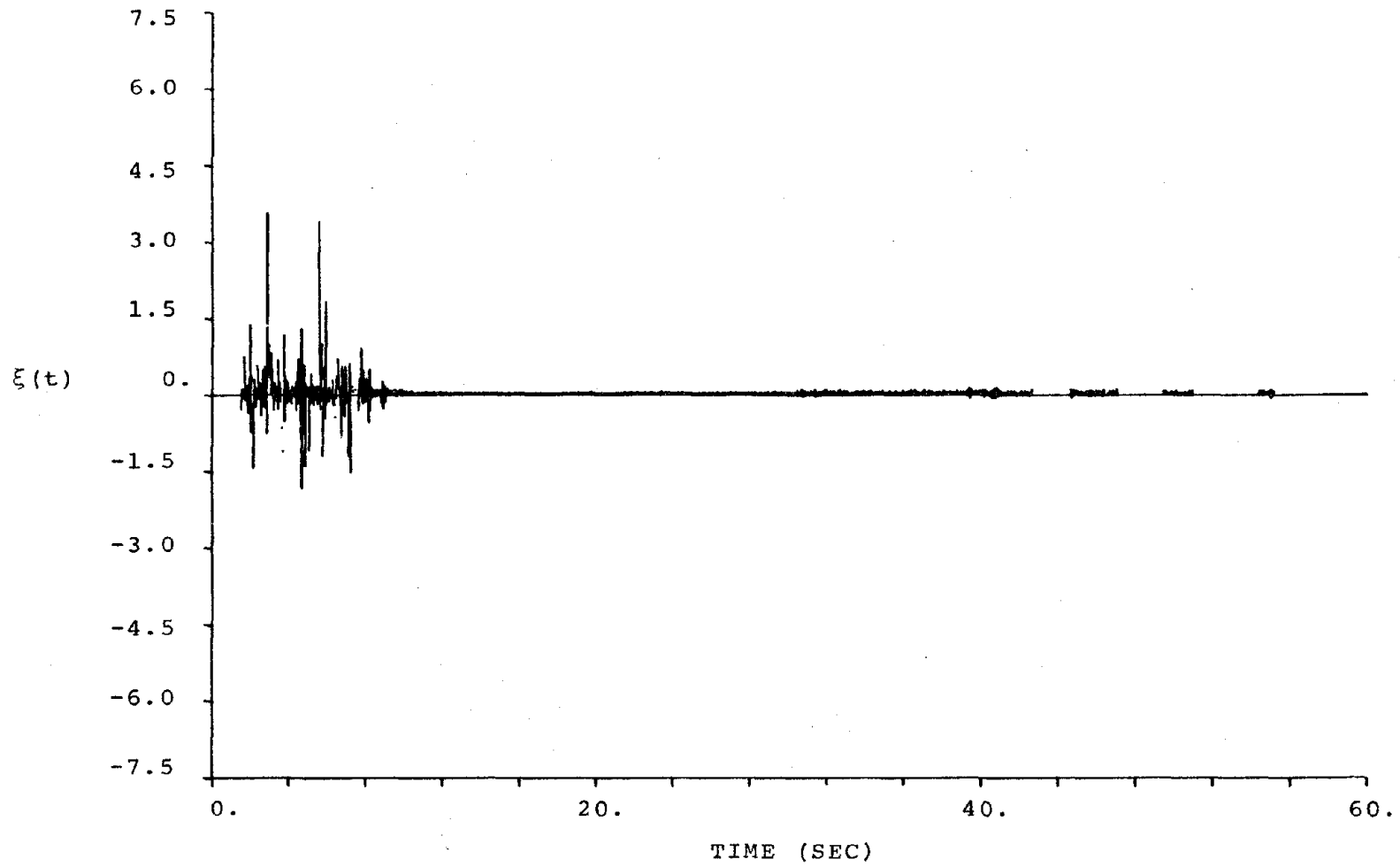


Figure 8. Damping Ratio Identified From the Data of Idealized Model and the Natural Frequency of Figure 4.

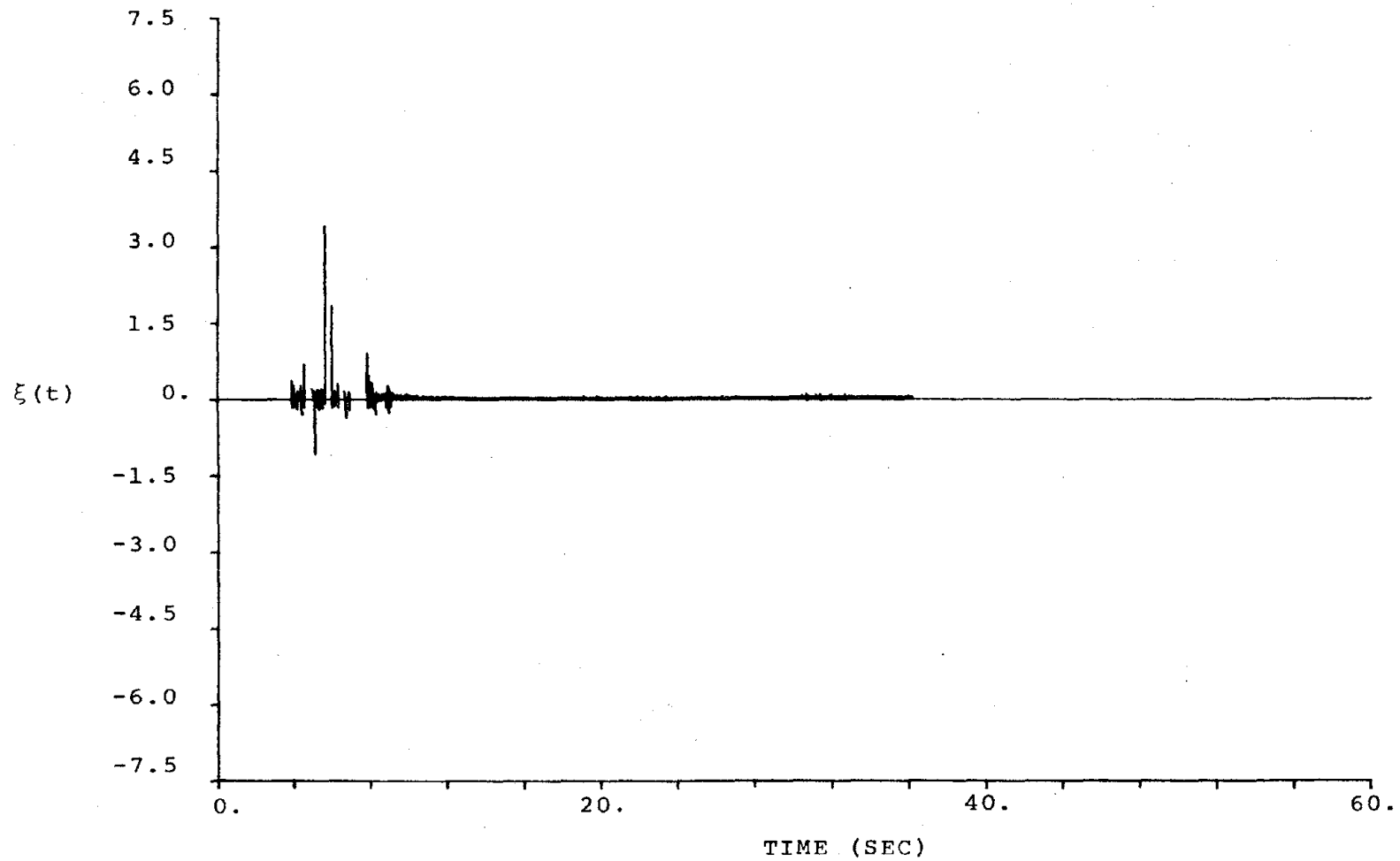


Figure 9. Damping Ratio Identified From the Data of Idealized Model and the Natural Frequency of Figure 5.

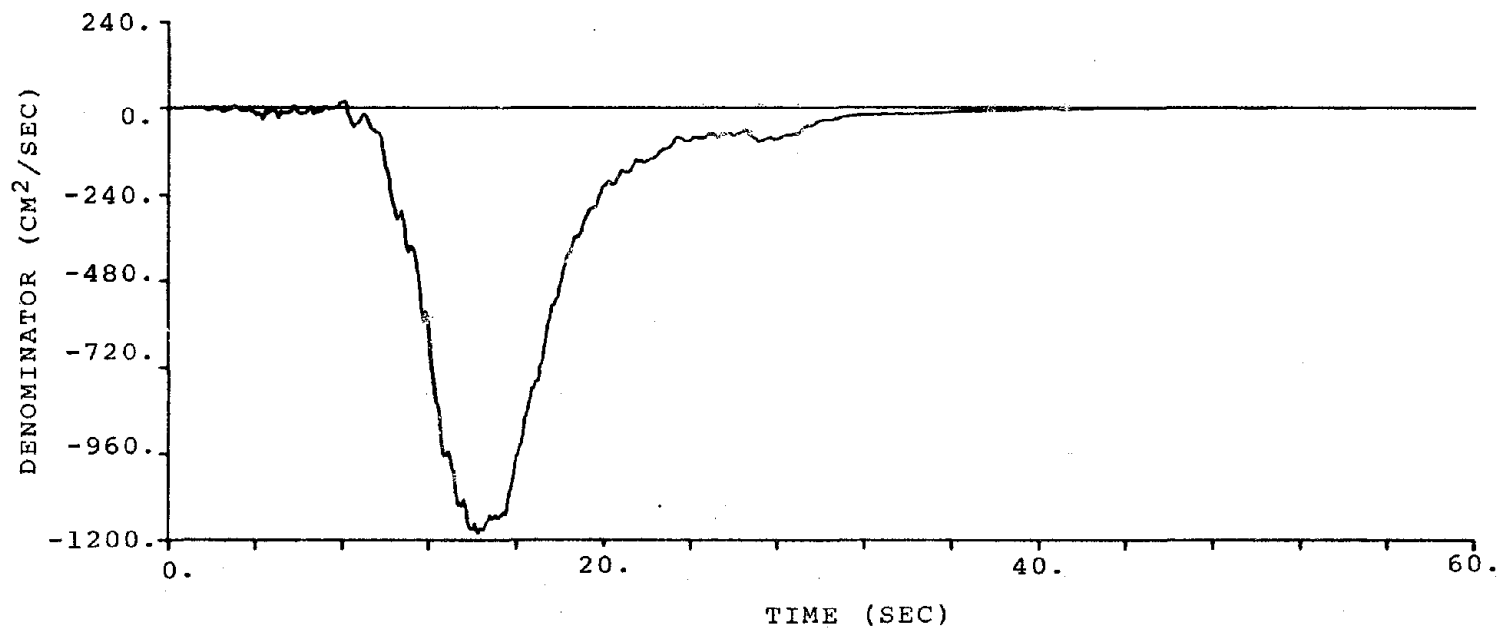


Figure 10. Denominator of Equation 11 Obtained From the Data of Idealized Model.

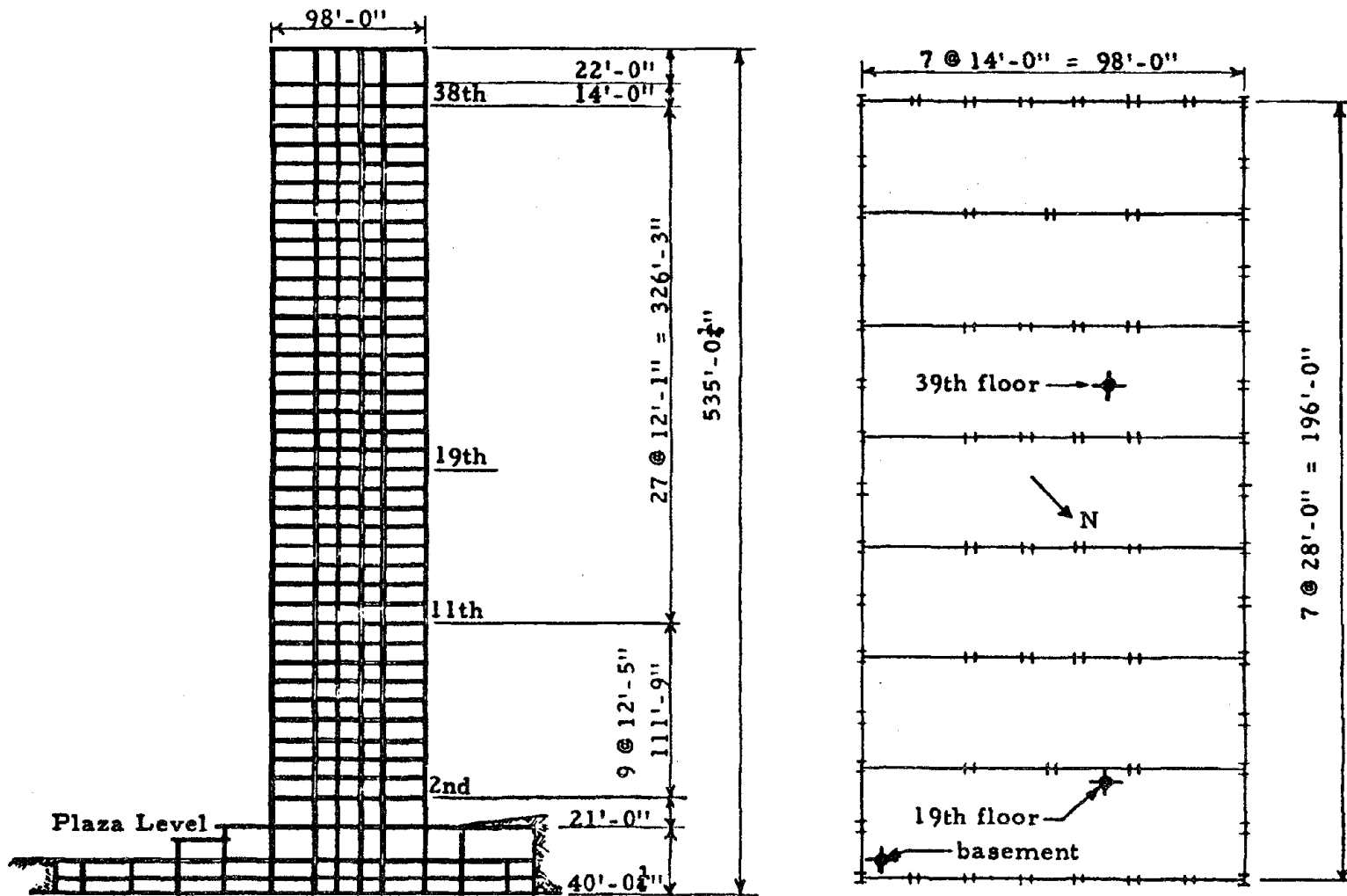


Figure 11. Transverse Section and Typical Floor Palm of Union Bank Building [4].  
 ◆ Location of accelerograph.

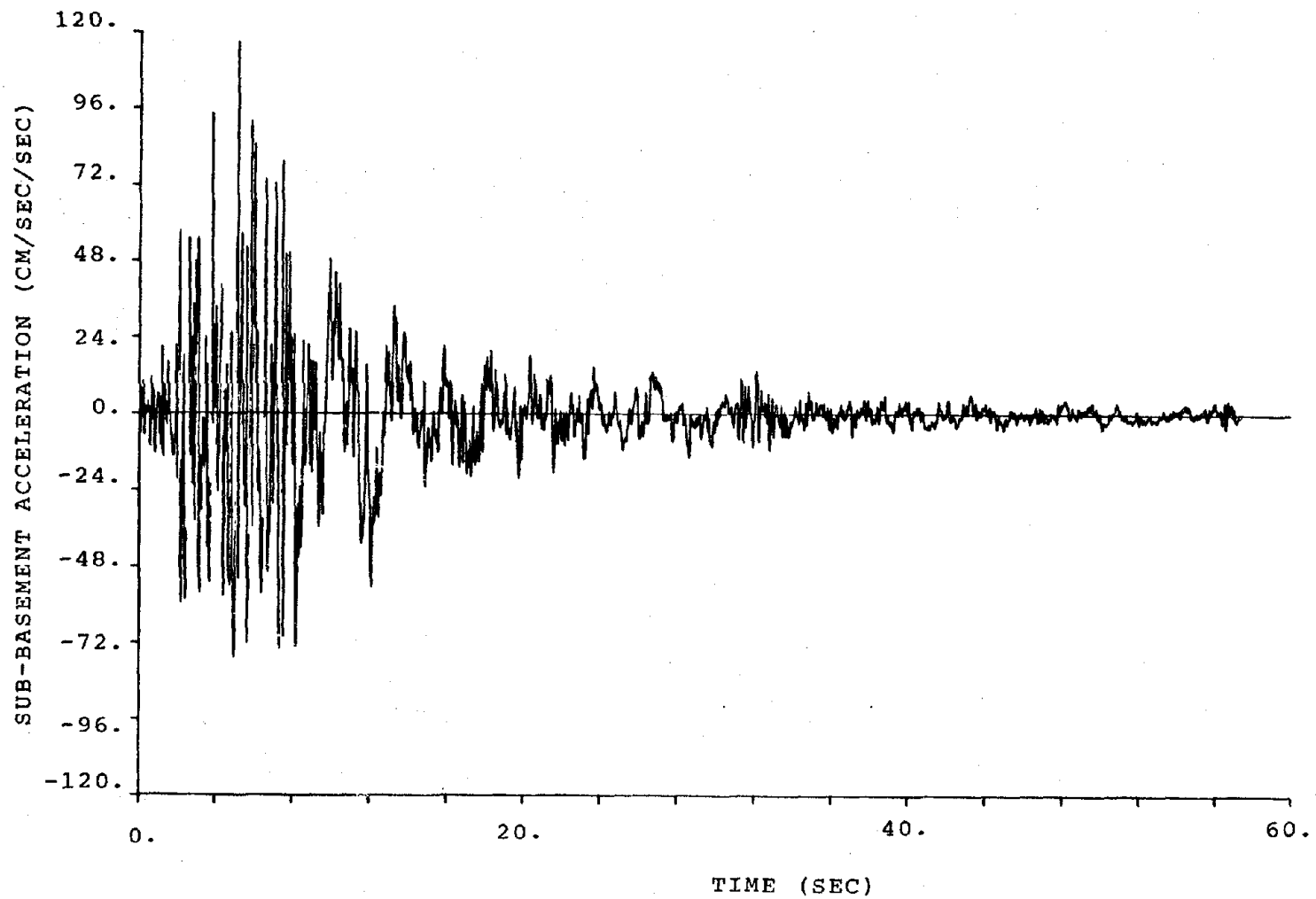


Figure 12. The Sub-basement Absolute Acceleration of Union Bank Building (1971 San Fernando Earthquake).

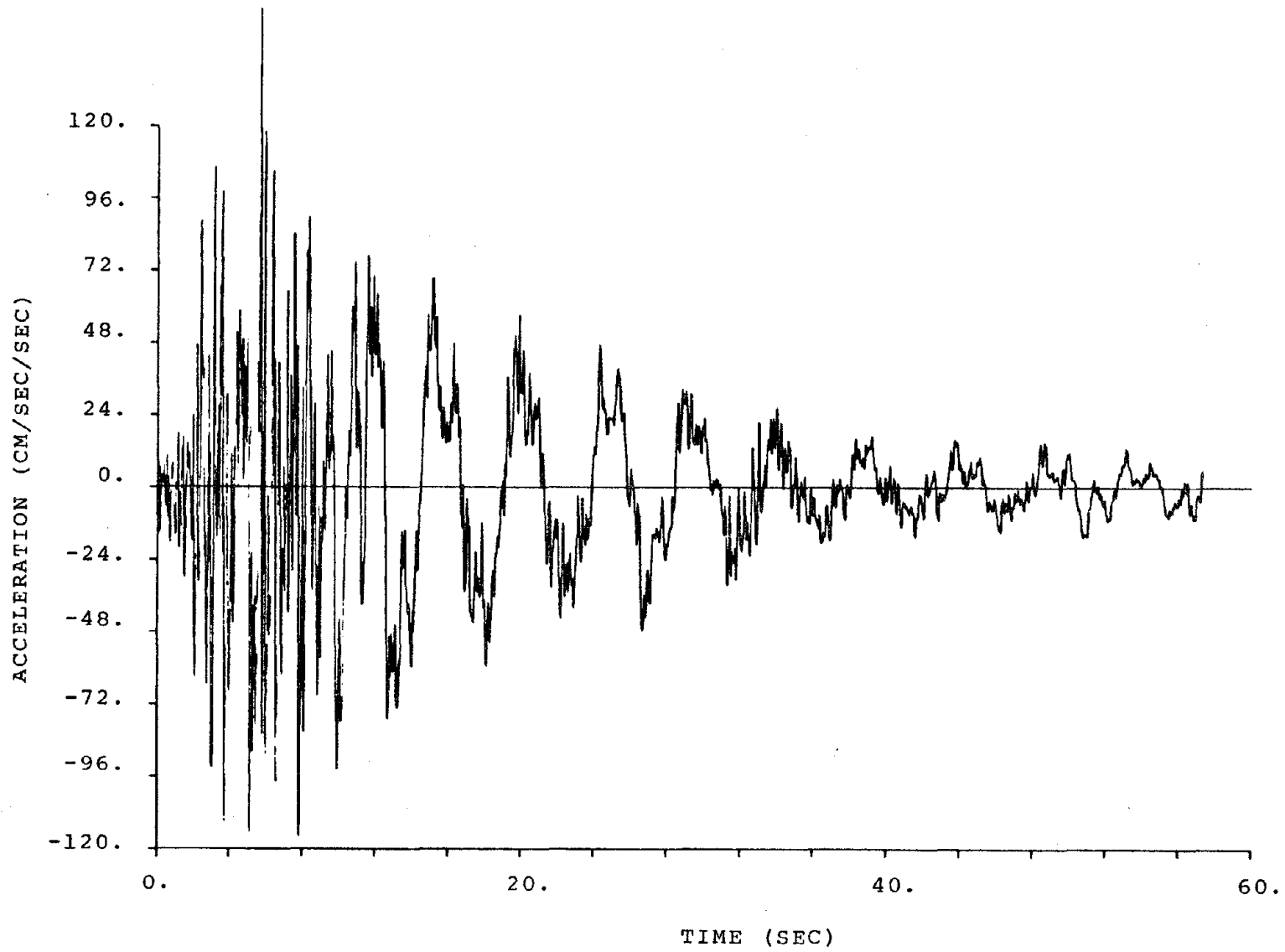


Figure 13. Relative Acceleration at the 19th Floor of Union Bank Building.

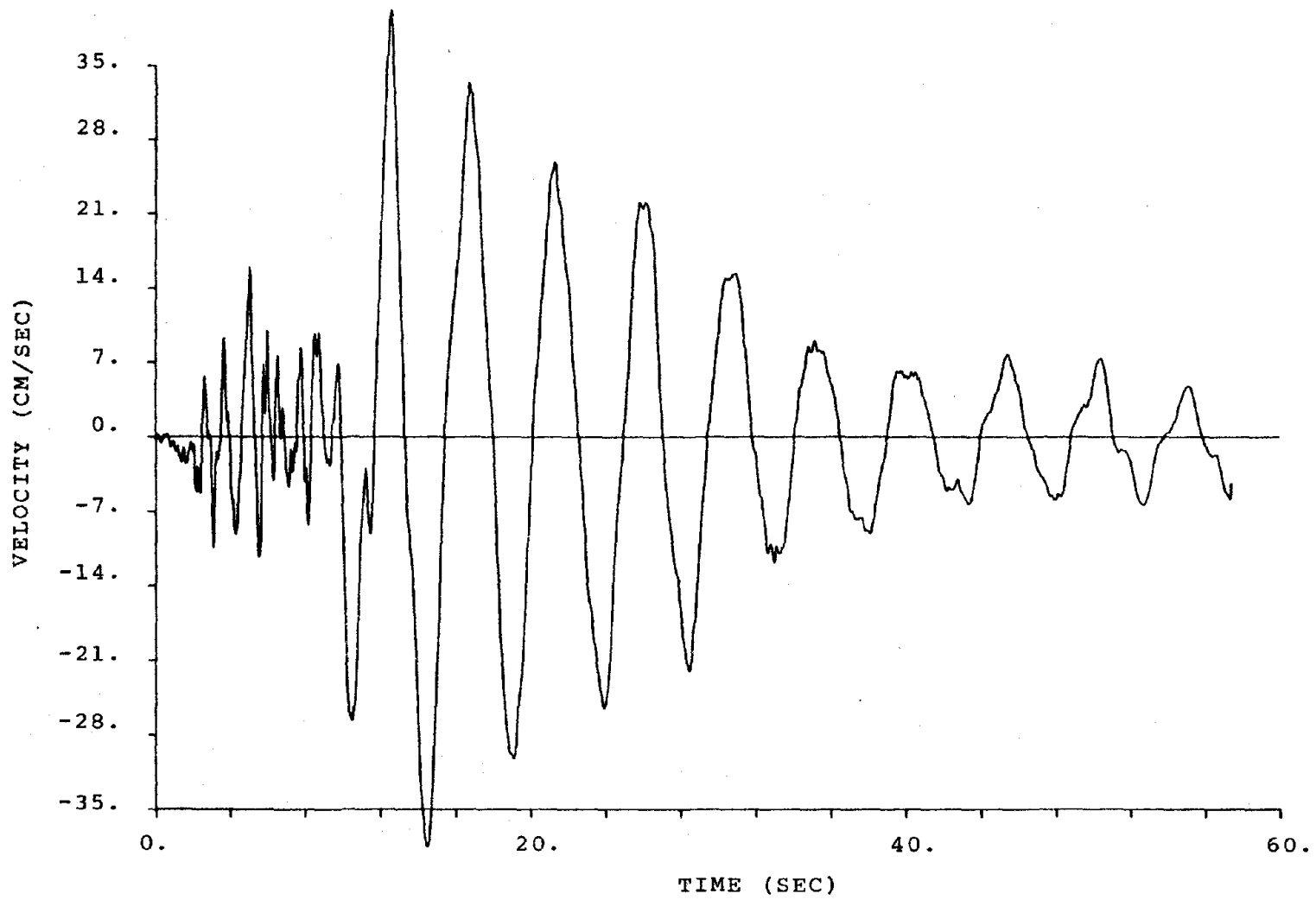


Figure 14. Relative Velocity at the 19th Floor of Union Bank Building.

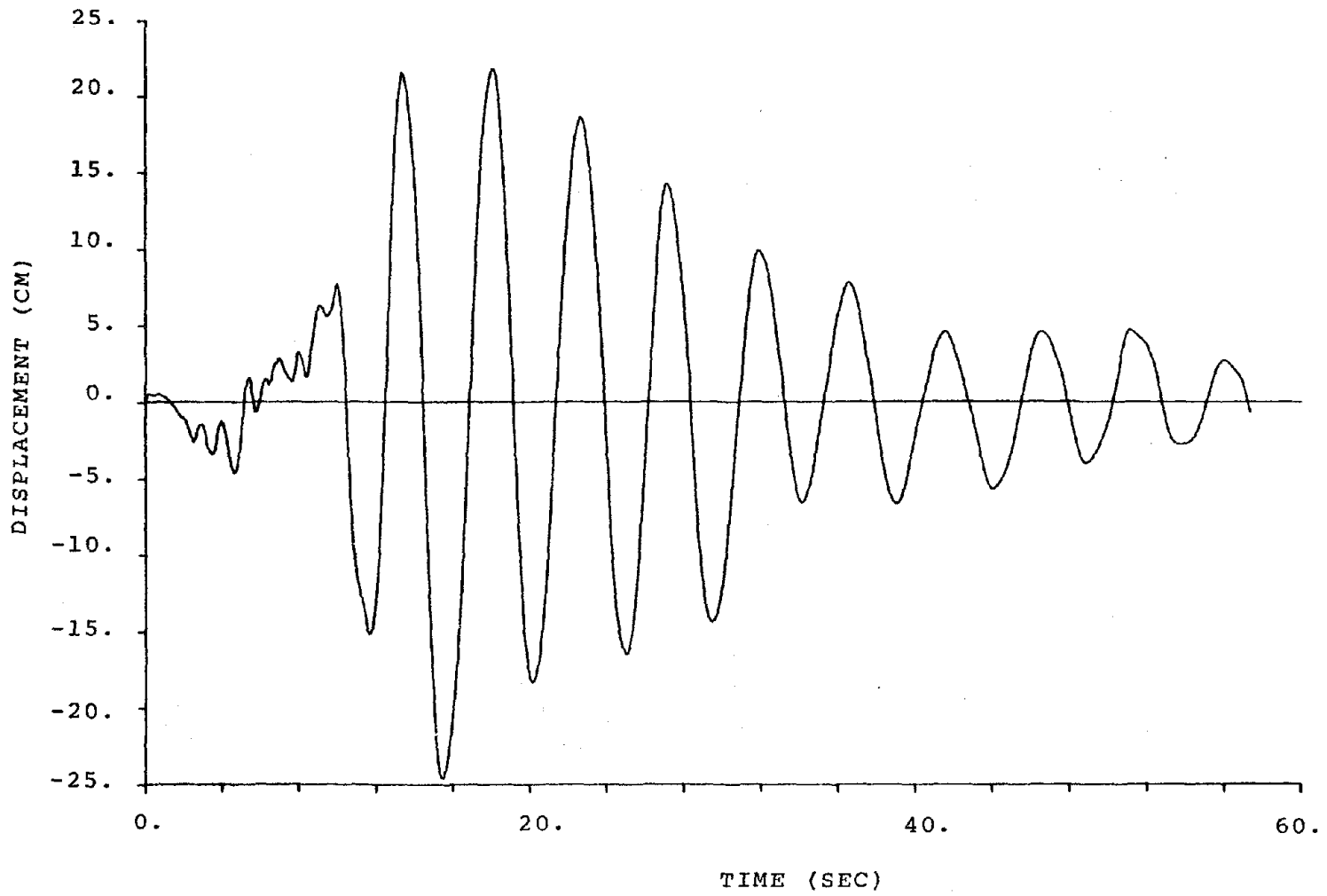


Figure 15. Relative Displacement at the 19th Floor of Union Bank Building.

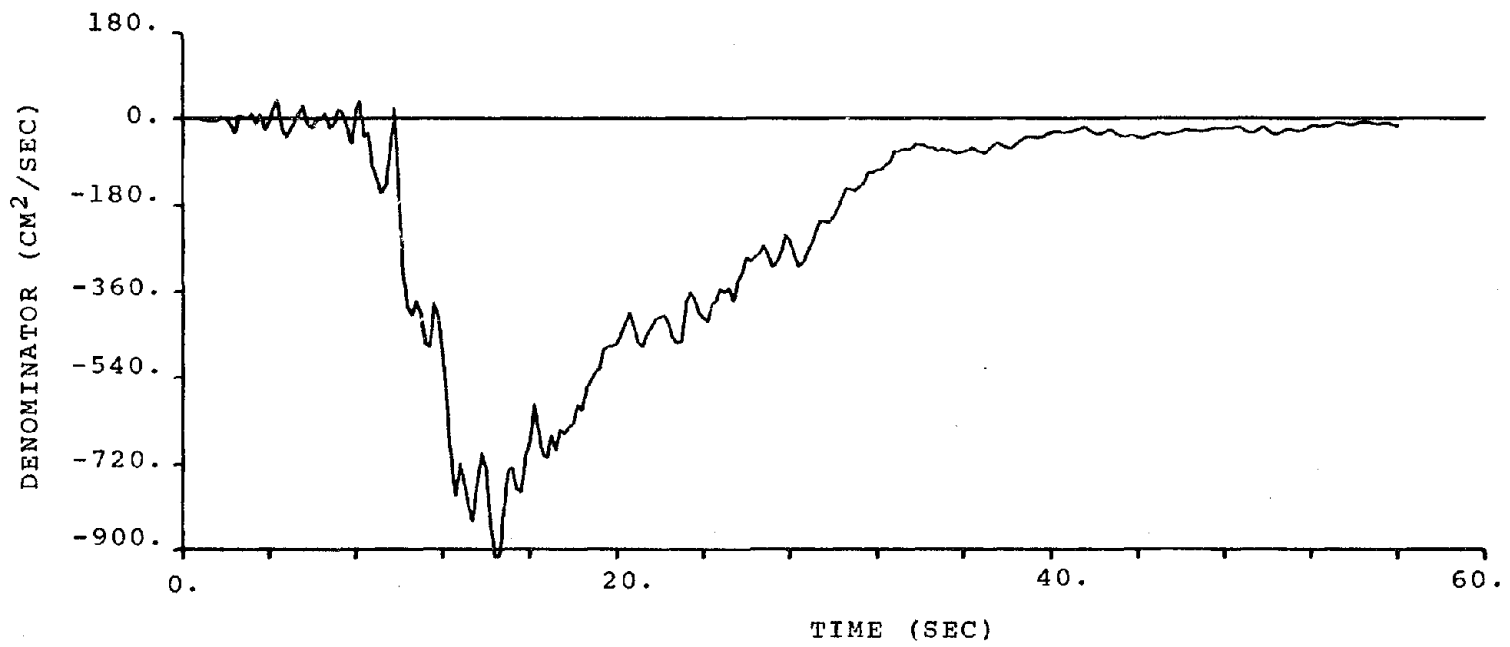


Figure 16. Denominator of Equation 11 Obtained from Union Bank Building.

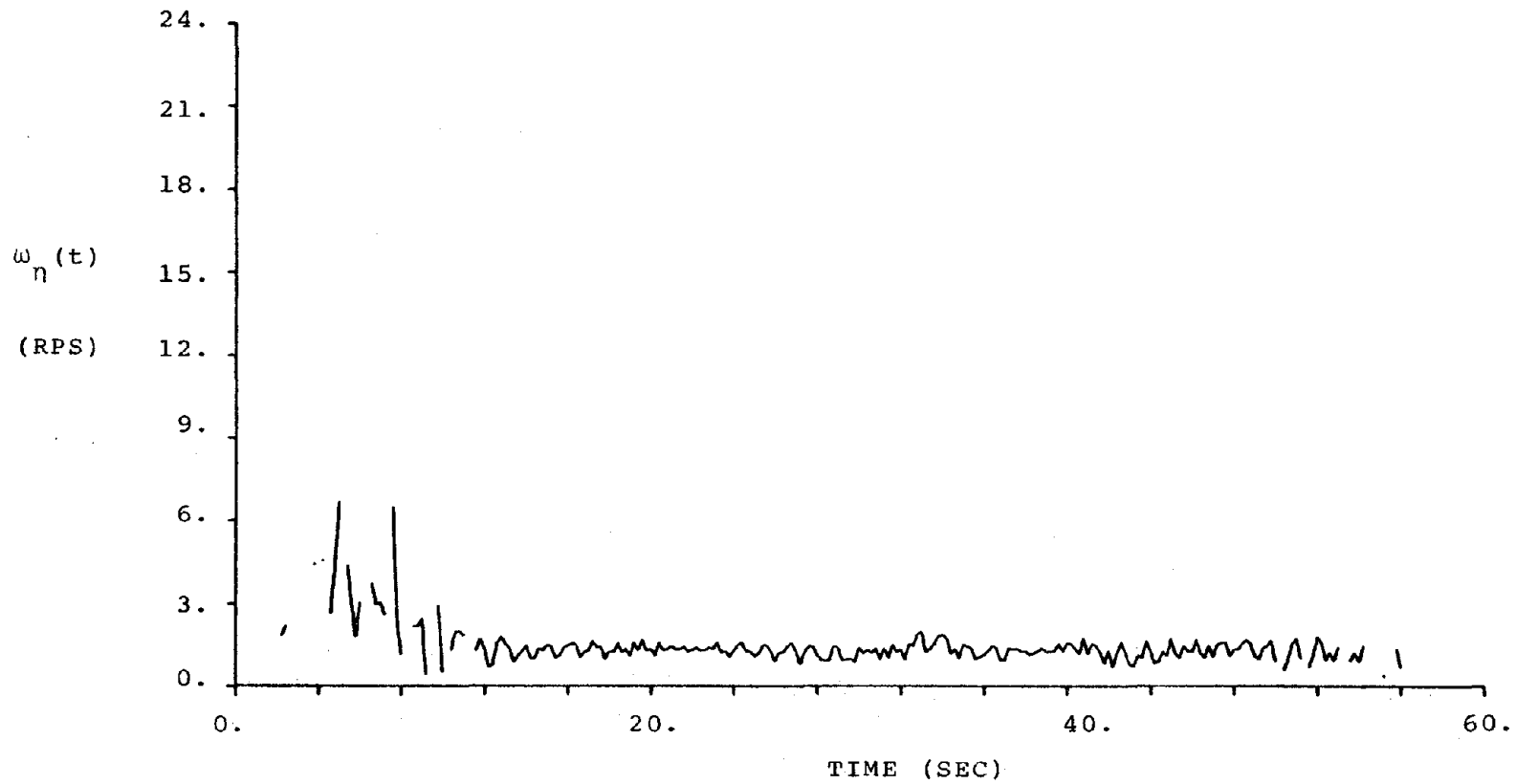


Figure 17. Natural Frequency Identified From Union Bank Data Under Two Conditions.

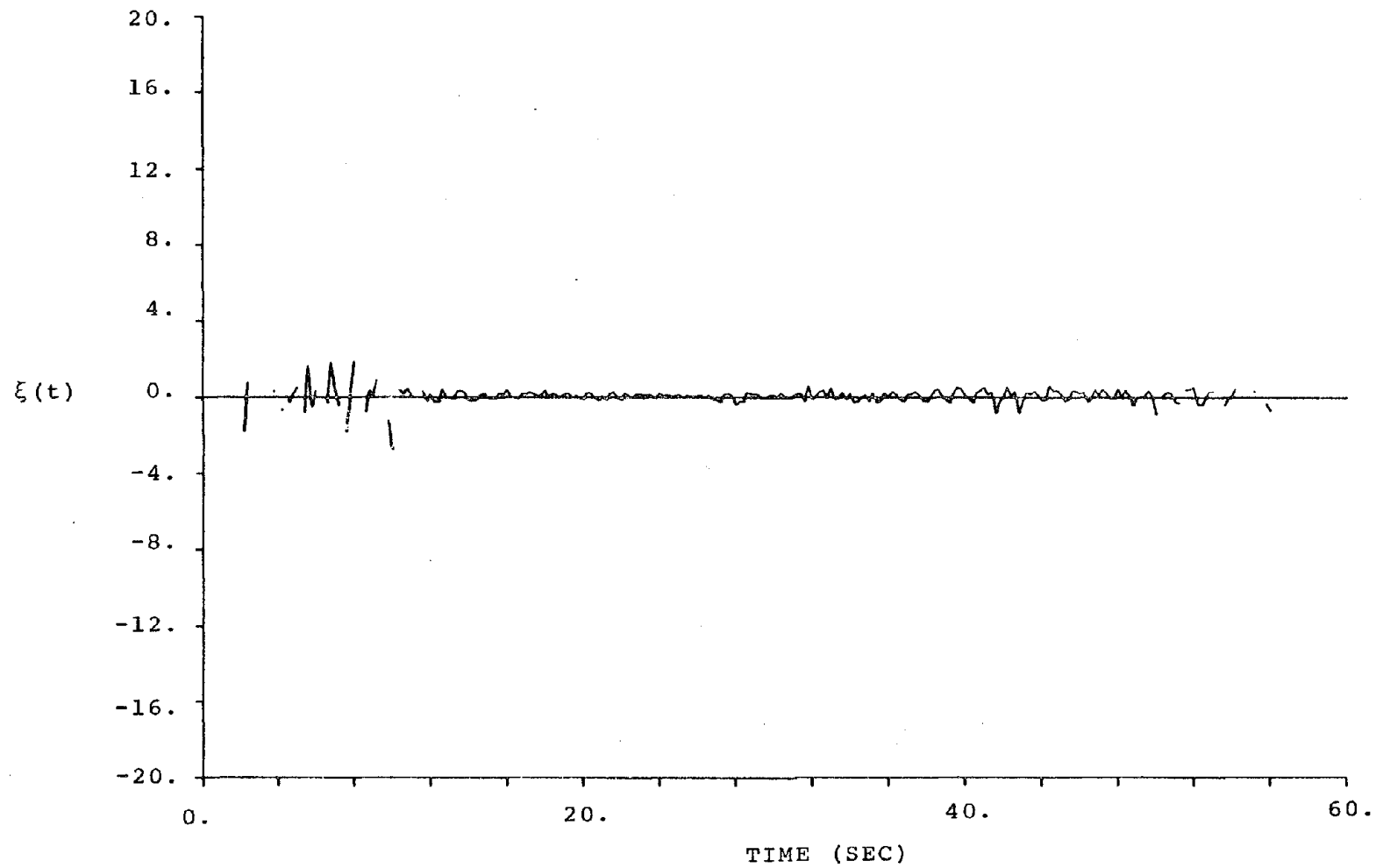


Figure 18. Damping Ratio Identified From Union Bank Data.

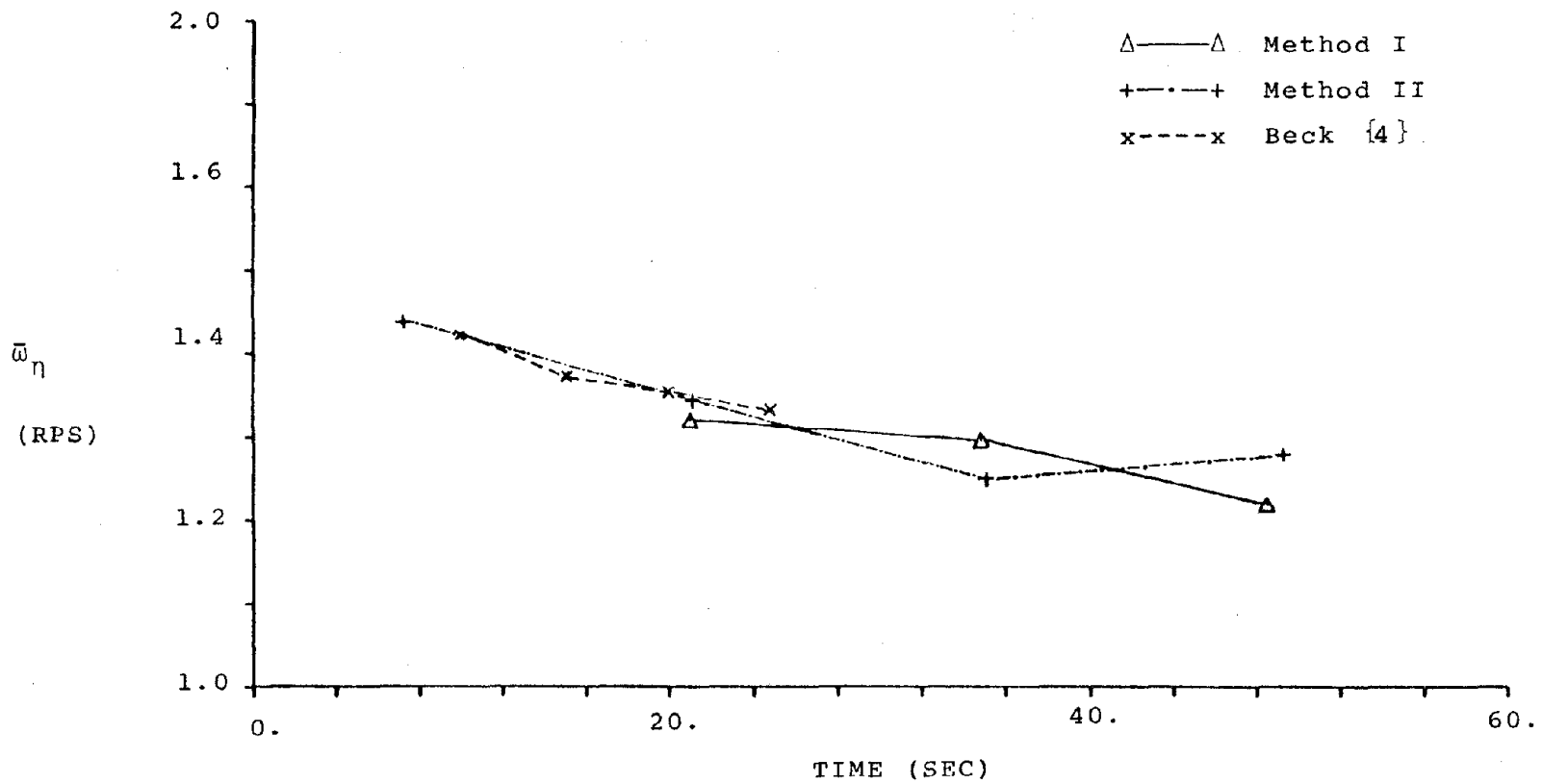


Figure 19. Comparison of the Natural Frequency Identified From Different Methods for Union Bank Building.

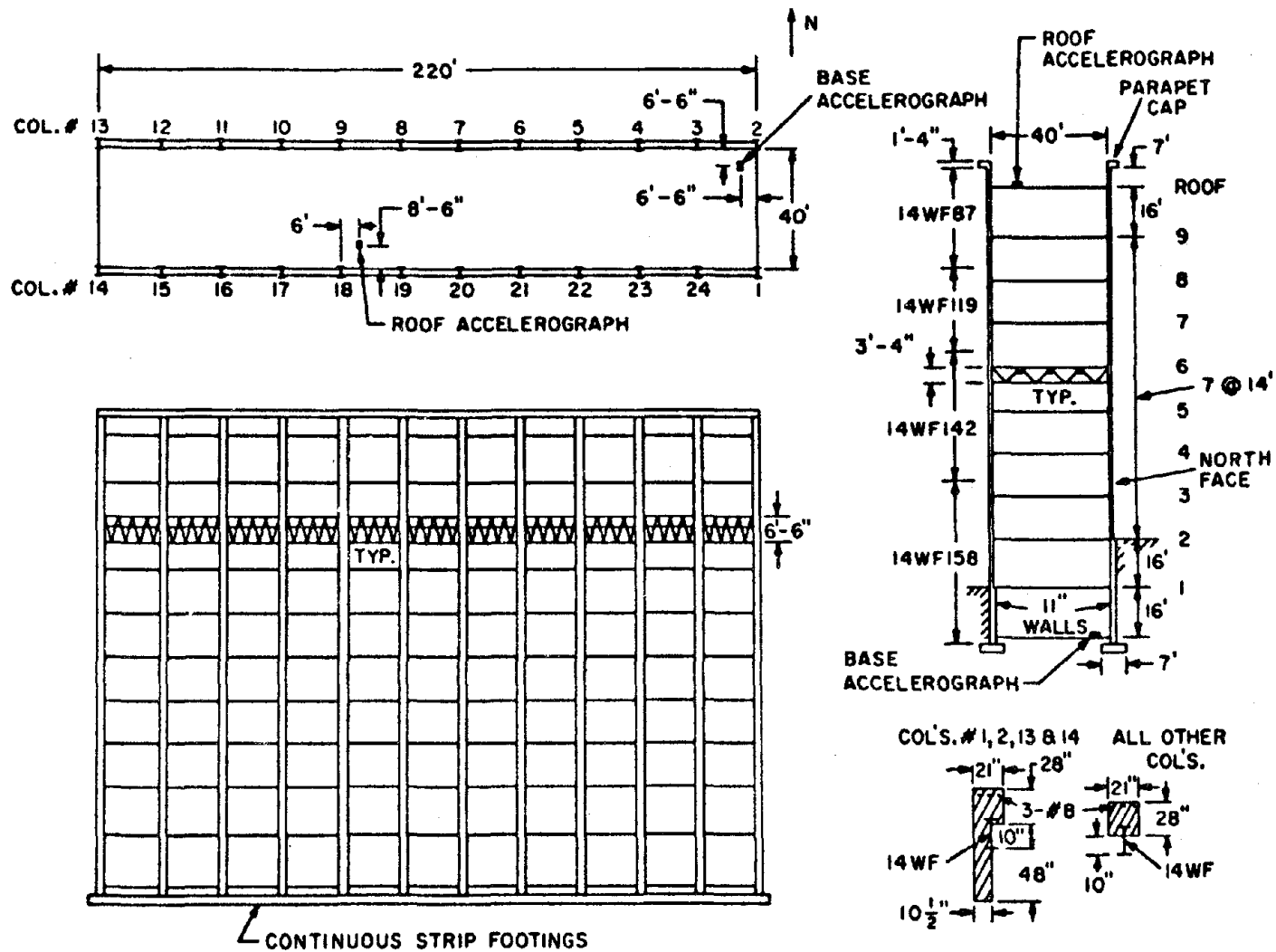


Figure 20. Typical Floor Plan and Longitudinal and Transverse Sections of JPL Building 180 {4}.

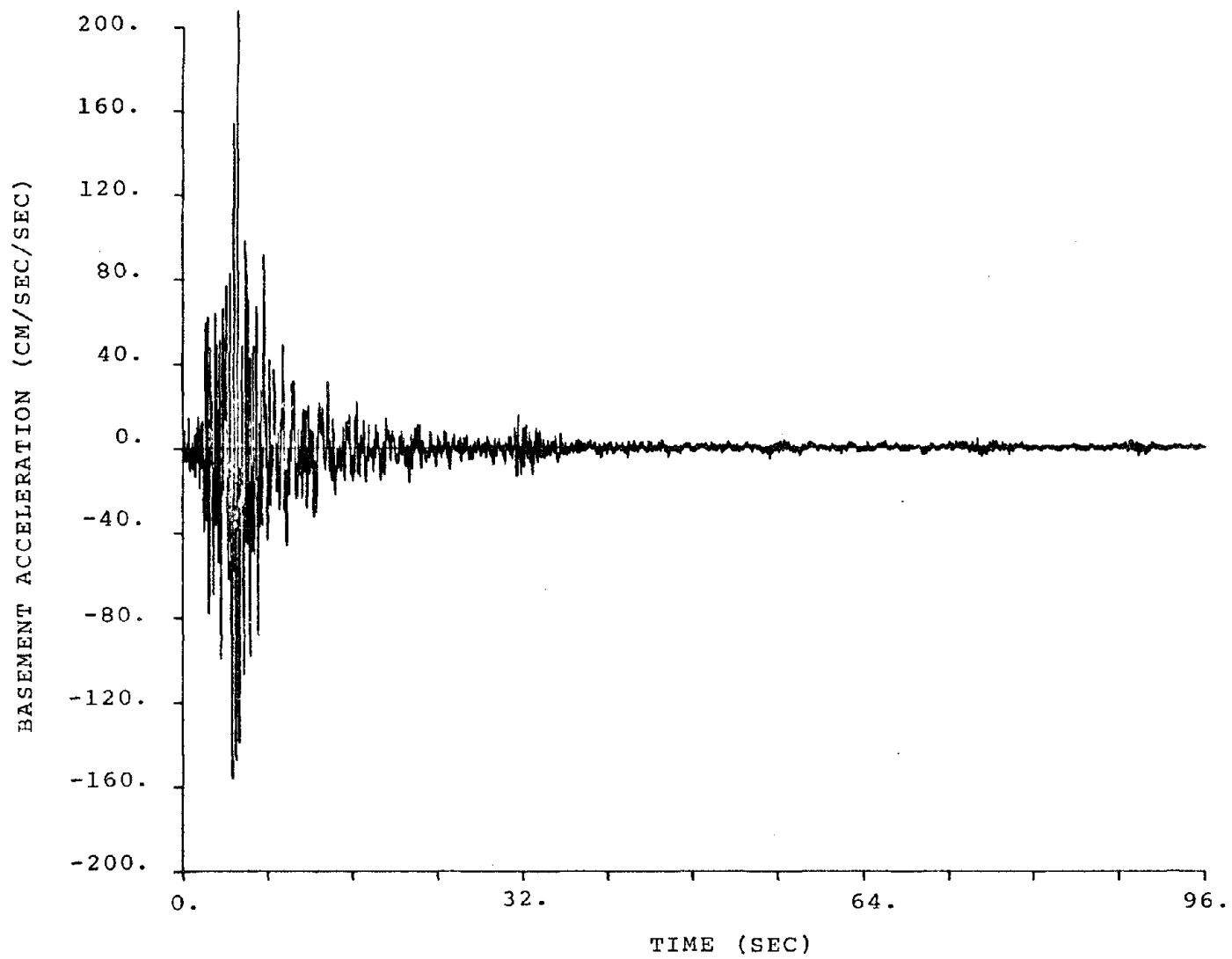


Figure 21. S82°E Component of the Basement Absolute Acceleration in JPL Building 180 (1971 San Fernando Earthquake).

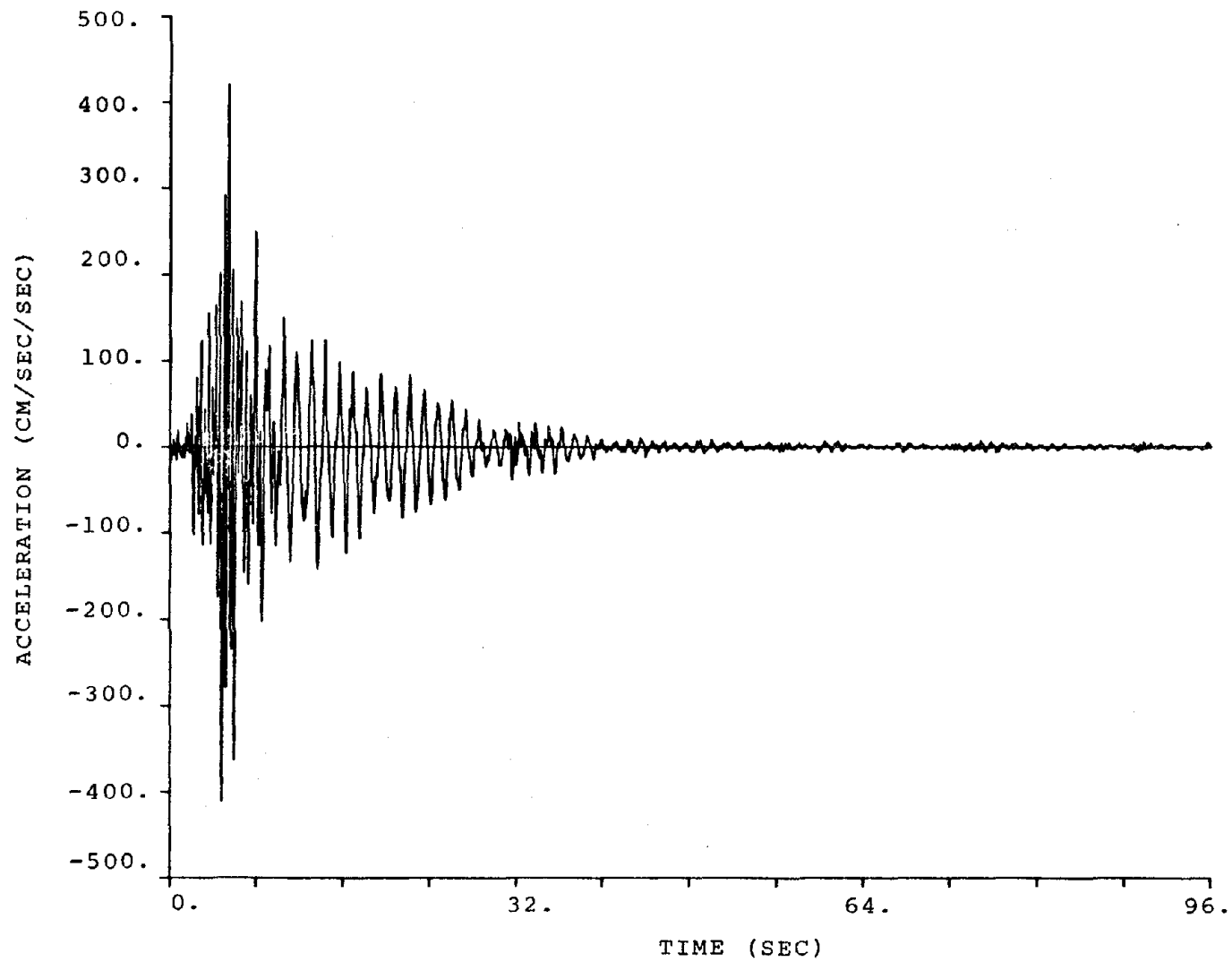


Figure 22. Relative Acceleration at the Roof of JPL Building 180.

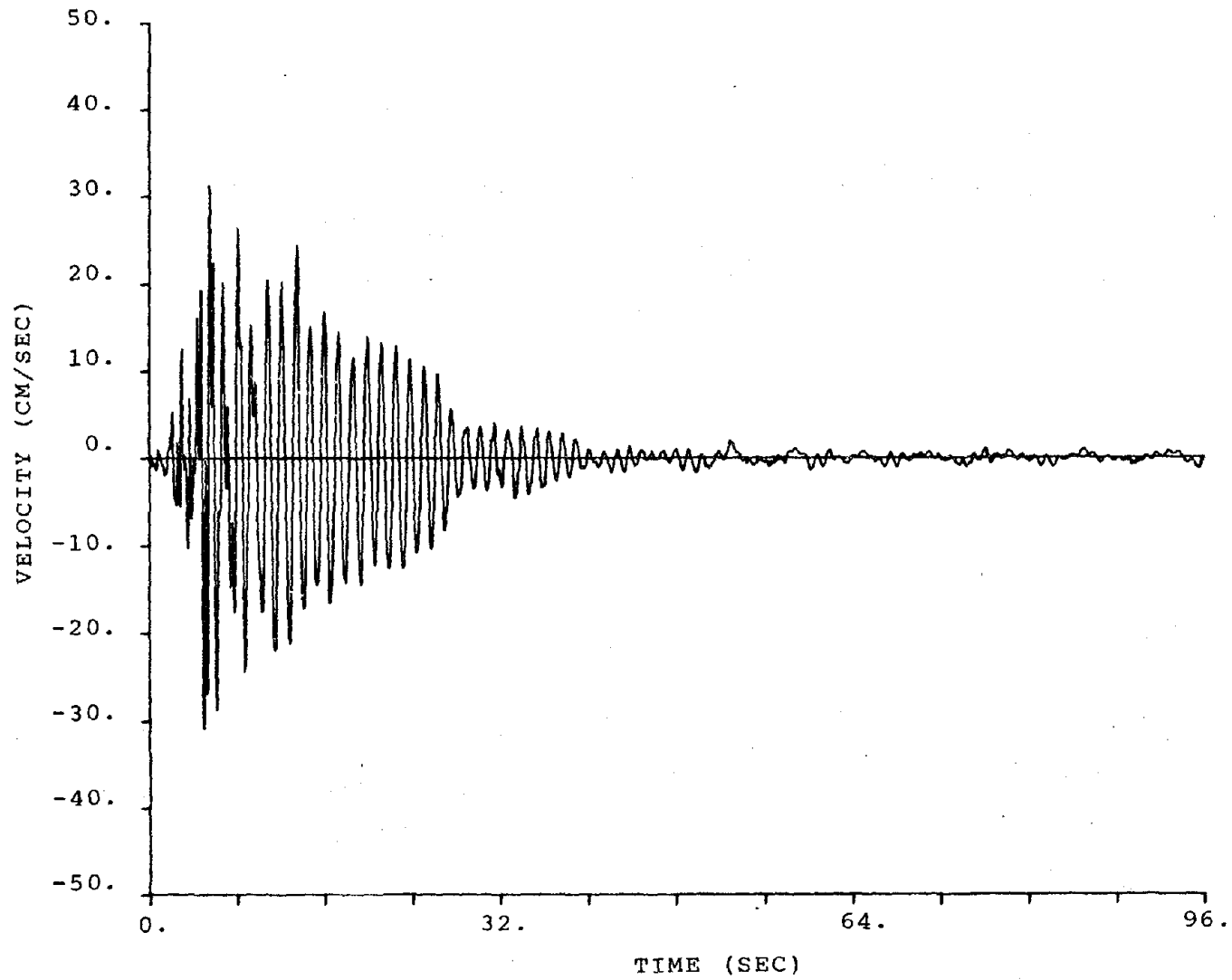


Figure 23. Relative Velocity at the Roof of JPL Building 180.

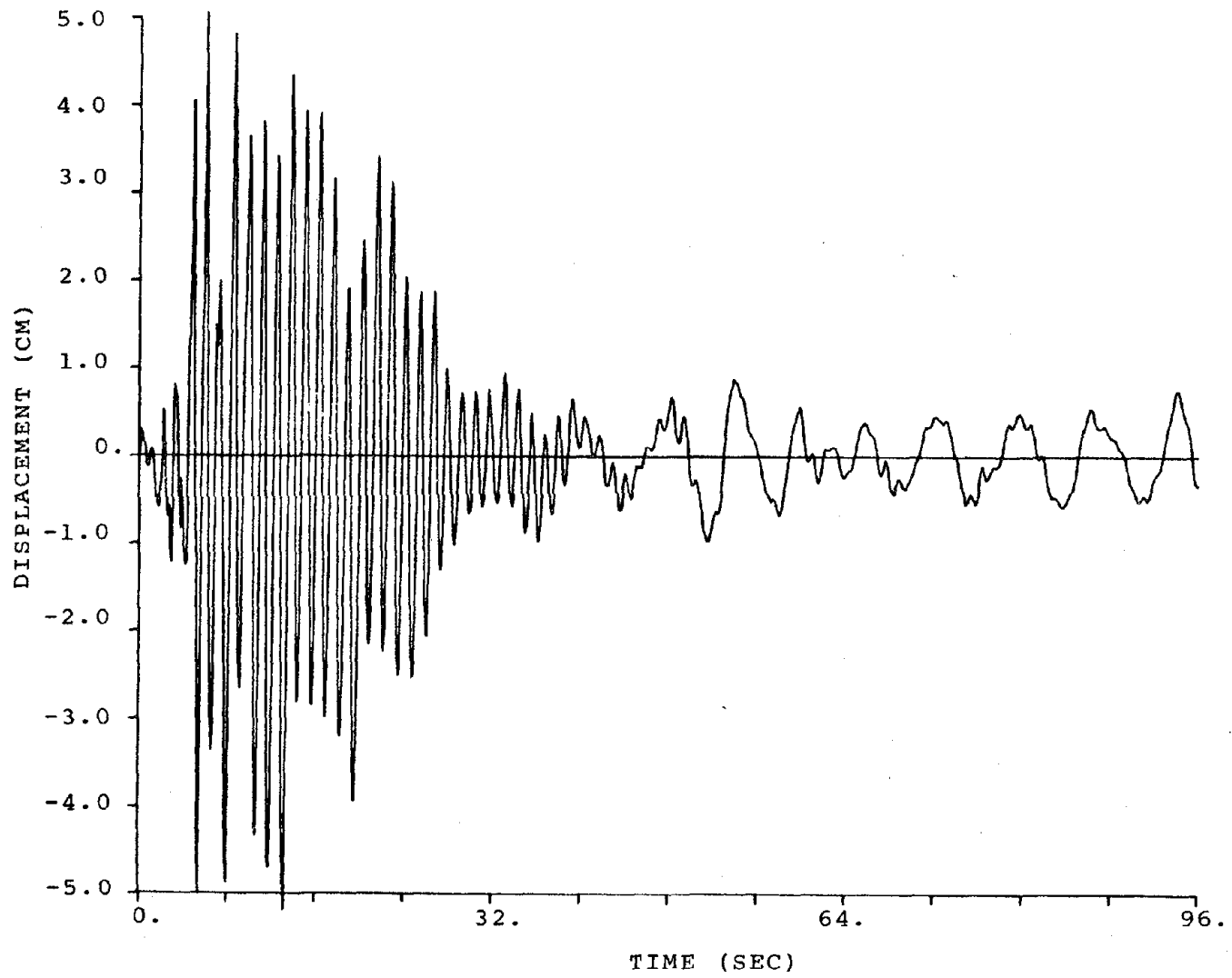


Figure 24. Relative Displacement at the Roof of JPL Building 180.

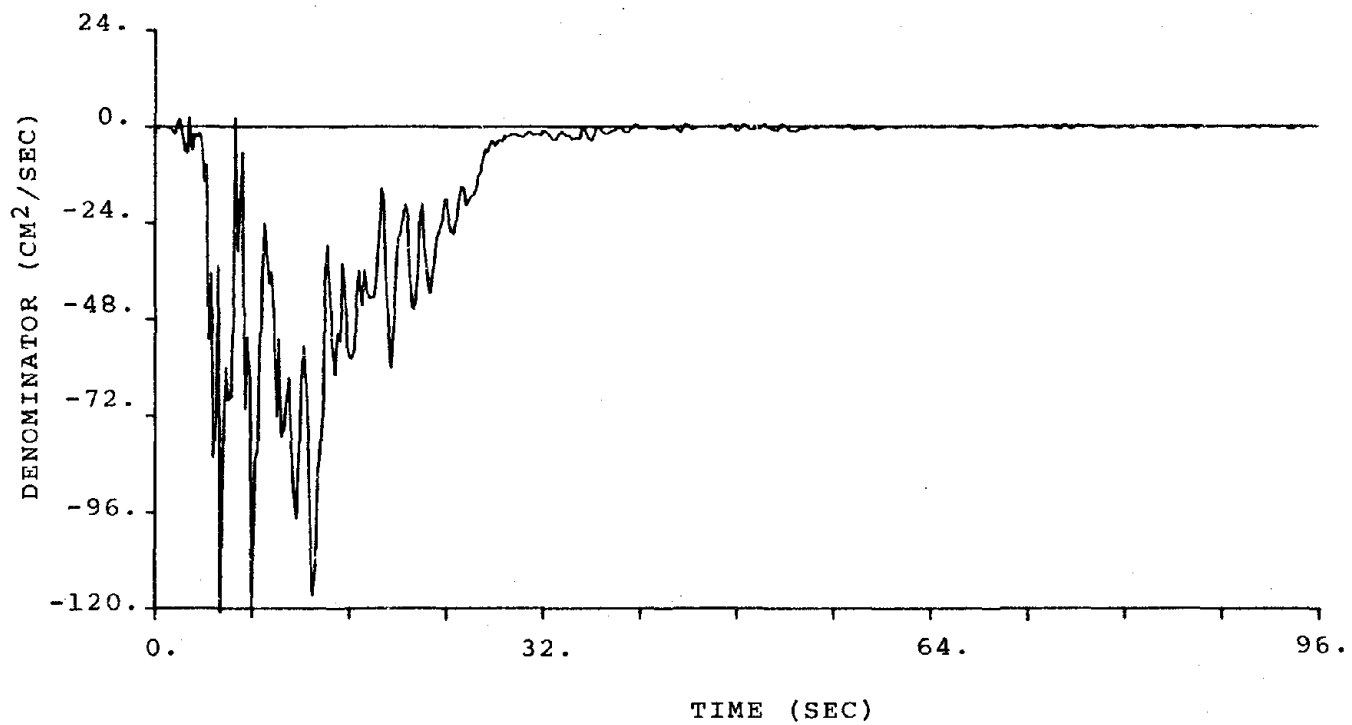


Figure 25. Denominator of Equation 11 Obtained From the Data of JPL Building 180.

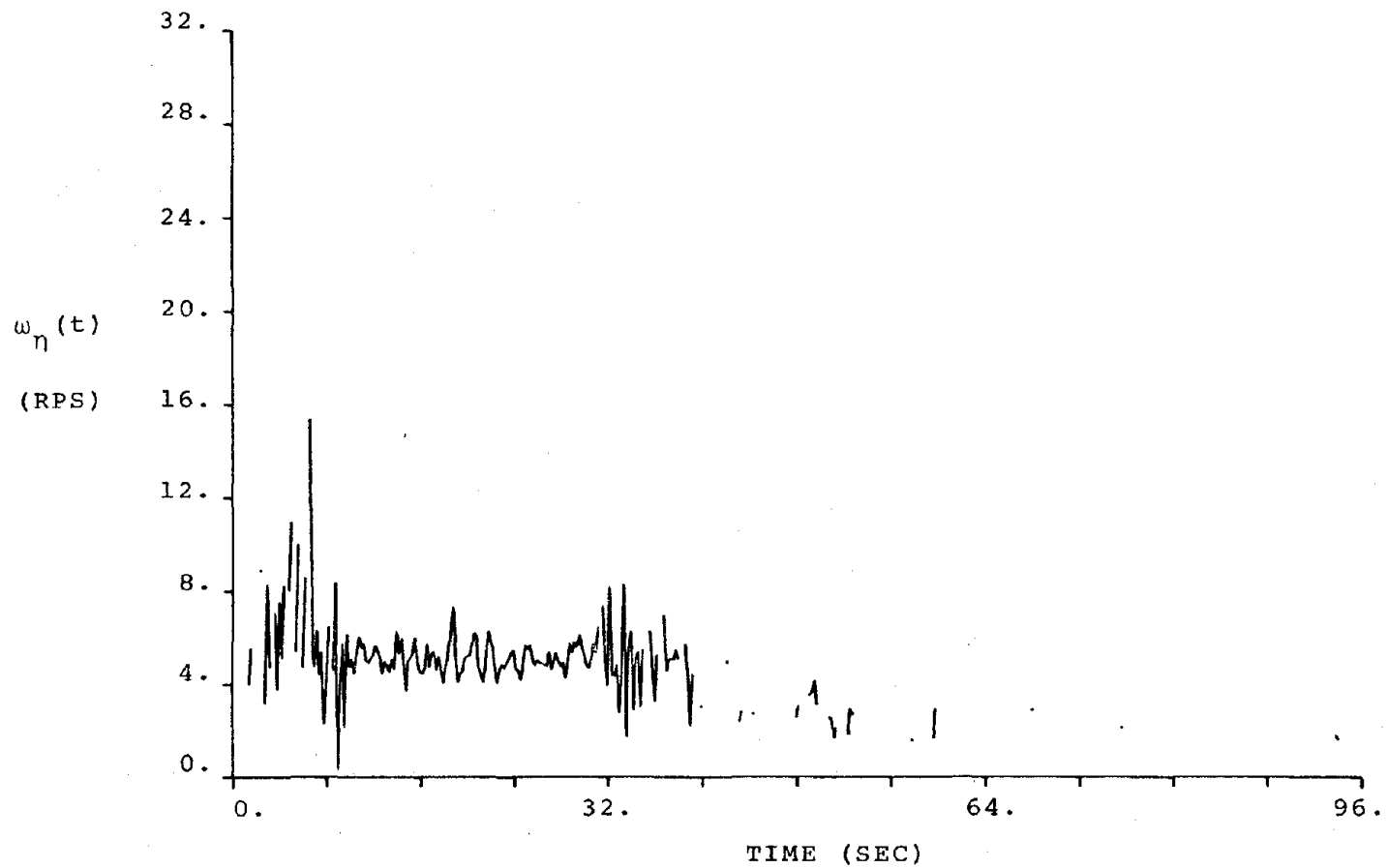


Figure 26. Natural Frequency Identified From the Data of JPL Building 180 Under Two Conditions.

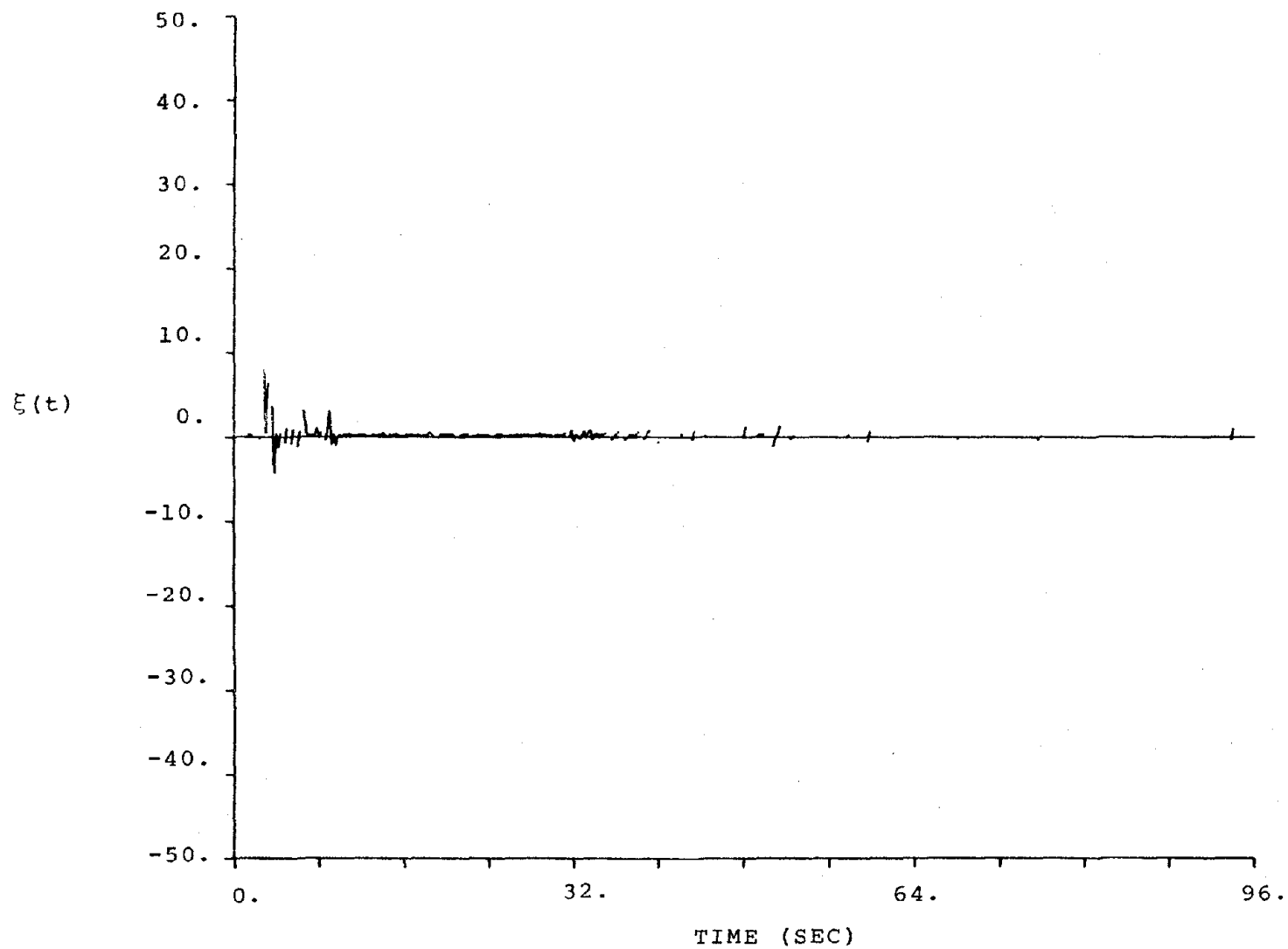


Figure 27. Damping Ratio Identified From the Data of JPL Building 180 and Natural Frequency of Figure 26.

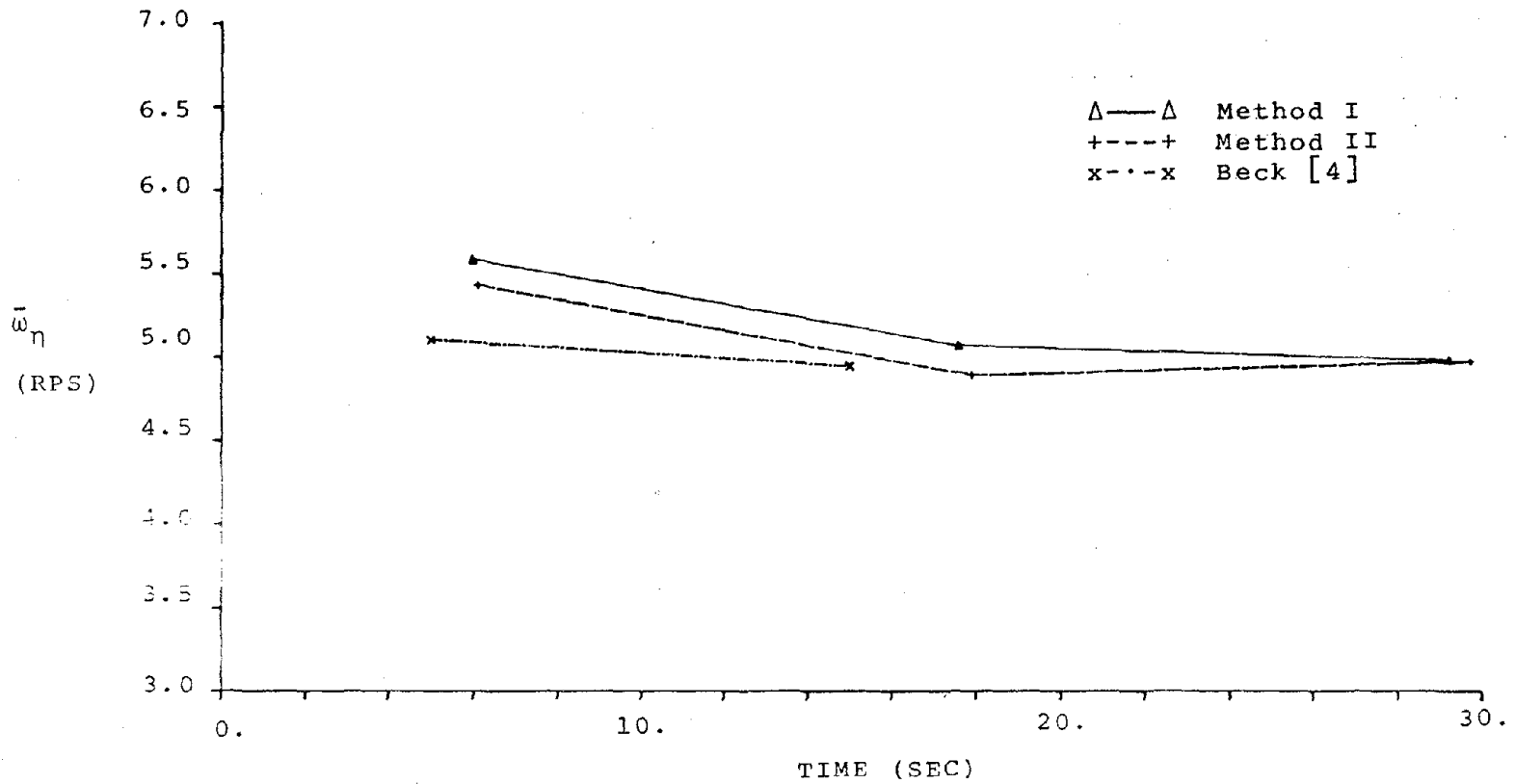


Figure 28. Comparison of the Natural Frequency Identified From Different Methods for JPL Building 180.

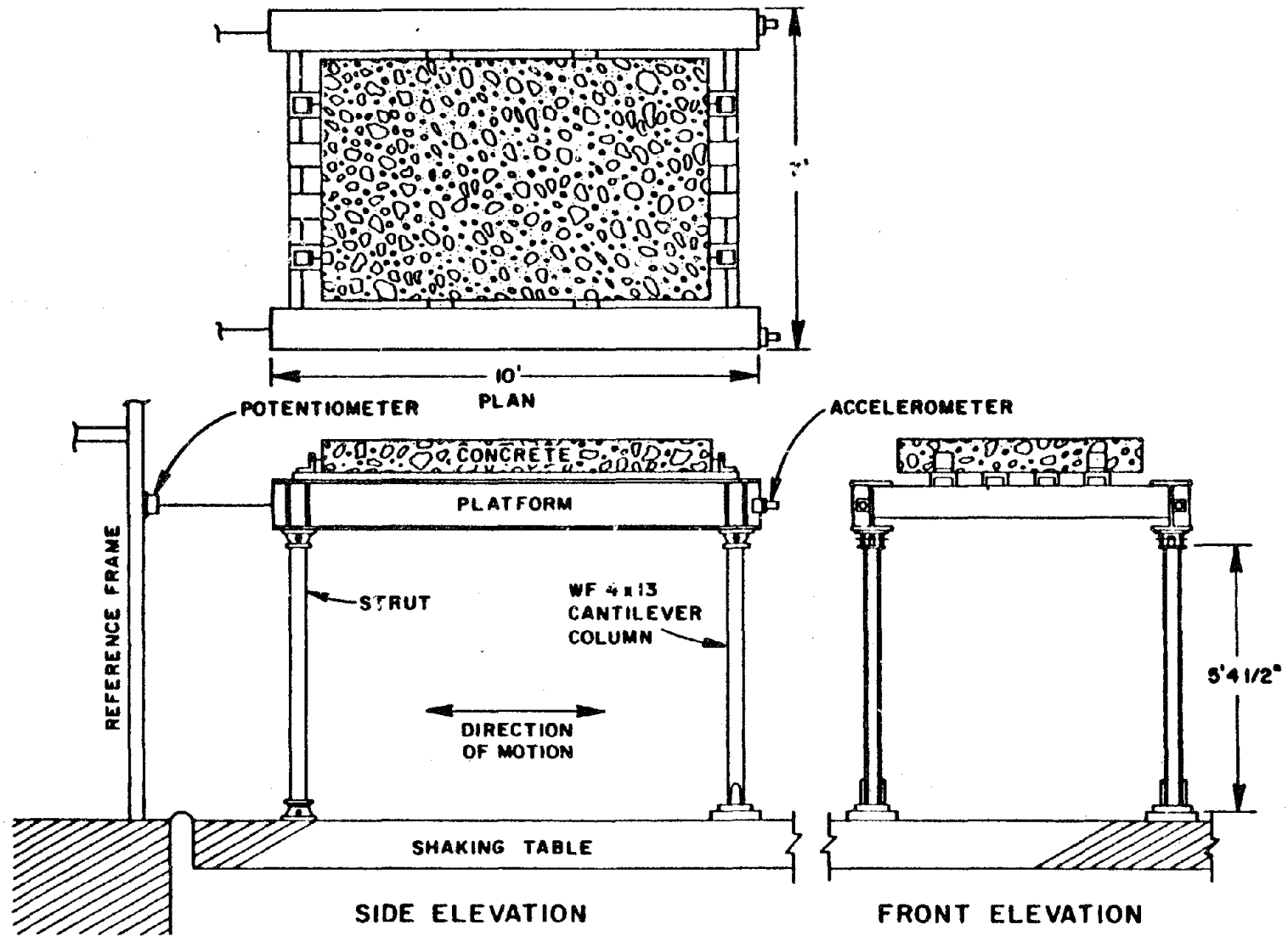


Figure 29. Plan and Elevation Views of Test Structure {27}.

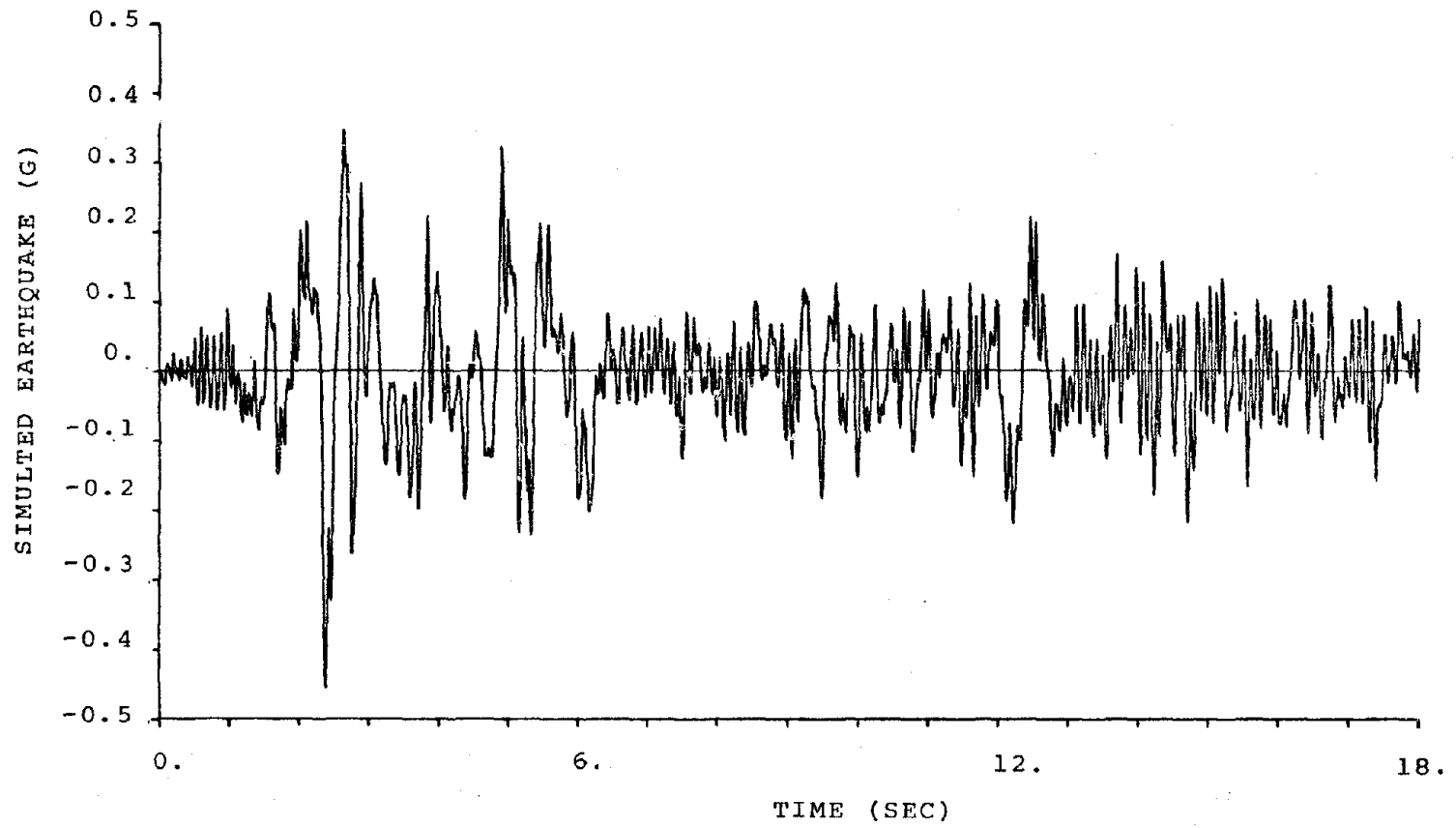


Figure 30. Simulated Earthquake Input to a Single-Story Steel Frame or Nonlinear Model I.

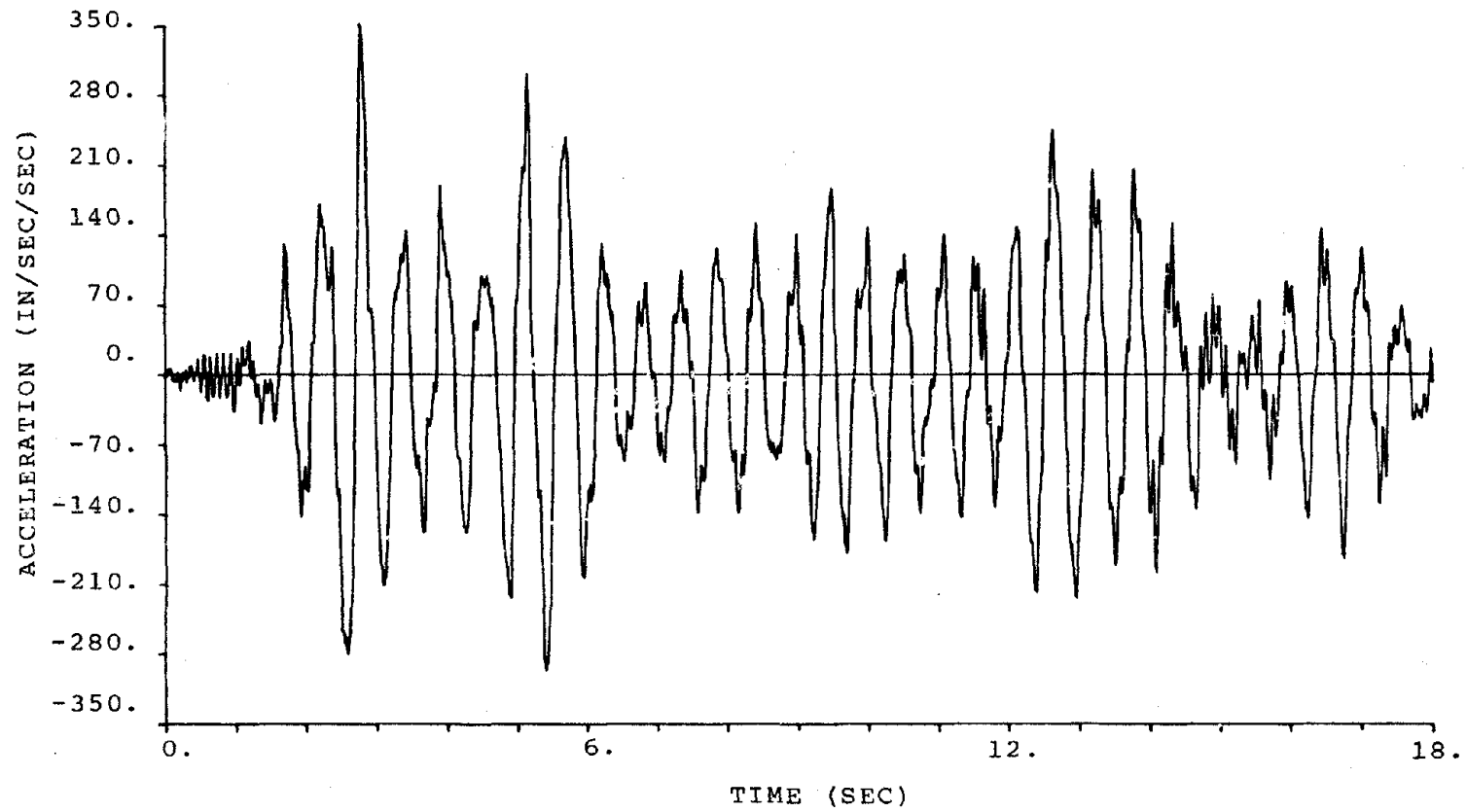


Figure 31. Measured Acceleration of Nonlinear Model I.

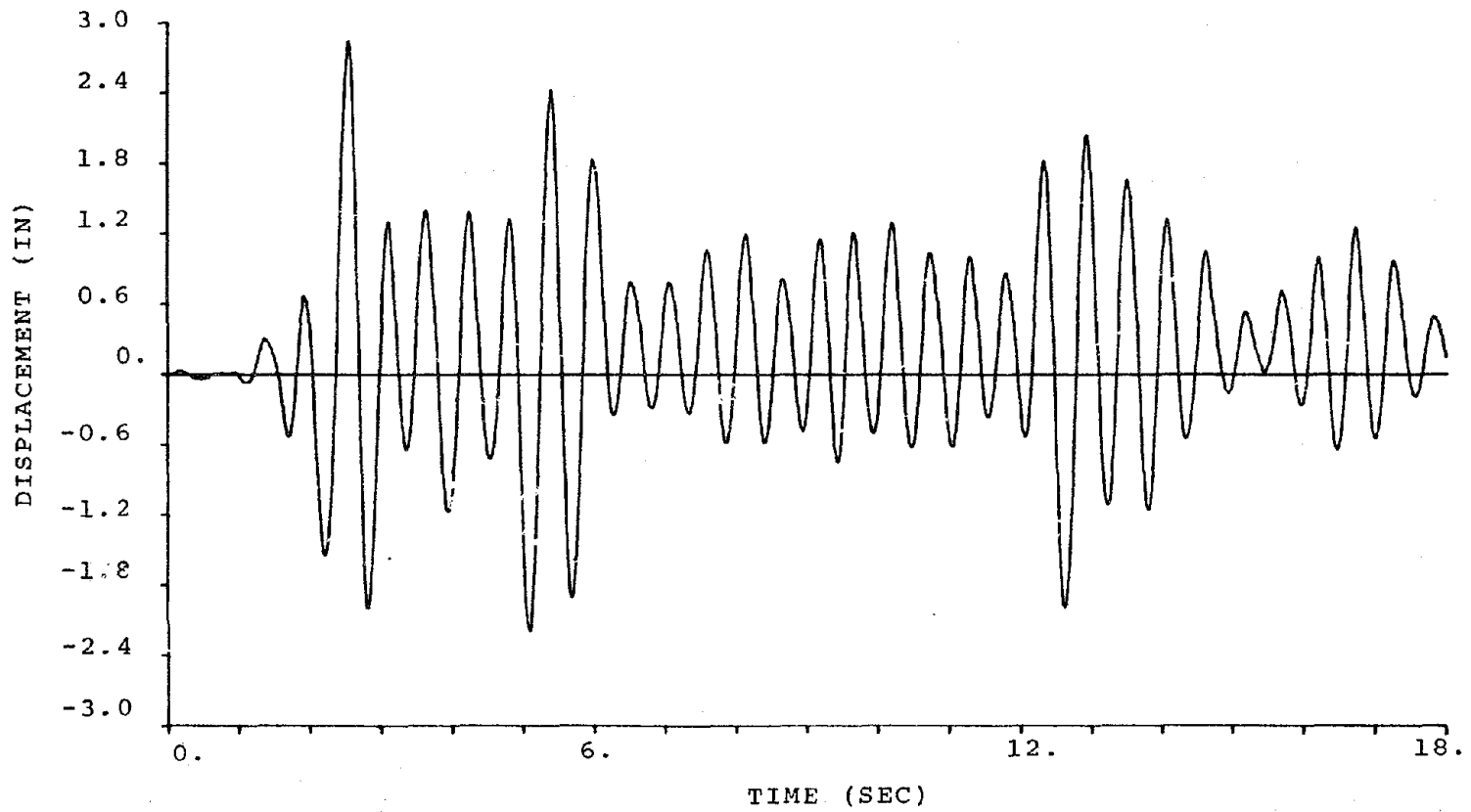


Figure 32. Measured Displacement of Nonlinear Model I.

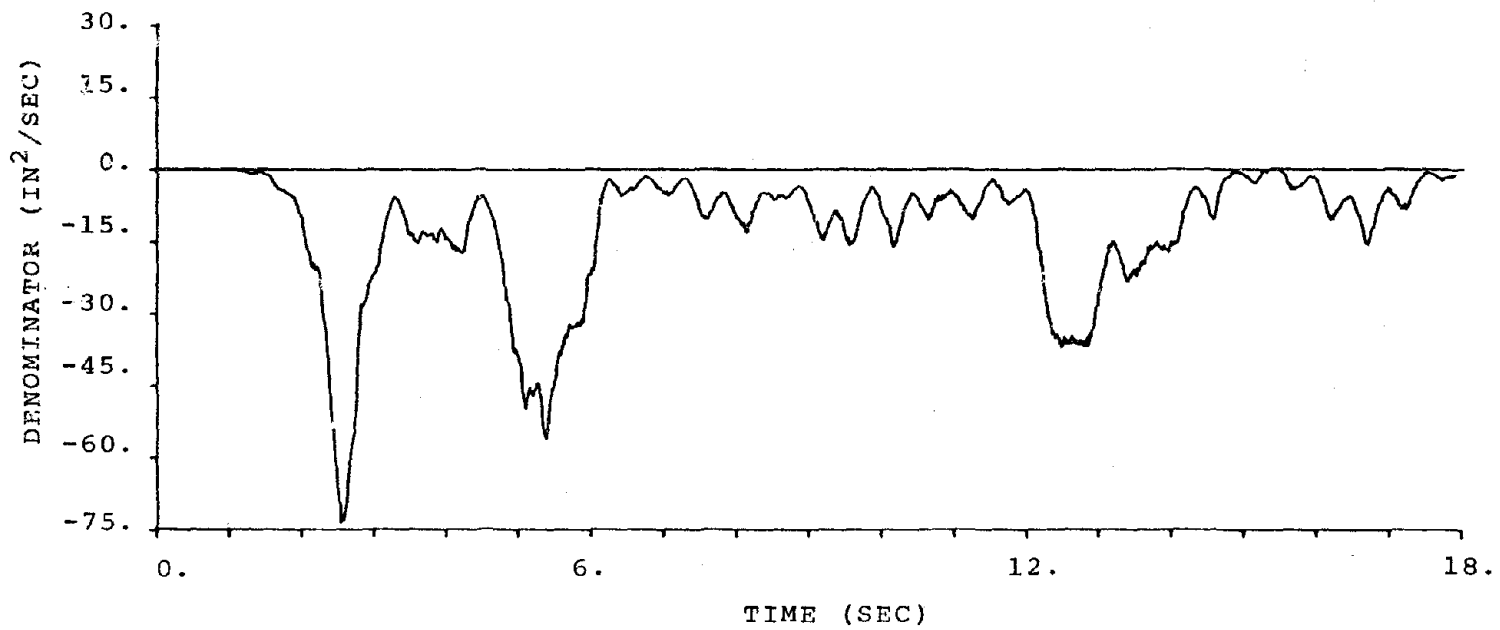


Figure 33. Denominator of Equation 11 Obtained From the Data of Nonlinear Model I.

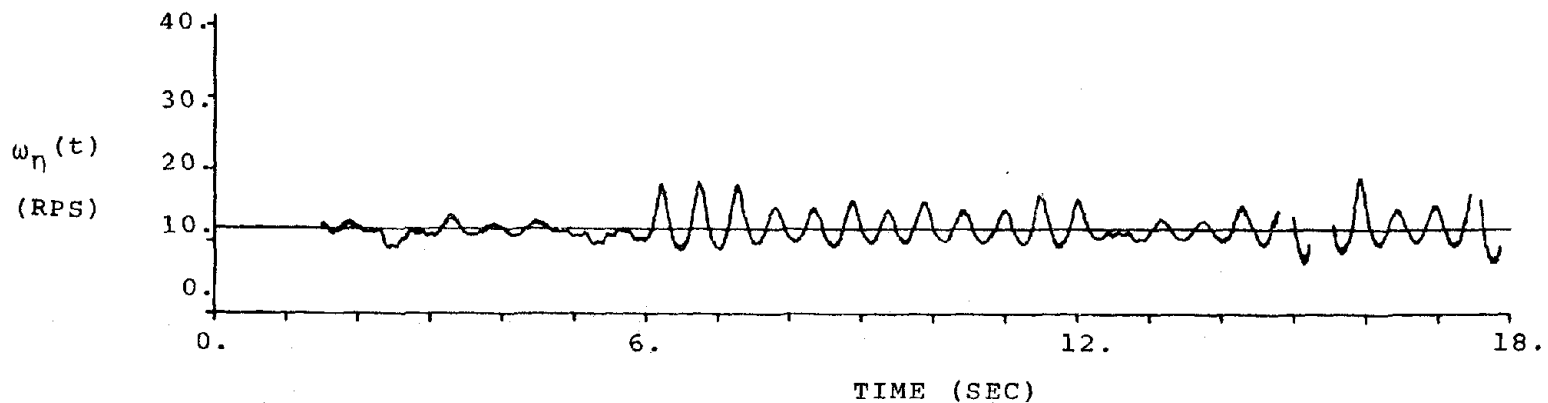


Figure 34. Natural Frequency Identified From the Data of Nonlinear Model I Under Two Conditions.

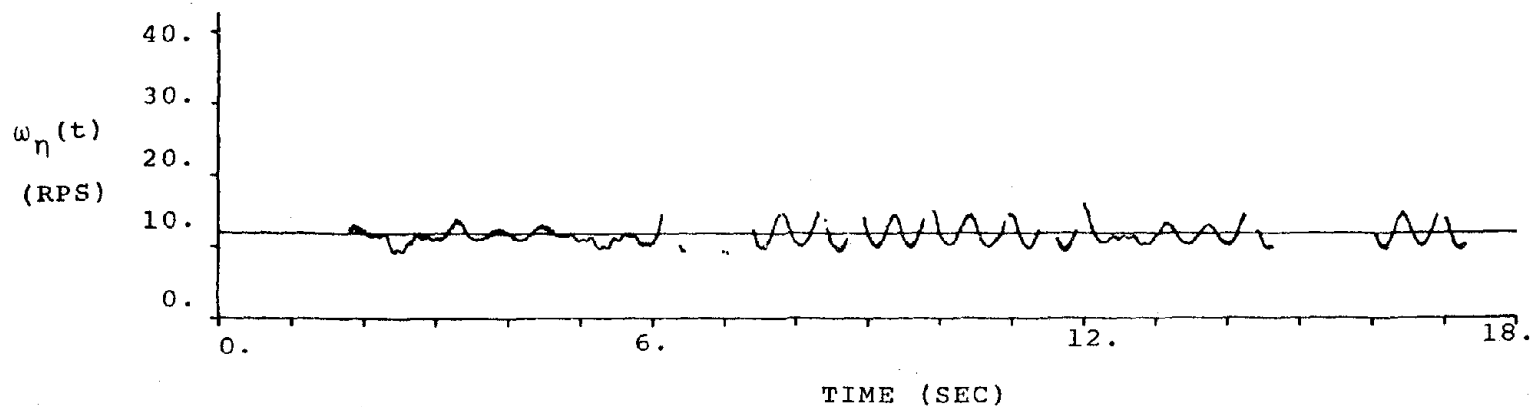


Figure 35. Natural Frequency Identified From the Data of Nonlinear Model I Under Two Conditions With More Restricted Denominator.

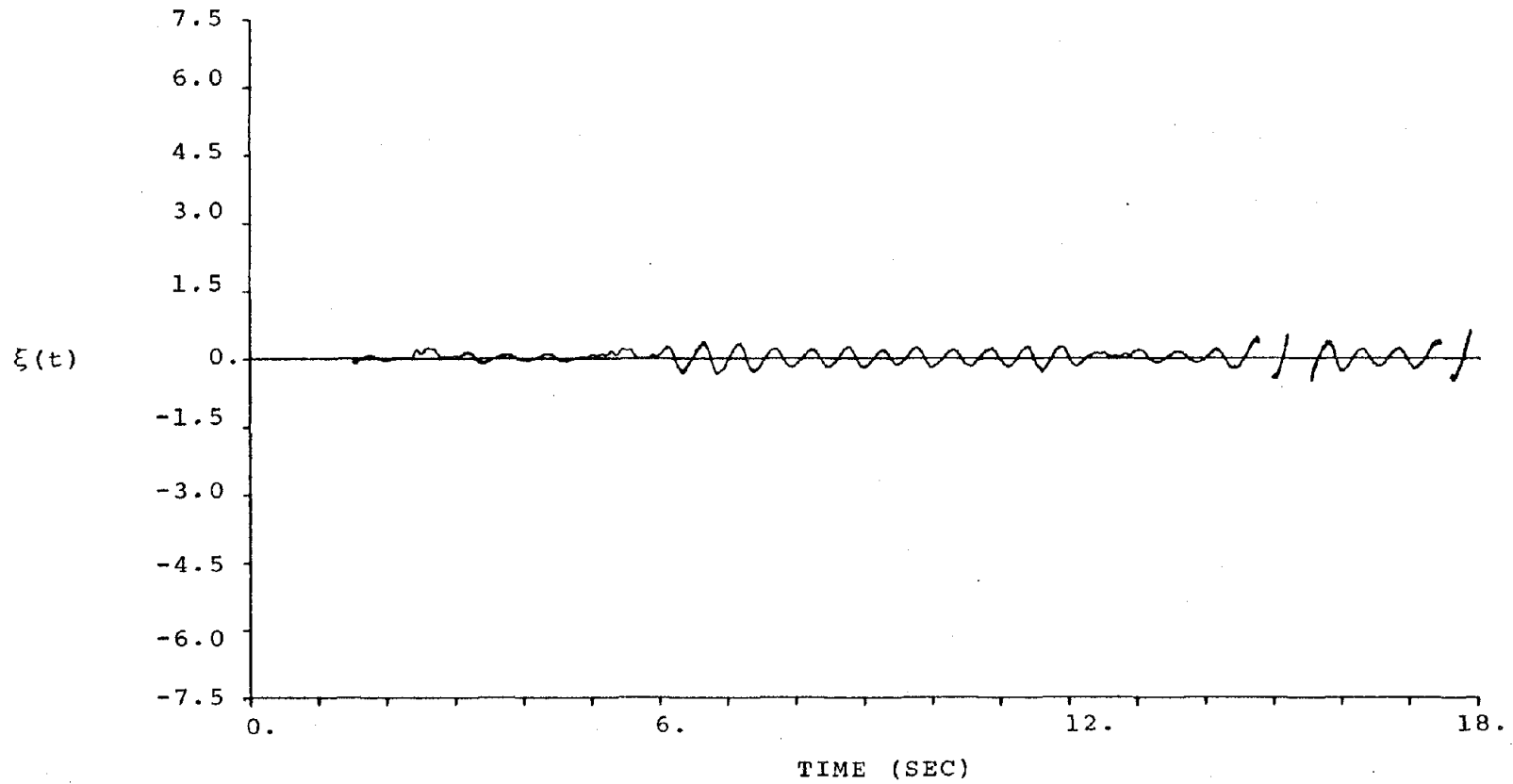


Figure 36. Damping Ratio Identified From the Data of Nonlinear Model I and the Natural Frequency of Figure 34.

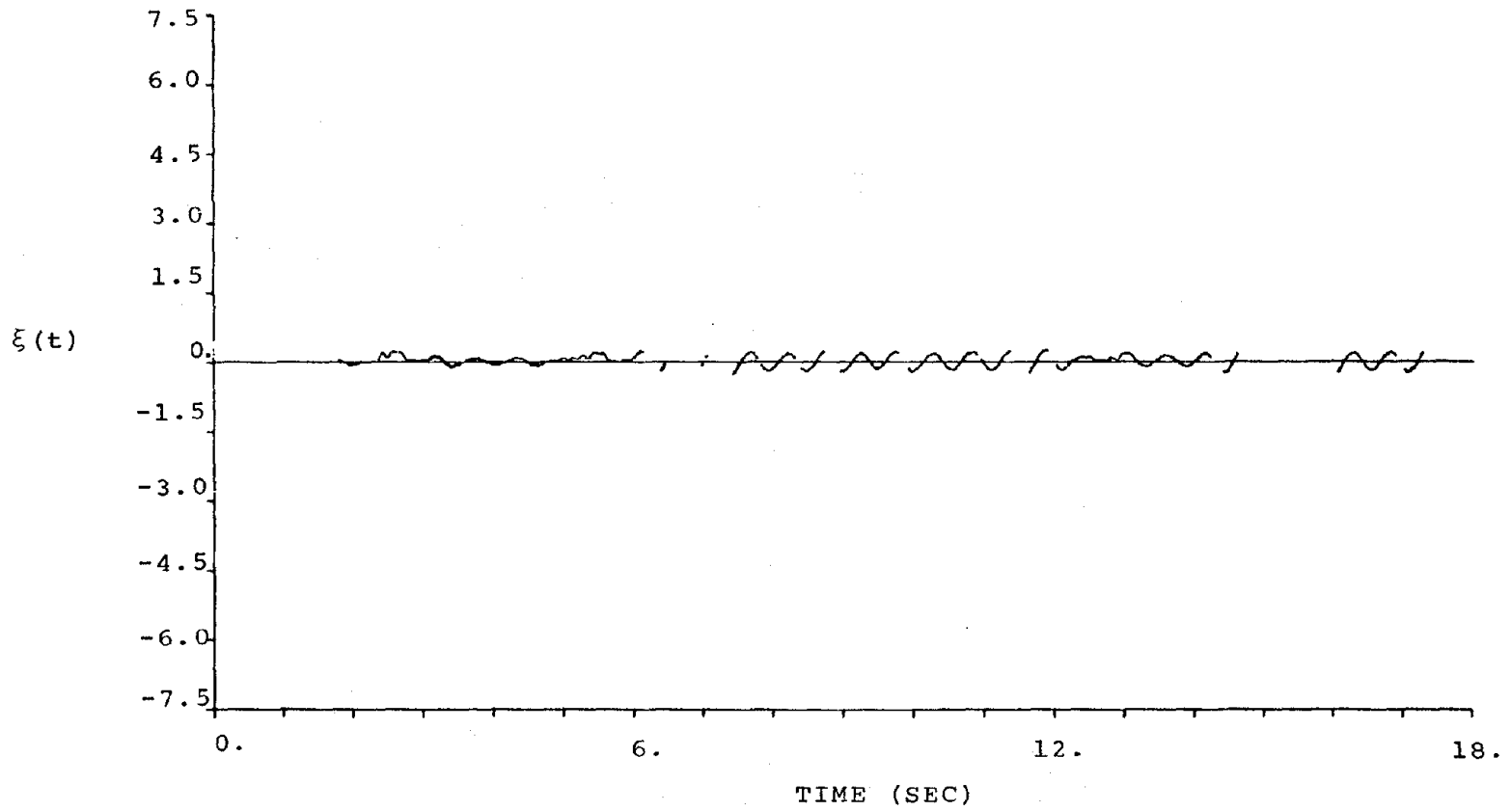


Figure 37. Damping Ratio Identified From the Data of Nonlinear Model I and the Natural Frequency of Figure 35.

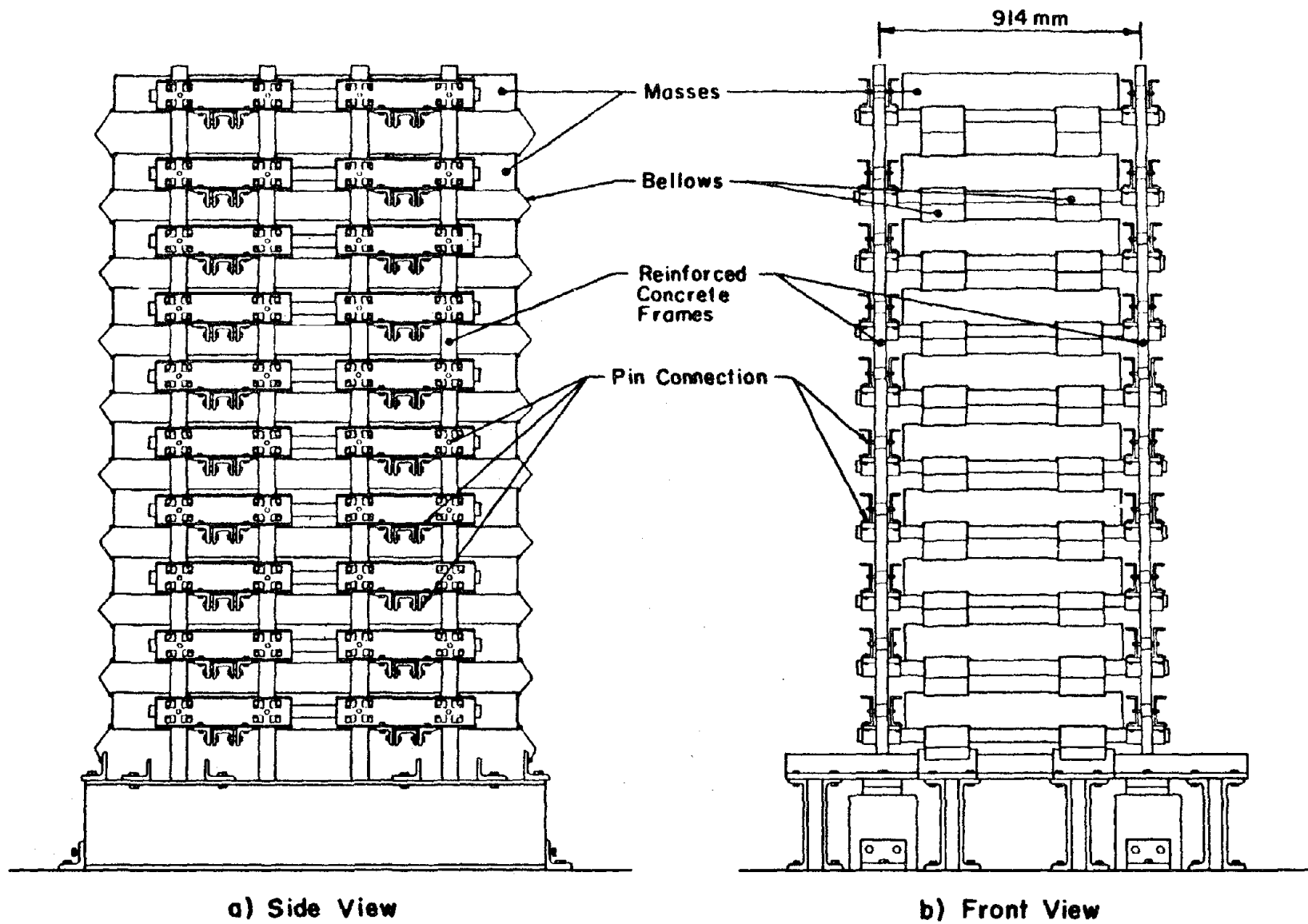


Figure 38. Test Structure {18}.

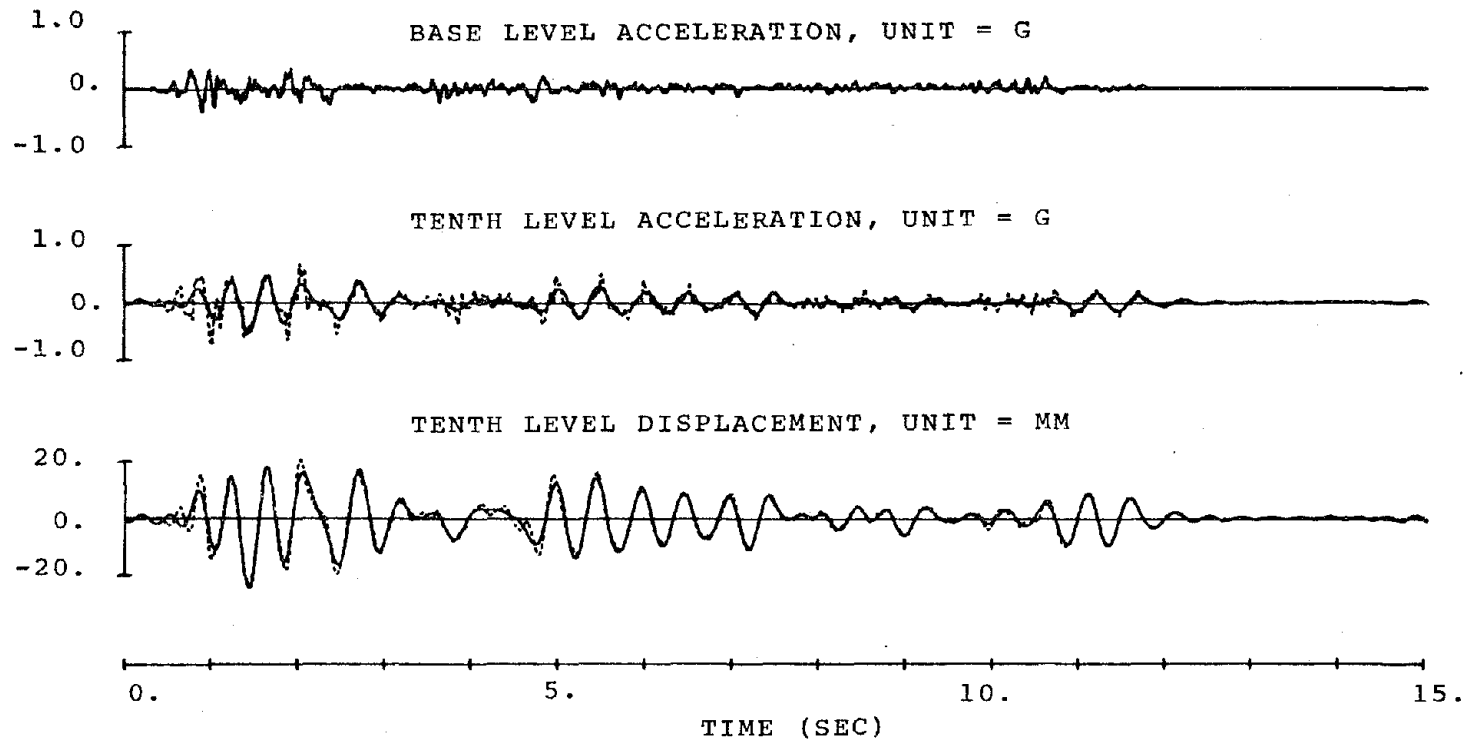


Figure 39. Observed Test Data, Run One.

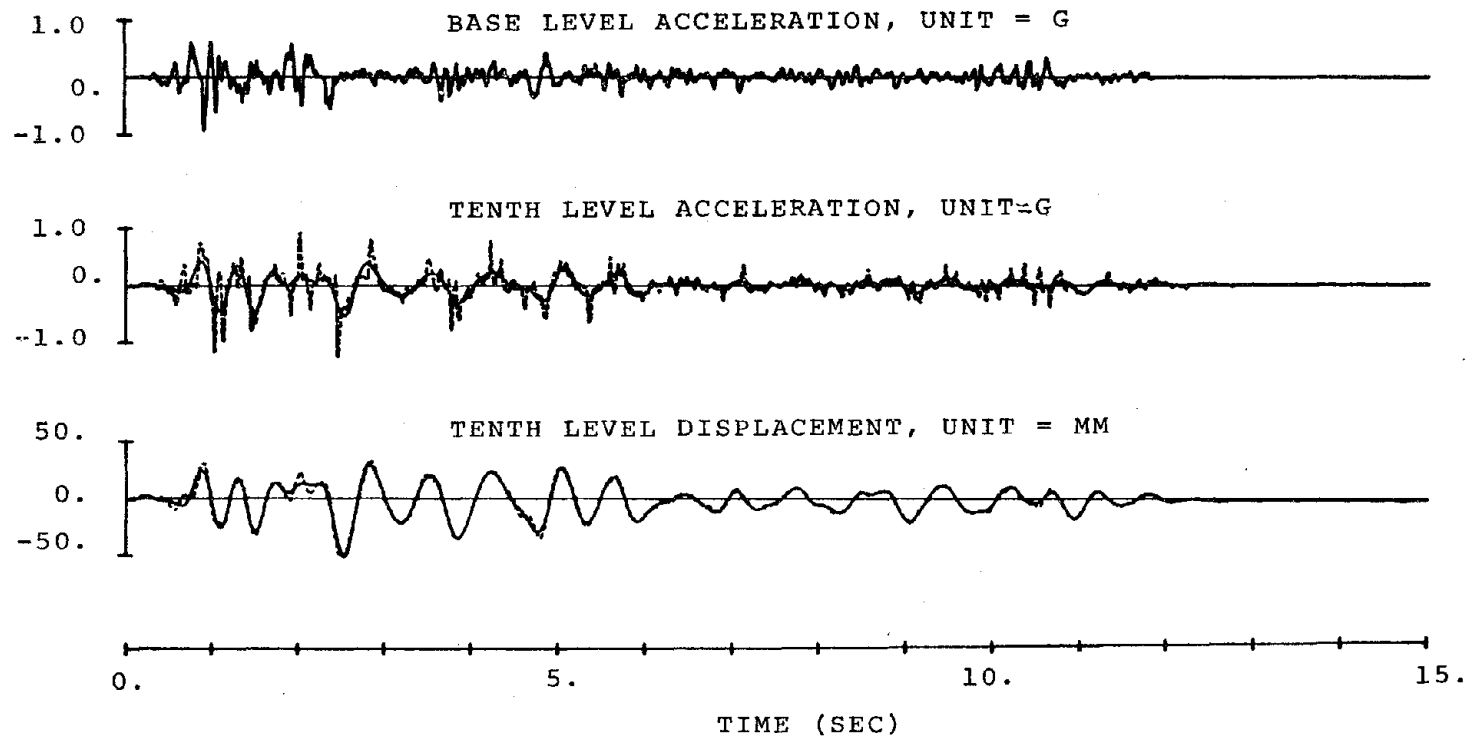


Figure 40. Observed Test Data, Run Two.

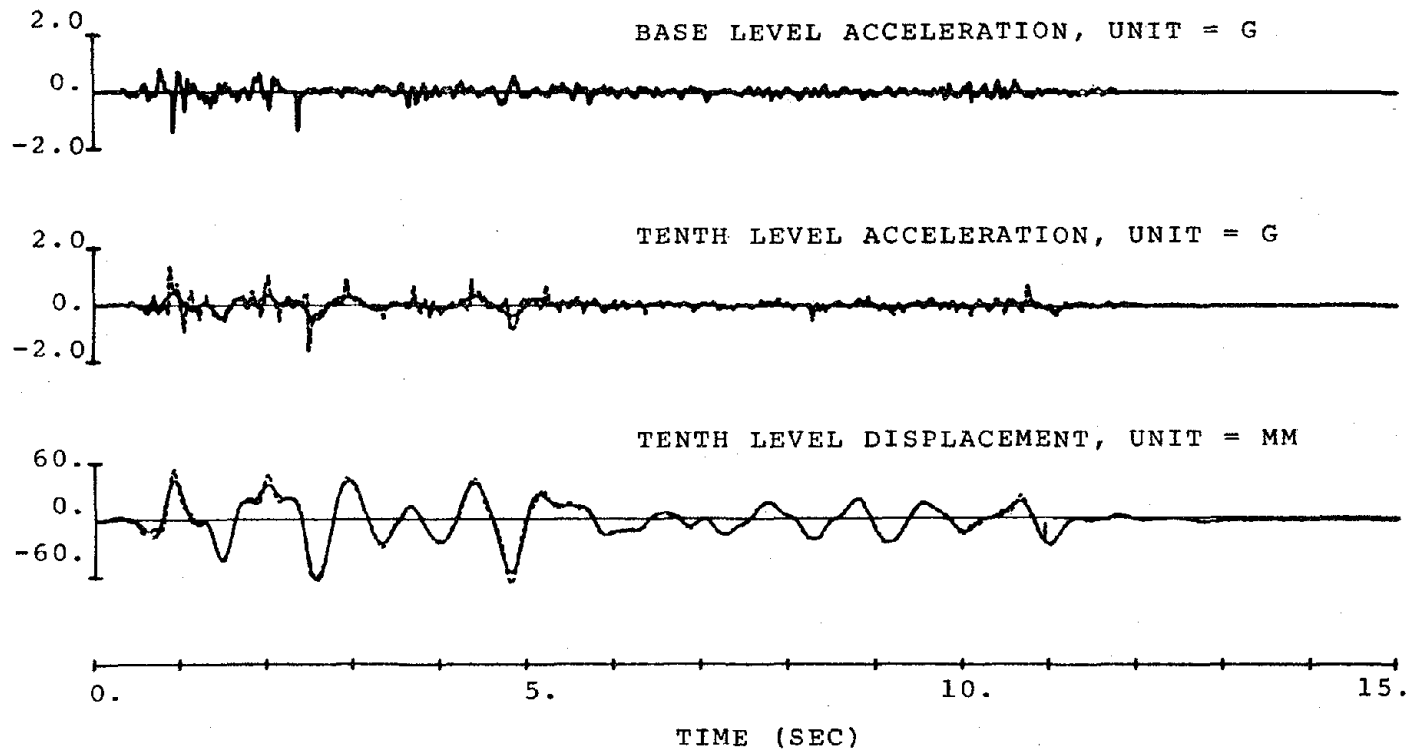


Figure 41. Observed Test Data, Run Three.

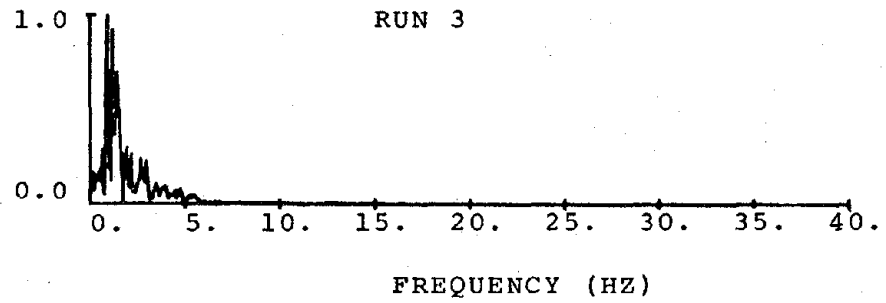
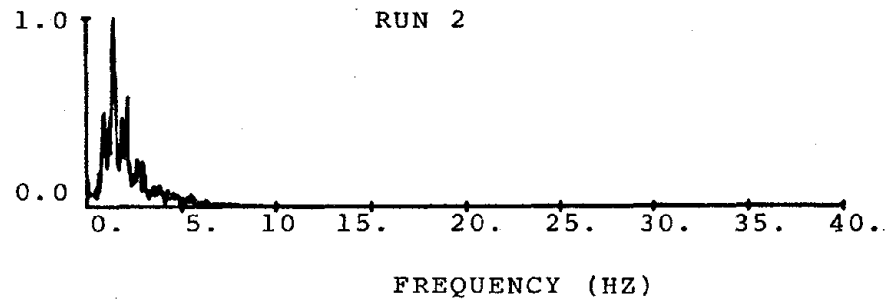
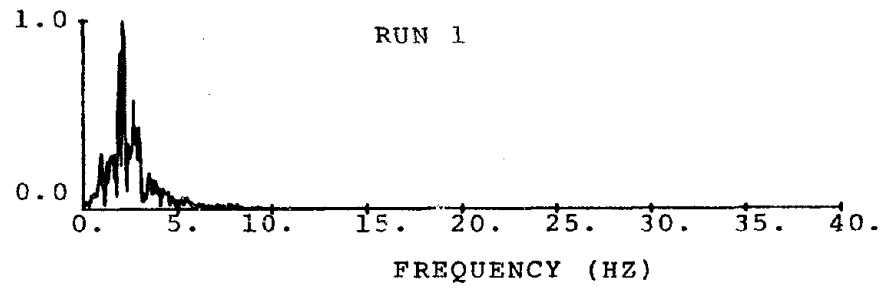


Figure 42. Fourier Amplitude Spectra of Tenth Level Displacement at Different Test Runs {18}.

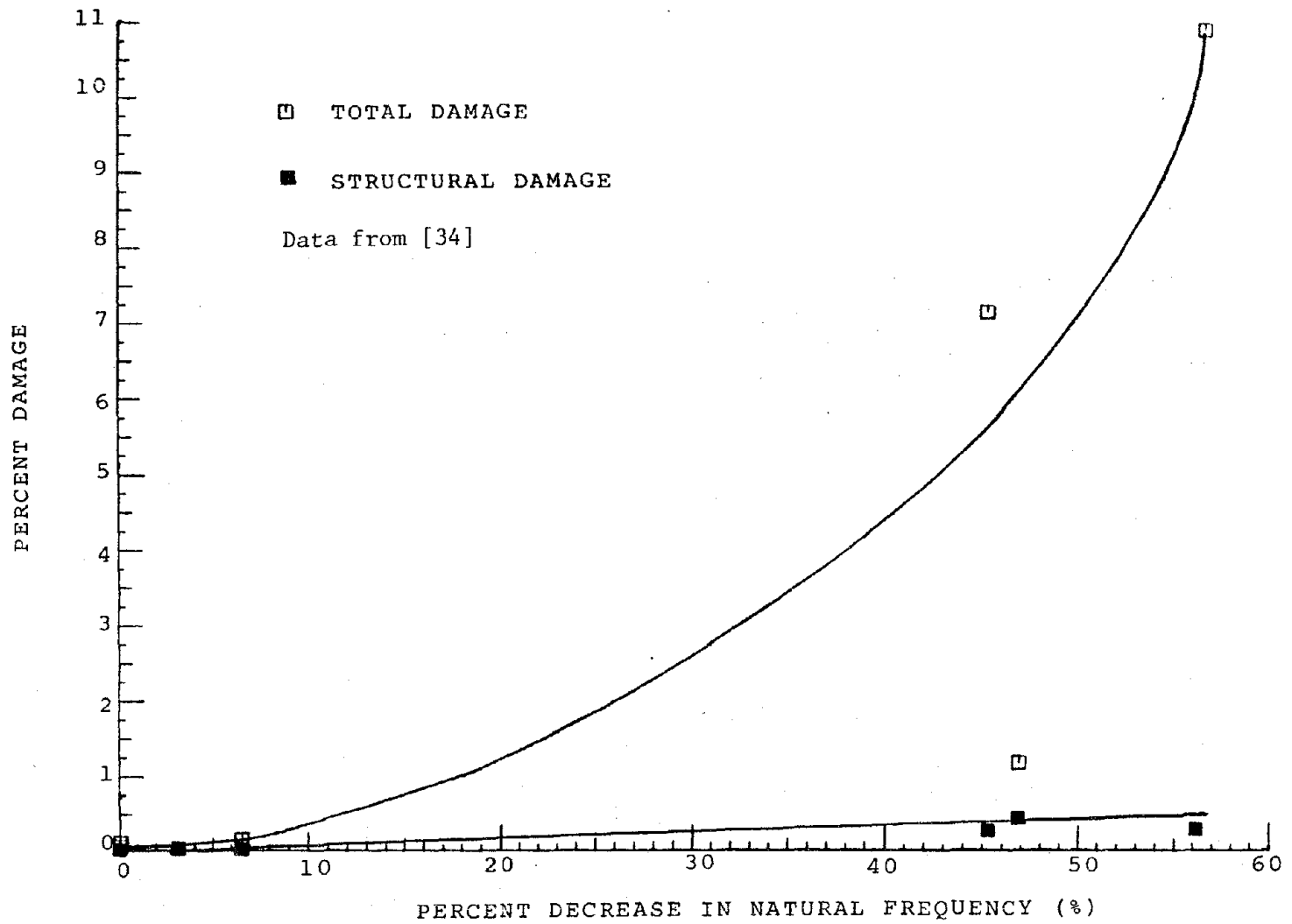


Figure 43. Damage Ratio Vs. Percent Decrease in Natural Frequency During Earthquake.

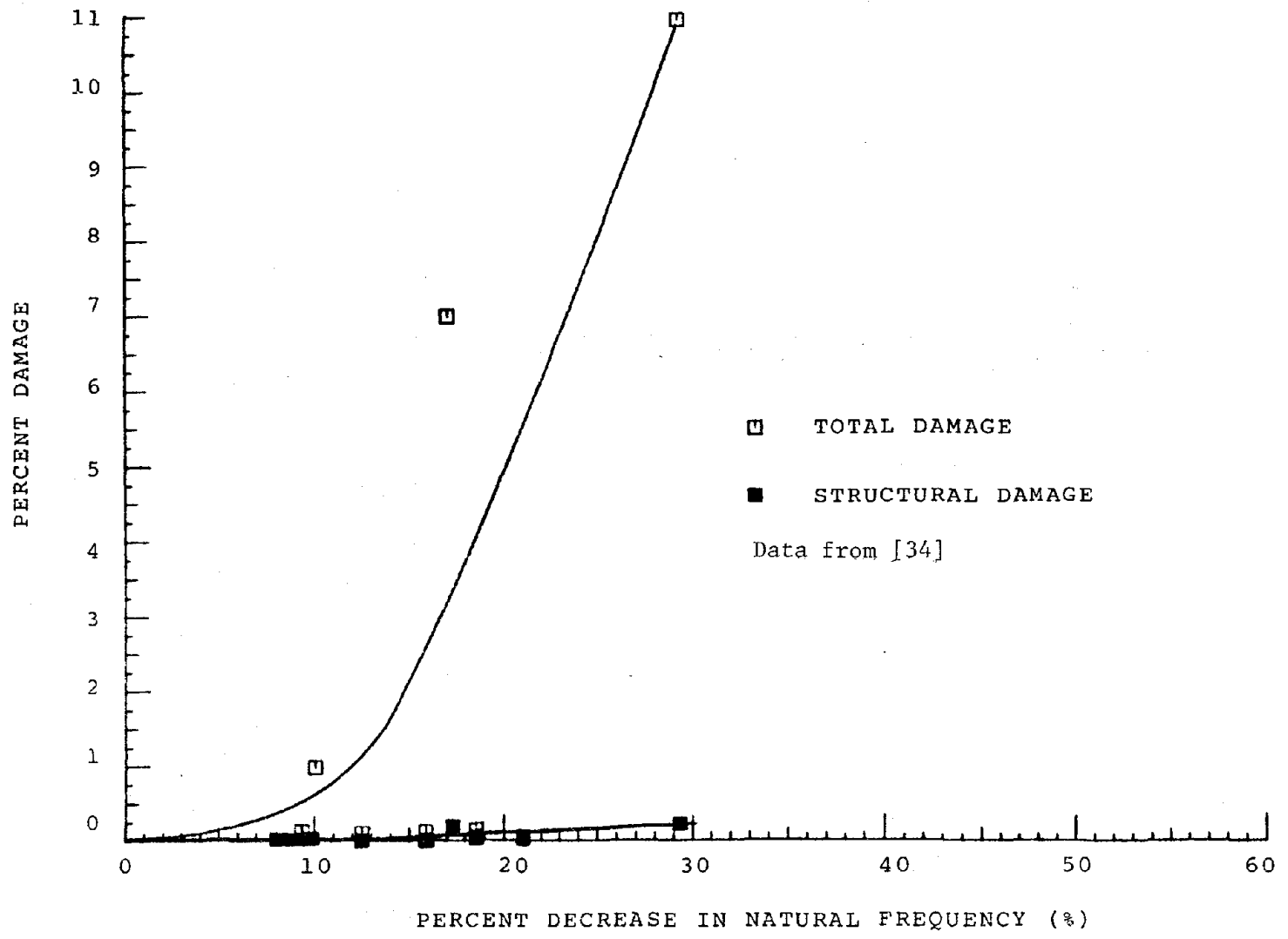


Figure 44. Damage Ratio Vs. Percent Decrease in Natural Frequency From Preearthquake to Postearthquake.

